



CHALMERS
UNIVERSITY OF TECHNOLOGY



The Mechanical Behavior of the Glued-in Plate Connection

An experimental study on bonded timber
connections

Master's thesis in Structural Engineering and Building Technology

LINN VERNERSSON & VENDELA ÖRNDAL

DEPARTMENT OF ARCHITECTURE AND CIVIL ENGINEERING

CHALMERS UNIVERSITY OF TECHNOLOGY
Gothenburg, Sweden 2025
www.chalmers.se

MASTER'S THESIS 2025

The Mechanical Behavior of the Glued-in Plate Connection

An experimental study of bonded timber connections

LINN VERNERSSON & VENDELA ÖRNDAL



CHALMERS
UNIVERSITY OF TECHNOLOGY

Department of Architecture and Civil Engineering
Division of Structural Engineering
Lightweight Structures
CHALMERS UNIVERSITY OF TECHNOLOGY
Gothenburg, Sweden 2025

The Mechanical Behavior of the Glued-in Plate Connection
An experimental study of bonded timber connections
LINN VERNERSSON & VENDELA ÖRNDAL

© LINN VERNERSSON & VENDELA ÖRNDAL, 2025.

Examiner: Full Professor Mohammad al-Emrani
Architecture and Civil Engineering
Chalmers University of Technology

Supervisor: Post-doc Zhengyao Li
Architecture and Civil Engineering
Chalmers University of Technology

Supervisor: Marco Pagliarin
Technical Project Manager Timber
Hilti AG

Master's Thesis 2025
Department of Architecture and Civil Engineering
Division of Structural Engineering
Lightweight Structures Group
Chalmers University of Technology
SE-412 96 Gothenburg
Telephone +46 31 772 1000

Cover: Test specimens in a pile from the experimental testing conducted in this study.

Typeset in L^AT_EX
Printed by Chalmers Reproservice
Gothenburg, Sweden 2025

The Mechanical Behavior of the Glued-in Plate Connection

An experimental study of bonded timber connections

LINN VERNERSSON & VENDELA ÖRNDAL

Department of Architecture and Civil Engineering

Chalmers University of Technology

Abstract

Glued-in plates is a novel connection for timber construction and limited research has been done on the subject. The connection consists of a timber element with a slot, in which a steel plate is mounted and set with adhesive. Previous research shows that this connection has many advantages compared to traditional timber fastening methods. Similarities can be found with the glued-in rod connection, where both connections are made with the same three materials and have the same basic mechanical behavior.

In this project, an experimental study was conducted where different parameters were investigated to gain further insights in the load carrying capacity of the glued-in plates connection. Geometrical parameters were changed depending on the test series, and one of the main focuses was to investigate the properties of the glue dowel formed in the perforation of the steel plate.

Results from the experimental testing shows that glue dowels increase the load capacity of the connection and contributes a less brittle failure compared to unperforated plates. The shear area of the glue dowel has a linear increasing correlation to the load capacity. Both plate thickness and embedment length have an influence on load capacity up to a certain limit and then plateaus. Distributing the perforation of the plate, gives a higher load capacity due to a better stress distribution in the adhesive. Although, the perforation should not be placed closer than 2.5 times the dowel diameter to the edge of the plate to ensure that there is no failure in the timber.

The connection is proven to exhibit high stiffness and strength. However, there are many areas that need studying before the connection can be used in real life applications. One of the areas is how the application of adhesive should be conducted for reliable results and practical use, while also studying the occurrence of air bubbles. Furthermore, a design standard with demands, requirements and calculation method should be developed as to consider all aspects and variables of the connection design.

Keywords: glued-in plates, timber connection, bonded connection, experimental testing, pull-out testing, glue dowel

Acknowledgements

This Masters thesis was conducted at Chalmers University of Technology, Department of Architecture and Civil Engineering. The thesis has been carried out during the 2025 spring semester as the final project in the Master's program Structural Engineering and Building Technology.

We would like to bring to the attention all the people who has in any way helped the process of this thesis. Firstly, thank you to our supervisor Zhengyao Li for the advice and guidance throughout the entirety of this project. We would also like to thank examiner professor Mohammad al-Emrani for challenging and improving this thesis with his observations and experience.

The thesis is a cooperation between Chalmers and Hilti. All of the experimental tests was funded by Hilti and performed in their in-house test lab. We would like to thank Raffael Gstöhl, Max Volk, Jakub Raczy and Max Fehr for always helping and explaining. Furthermore, we would like to express our gratitude to our supervisor Marco Pagliarin for providing his guidance and experience. Your contributions to this project have been invaluable. Thank you for the warm welcome and the incredible opportunity provided by the Hilti team.

Lastly, thank you to our opponents and dear friends, Lisa Ryrstedt and Peter Stanek Sörner, for providing feedback that improved us and our work.

Linn Vernersson & Vendela Örndal, Gothenburg, June 2025

List of Acronyms

Below is the list of acronyms that have been used throughout this thesis listed in alphabetical order:

CoV	Coefficient of Variance
DIC	Digital Image Correlation
EWP	Engineered Wood Products
EPX	Epoxy
GIP	Glued-in plate
GIR	Glued-in rod
LVL	Laminated Veneered Lumber

Contents

List of Acronyms	ix
List of Figures	xiii
List of Tables	xix
1 Introduction	1
1.1 Background	1
1.2 Aim and objective	2
1.3 Methodology	3
1.4 Thesis questions	3
1.5 Limitations	4
2 Previous research on bonded connections	5
2.1 Main components of a glued-in plate connection	5
2.1.1 Timber	6
2.1.2 Steel	8
2.1.3 Adhesive	9
2.2 Previous testing on glued-in plates	11
2.3 Glued-in rods and possible take aways	15
2.4 Other bonded connections and possible take aways	19
2.5 Method of literature review	21
2.6 Summary	22
3 Experimental Testing	23
3.1 Description of test series	23
3.1.1 Test series 1	24
3.1.2 Test series 2	25
3.1.3 Test series 3	26
3.1.4 Test series 4	26
3.1.5 Test series 5	27
3.1.6 Test series 6	27
3.1.7 Test series 7	28
3.1.8 Test series 8	28
3.2 Specimen geometry	29

3.3	Preparing of specimens	31
3.4	Testing method	34
4	Results	39
4.1	Test series 1	43
4.2	Test series 2	46
4.3	Test series 3	46
4.4	Test series 4	50
4.5	Test series 5	52
4.6	Test series 6	54
4.7	Test series 7	56
4.8	Test series 8	58
5	Discussion	61
5.1	The glue dowel and its geometry	61
5.2	The influence of plate thickness on connection behaviour	62
5.3	Geometry of the adhesive and the effect on connection stiffness	63
5.4	Geometry of the timber section	64
5.5	The influence of plate design	65
5.6	Gluing method and air bubbles	65
5.7	Design of geometry and calculation method	66
5.8	Greased plates	67
5.9	Testing method	67
5.10	Further research	68
6	Conclusion	71
A	Appendix A - Geometry of test specimen	I
B	Appendix B - Tables of results from hand calculations	VII
C	Appendix C - Results from experimental testing	XIII
D	Appendix D - Load-displacement curves from experimental testing	XIX

List of Figures

2.1	The components of a GIP connection.	6
2.2	The coordinate system of timber. The longitudinal direction follows the direction of the fibers and the tree trunk. Radial direction moves from the center of the tree outwards. Transversal direction is the tangential direction of the annual rings, and is directly perpendicular to the radial direction.	6
2.3	Schematic drawing of the timber specimen. W is the width of the specimen, H is the height, E is the embedment length of the plate and S is the width of the slot	7
2.4	Schematic drawing of the steel plate. w is the width, l is the length and t is the thickness of the plate, d is the diameter of the hole and e is the embedment length of the plate.	9
2.5	Stress distribution in bondline for a single lap joint, according to Volkersen's Model.	10
2.6	Results from Vallée et al. (2011). To the left: Relation between capacity and embedment length in glued-in plates. To the right: Load-displacement curves for bonded joints in red and doweled joints in blue.	12
2.7	Results from Vallée et al., 2011, where the load-displacements curve for bonded and doweled trusses are shown.	13
2.8	Drawing of the specimens tested in Jockwer et al., 2023.	13
2.9	Images from Jockwer et al., 2023. To the left: The test specimen after failure, showing the present failure modes. To the right: The test rig used for static tensile testing at RISE in Borås, Sweden. Observe that the test specimen in the picture is from another test series and not of the correct geometry.	14
2.10	Results from temperature and moisture tests on GIP from Norbäck et al., 2023.	15
2.11	Gluing method used in Norbäck et al., 2023.	15
2.12	The components of a GIR connection.	16
2.13	The two different adhesive insertion methods for GIR, as presented in Steiger et al., 2015.	17

2.14	Pictures from Otero Chans et al., 2013, showing different timber failure modes. To the left: Block failure in spruce glulam specimen. To the right: Shear failure along the rod/Timber-adhesive interface failure in eucalyptus glulam.	17
2.15	Results from Otero Chans et al., 2013, showing the failure load for spruce as a function of anchorage length.	18
2.16	Rod placements in testing made by Xu et al., 2020. Image 1 is a centrally placed rod, image 2 corresponds to eccentrically placed rod and image 3 is inclined rod.	19
2.17	The components and layout of a lap joint. To the left, a single lap joint is displayed. To the right, a double lap joint like the specimen used in Tannert et al. (2010).	19
2.18	Graphs from Tannert et al. (2010). To the left: Plot of failure load as a function of anchorage length, comparing experimental and finite element results. To the right: Plot of failure load as a function of glue line thickness, comparing experimental and finite element results.	20
2.19	The design of the TCC floor by Zeman et al. (2024), showing the glued-in and cast-in steel plate.	20
2.20	Results from pushout tests (Zeman et al., 2024). To the left: Load-displacement graph for TCC floor connected by inclined screws, distanced 150 mm in blue and 250 mm in red. To the right: Load-displacement graph for TCC floor connected with steel plate.	21
3.1	The three types of specimen in relative scale. The smallest version (to the left) is used to test hypothesis 1. The middle version (center) is used in test series 2-5. The largest version (to the right) are used in tests 6-8. Note that these measurements does not apply exactly to all test series. These are merely examples of test specimen. The largest specimen has a sufficiently strong dowel connection at one end, it does not necessarily look like the one in the drawing.	30
3.2	Picture showing the first iteration of centering and spacing for the steel plate. Two pices of 3D-printed plastic clamps with plexiglass slotted were screwed together. The lower clamp and the plexiglass had holes for filling the adhesive.	32
3.3	Left: Picture taken of the filling of adhesive, done with one hole drilled at 45° angle. Right: Picture taken of the filling of the adhesive, done with two holes on each side of embedment length. Both where glued laying horizontal on a flat surface. Black lines are drawn in to show the unevenness.	32
3.4	To the left: Picture showing the gluing process of multiple specimens at once. Clamps were used to keep the specimens together as well as keeping the plexiglass in place. To the right: Picture showing the spacers used to center the steel plates.	33

3.5	Grease test to make sure the glue didnt adhere to the steel plate. The tested types were, from left to right: WD-40, Hilti CMA3KA grease, SKF Bearing grease, Hilti Spray lubricant, Hilti Special lubricant. The flipped pieces of glue were loose.	34
3.6	The load curve according to ISO 6891/EN 26891 (International organization for standardization, 1983).	36
3.7	Picture showing the test rig used for double sided specimen.	37
4.1	An example of an air bubble in a glue dowel.	42
4.2	Mean load capacity as a function of plate thickness in test series 1.	44
4.3	Partial failure in glue dowel for a 1 mm thick plate. The thin plate cuts through the dowel, actual shear failure has not occurred.	44
4.4	Load-displacement for two different failure modes for the same plate thickness. This shows how the failure affects the post-failure behavior.	45
4.5	The dashed line is showing the perceived trend for laser cut plates with increasing thickness.	45
4.6	The load capacity per specimen as a function of the hole area. The dashed line is showing the perceived trend. The largest dowel size fails in timber-glue interface instead of a dowel failure. This is due to the dowel strength is increasing at a higher rate with a larger diameter than the adhesion to the timber for the increased area.	47
4.7	The slip modulus per specimen as a function of the hole area.	48
4.8	Grease has seeped into the dowel and decreased the load carrying area of the dowel (left side of the picture), combined with a big air bubble (right side).	48
4.9	The load capacity per specimen as a function of the plate thickness. The two values under 5 kN are both specimen with air bubbles/grease in the glue dowel. Marked with dashed line is the calculated capacities for shear and tensile capacity respectively.	49
4.10	The slip modulus per specimen as a function of the plate thickness. The two values under 20 kN/mm are both specimen with air bubbles in the glue dowel.	50
4.11	The load capacity per specimen as a function of the glue line thickness, grouped by failure mode. The data points marked have air bubbles present in the dowel, as discussed below.	51
4.12	The slip modulus per specimen as a function of the glue line thickness. The data points marked have air bubbles present in the dowel, as discussed below.	51
4.13	Load-displacement curve for typical specimen in test series 5. It has a very sudden failure in the interface between adhesive and steel, due to loss of adhesion.	53
4.14	The load capacity per specimen as a function of the glue line thickness. The different failure modes are illustrated by different colours.	53
4.15	The slip modulus per specimen as a function of the glue line thickness.	54
4.16	The peak load per specimen as a function of hole spacing.	55
4.17	The slip modulus per specimen as a function of hole spacing.	55

4.18	Opened specimen from series 7. Black is residue on from plates on glue, in red. As visible, a significant portion of the area has this residue.	56
4.19	The load capacity per specimen as a function of the timber net section.	57
4.20	The slip modulus per specimen as a function of the timber net section.	57
4.21	The peak load per specimen as a function of embedment length. The dashed line is showing the perceived trend.	58
4.22	The slip modulus per specimen as a function of the embedment length. The dashed line is showing the perceived trend.	59
A.1	The geometry of the specimen in test series 1	I
A.2	The geometry of the specimen in test series 2	II
A.3	The geometry of the specimen in test series 3	II
A.4	The geometry of the specimen in test series 4	III
A.5	The geometry of the specimen in test series 5	III
A.6	The geometry of the specimen in test series 6	IV
A.7	The geometry of the specimen in test series 7	V
A.8	The geometry of the specimen in test series 8	VI
D.1	Load-displacement curve for test 1-1D	XIX
D.2	Load-displacement curve for test 1-1P	XIX
D.3	Load-displacement curve for test 1-1L	XX
D.4	Load-displacement curve for test 1-2D	XX
D.5	Load-displacement curve for test 1-2P	XX
D.6	Load-displacement curve for test 1-2L	XXI
D.7	Load-displacement curve for test 1-4D	XXI
D.8	Load-displacement curve for test 1-4P	XXI
D.9	Load-displacement curve for test 1-4L	XXII
D.10	Load-displacement curve for test 1-6D	XXII
D.11	Load-displacement curve for test 1-6L	XXII
D.12	Load-displacement curve for test 3-10d and 3-06t	XXIII
D.13	Load-displacement curve for test 3-08t	XXIII
D.14	Load-displacement curve for test 3-10t	XXIII
D.15	Load-displacement curve for test 3-12t	XXIV
D.16	Load-displacement curve for test 3-12d	XXIV
D.17	Load-displacement curve for test 3-16d	XXIV
D.18	Load-displacement curve for test 3-20d	XXV
D.19	Load-displacement curve for test 4-4A	XXV
D.20	Load-displacement curve for test 4-6A	XXV
D.21	Load-displacement curve for test 4-8A	XXVI
D.22	Load-displacement curve for test 5-4A	XXVI
D.23	Load-displacement curve for test 5-6A	XXVI
D.24	Load-displacement curve for test 5-8A	XXVII
D.25	Load-displacement curve for test 6-1S	XXVII
D.26	Load-displacement curve for test 6-2S	XXVII
D.27	Load-displacement curve for test 6-3S	XXVIII
D.28	Load-displacement curve for test 6-4S	XXVIII
D.29	Load-displacement curve for test 7-100H	XXVIII

D.30 Load-displacement curve for test 7-80H	XXIX
D.31 Load-displacement curve for test 7-60H	XXIX
D.32 Load-displacement curve for test 8-50E	XXIX
D.33 Load-displacement curve for test 8-100E	XXX
D.34 Load-displacement curve for test 8-150E	XXX
D.35 Load-displacement curve for test 8-200E	XXX

List of Tables

3.1	The different test variations for test series 1.	25
3.2	The different test variations for test series 2.	25
3.3	The different test variations for test series 3.	26
3.4	The different test variations for test series 4.	27
3.5	The different test variations for test series 5.	27
3.6	The different test variations for test series 6.	28
3.7	The different test variations for test series 7.	28
3.8	The different test variations for test series 8.	29
4.1	Classification of failure modes.	39
4.2	The average maximum load for test series 1. Results with large CoV show air bubble in the dowel for at least one specimen.	43
4.3	The average peak load and slip modulus for test series 3. Results with large CoV show air bubble in the dowel for at least one specimen.	46
4.4	The average peak load for test series 4.	50
4.5	The average peak load and slip modulus for test series 5.	52
4.6	The average peak load and slip modulus for test series 6.	54
4.7	The average load capacity and slip modulus for test series 7.	56
4.8	The average peak load and slip modulus for test series 8.	58
B.1	Results from test series 1	VIII
B.2	Results from test series 2	IX
B.3	Results from test series 3	IX
B.4	Results from test series 4	X
B.5	Results from test series 5	X
B.6	Results from test series 6	XI
B.7	Results from test series 7	XI
B.8	Results from test series 8	XII
C.1	The max load and failure mode for test specimens in test series 1. . .	XIII
C.2	The max load and failure mode for test specimens in test series 3. . .	XIV
C.3	The max load and failure mode for test specimens in test series 4. . .	XV
C.4	The max load and failure mode for test specimens in test series 5. . .	XV
C.5	The max load and failure mode for test specimens in test series 6. . .	XVI
C.6	The max load and failure mode for test specimens in test series 7. . .	XVI
C.7	The max load and failure mode for test specimens in test series 7. . .	XVII

1

Introduction

There is a long tradition of using timber as a building material, dating back to the 13th century in Sweden (Swedish Wood, n.d.-c). Due to its abundance in the Scandinavian nature, timber has been utilized in a wide variety of structures, such as churches, bridges and residences.

Using timber as a construction material has many benefits, where one of the main ones being the lower environmental impact compared to other conventional building materials like steel and concrete (Swedish Wood, n.d.-c). It is high-achieving in fire safety and strength-to-weight ratio, while being the only of the three materials that is renewable and that stores bound CO₂ during the lifetime of the material.

During the last decades, there has been a significant technological development and following increase in timber construction with a larger range of utility (Swedish Wood, n.d.-c). For example, the development of engineered wood products (EWP) has contributed to the possibility of more high performance applications. Modular and prefabricated elements has decreased building time and made timber compete with concrete and steel constructions in larger projects. This new development within timber construction has lead to a need of connections with higher capacities.

1.1 Background

The connections in timber structures are a crucial part since these generally are the weakest link (Swedish Wood, 2017). Connections are used to transfer loads and forces between building elements and are therefore critical to the overall load capacity. By improving the performance of connections, there is a possibility to minimize both material in the connection but also possibly allow overall dimension changes.

There is an increased interest in using timber as the main building material, which is a part of the global shift to renewable materials and the strive for circular economy and sustainable construction. With more complex structures being built in timber, a need for more advanced timber connections has evolved. These advanced connections need in-depth analysis containing both numerical analysis and experimental

testing to properly predict non-linearities and other weaknesses introduced due to its complexities.

Glued connections first emerged within the aircraft industry, and has since the 1950's been used within the construction sector (Tannert et al., 2010). In order to broaden the use of bonded connections in timber construction, there is a need to develop design parameters and criteria that can be implemented in Eurocode and national standards. A tried glue connection within construction is bonding threaded steel rods into timber, so called glued-in rods (GIR). GIR has been developed since the 1980's, with the GIROD project most notably in the 1990's (Tlustochowicz et al., 2011). GIROD strived to create design requirements for GIR connections with the intention to include it into the next generation Eurocode.

The GIR connection have plenty of similarities to to the less researched connection called glued-in plate (GIP). Instead of bonding a rod, a steel plate is glued into a slot in the timber. The idea is that a plate will have better shear and moment resistance than a rod, creating a stiffer connection. GIR findings are interesting in the context of GIP as the connections consist of the same three material components and the basic mechanical behaviour is believed to be similar.

Hilti is a company that develops, manufactures and markets products for the construction industry, where connection solutions – both mechanical and chemical - is one of their main core business and research topic. Currently Hilti is actively doing research and development on new connection solutions for mass timber structures with the target of bringing innovation on structural performance and efficiency. Their interest in glued-in plates is lead by their wish of contributing with their expertise on chemical anchors in the mass timber field.

1.2 Aim and objective

The intent of this study is to evaluate the mechanical behaviour of glued-in plates as a timber connection, testing the performance under tensile load. The focus will be on evaluating the effects on the load bearing capacity based on the geometrical aspects of the connection. The end goal would be to find any relation that could help predict behaviour of the connection and possibly aid in creating a mathematical model that can be used for dimensioning, designing and optimizing glued-in plate connections.

The study will be conducted with the following objectives:

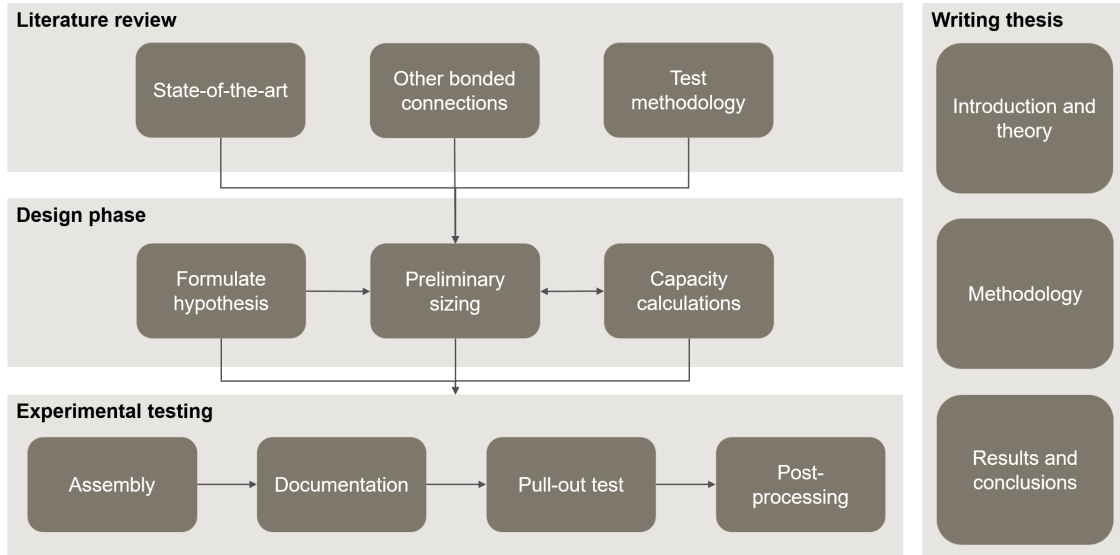
1. Research the state-of-the-art and identify possible knowledge gaps or discrepancies between studies.
2. Identify geometrical parameters and analyze how they contribute to strength, stiffness and/or ductility.

3. Design and perform experimental tests to evaluate the mechanical behaviour of glued-in plate connections under tensile load.
4. Analyze load-displacement curves and failure modes, put data into context and draw conclusions regarding of the effect of geometry on the connection strength, stiffness, ductility and failure mode.

1.3 Methodology

The masters project is divided into four phases:

1. Review the current status of research and knowledge.
2. Formulating hypotheses based on the information from phase one and designing tests for the upcoming phases.
3. Experimental testing is the third phase. This consists of assembling test specimen, performing tensile testing and documenting the process.
4. Thesis writing spans the entire project. The ongoing task is to document the progress, the findings and insights gained through the work.



1.4 Thesis questions

The following main questions have been formulated to be able to get a holistic view of the study of the glued-in plate connection.

- What geometrical parameters affects the connection strength, stiffness or ductility and in what way?

- Which (brittle) failure modes are present and how does failure mode affect the deloading/load redistribution after failure?

1.5 Limitations

Timber and its strength properties are highly dependent on climate parameters such as temperature and moisture. These parameters will be recorded during testing to ensure consistency, the effect of these parameters will however not be considered in this study. Furthermore, these parameters have already been investigated in the publication Norbäck et al., 2023, along with the effects of adhesive curing time on connection strength.

This study is designed to explore specifically the behaviour of adhesive and timber. Because of that, the steel plate will be overdimensioned as to not fail first. This is not a realistic way of designing connections, as it is preferred to create a ductile failure mode, i.e. force a failure in the steel. The results of this study may be applicable on the mechanical behaviour of adhesive and timber in a glued-in plate connection, but not the connection as a whole entity. This is because the steel plates in this study is overdimensioned on purpose, in order to analyze the behaviour of the weaker and brittle materials in the connection.

Comparing different materials is outside the scope of this study. All material remains constant throughout the study, with the exception for using two different types of timber, due to long delivery times. Within each test series the type of timber material will remain the same. Comparisons and conclusions will be drawn within each test series, and therefore changing timber between different test series will not affect the results.

During the testing, only one type of adhesive will be used and the curing time will be constant for all specimen. Therefore, the results from this testing are not applicable to all types of adhesive. There are a multitude of adhesive products on the market, with a large range of capacity and stiffness that will contribute to the joint displaying a different behaviour.

All plates will be of the same grade of steel for all tests. Steel is a well researched material, and investigating the effect of different steel grades is not within the scope of this study. Furthermore, all materials used in the testing is assumed the strength class as ordered from supplier. The material is not tested for its specific strength or stiffness parameters.

2

Previous research on bonded connections

A connection is the joining element between different parts of a structure. In general, they constitute the weakest points in the construction and is hence governing for the load bearing capacity of the entire structure (Swedish Wood, 2017).

2.1 Main components of a glued-in plate connection

The glued-in plate connection consists of three main components: timber, adhesive and steel (as pictured in Figure 2.1). They each contribute to different behaviour in the connection. When designing the connection it is important to make the steel component the weak link, because of its ductile failure. Both adhesive and timber have comparatively brittle failures which results in immediate strength loss (Swedish Wood, 2017; Yurrita & Cabrero, 2021; Zeman et al., 2024). By designing in this way, the connection have extra capacity after reaching maximum design load in case of failure.

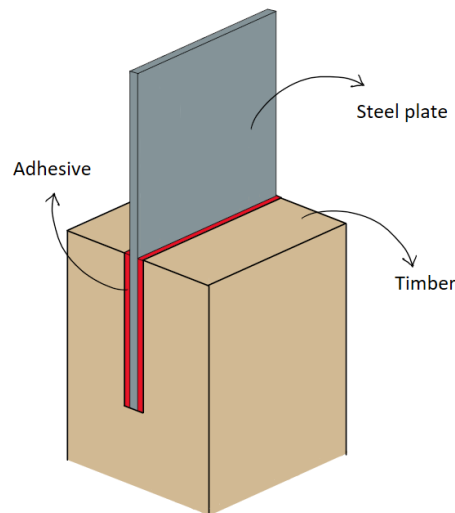


Figure 2.1: The components of a GIP connection.

2.1.1 Timber

Timber is an anisotropic, fibrous material of natural origin. Unlike for isotropic materials, orientation of the material is very important to account for the fiber structure. Hence, there is a special coordinate system used to describe the location and the forces within the material. Commonly, the different directions are referred to as longitudinal, radial and tangential, see Figure 2.2.

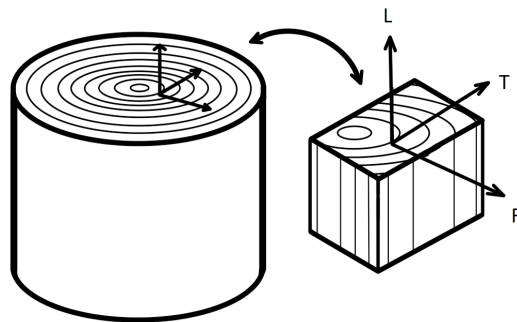


Figure 2.2: The coordinate system of timber. The longitudinal direction follows the direction of the fibers and the tree trunk. Radial direction moves from the center of the tree outwards. Transversal direction is the tangential direction of the annual rings, and is directly perpendicular to the radial direction.

The material also has imperfections as a result of its origin in nature. Knots are interruptions in the fibers caused by the branches of the timber that result in decreased material strength. Knots are only one of the many types of imperfections that occur in timber. More include the effects of rot, fungi, cracks, inconsistent grain direction, scarring and resin/pitchwood.

Glulam is short for glued laminated timber and is one type of EWP. As the name suggest, it consists of glued together lamellae of 45 mm thickness, where the fibers in the lamellae spans in the length direction of the piece. Laminating the material provides different perks compared to regular construction timber (Swedish Wood, n.d.-a). Firstly, any imperfections in the material is less governing in the strength of the piece than in a corresponding structural timber specimen. Glulam also makes it possible to overcome the size limitations of structural timber, making it possible to create larger and more high performance structures.

Laminated Veneer Lumber (LVL) is another type of EWP that consists of multiple layers of thin wood veneers (approx. 3 mm thick lamellae), that is glued and pressed together (Swedish Wood, 2022). The thin lamellae contribute to a very homogenous material compared to structural timber. The layers can be arranged with all fiber directions in the same direction, or with varying direction to decrease strength differences between the material directions. One of the benefits of LVL is that the strength capacity in tension, compression, shear and bending are high compared to other timber products.

The main differences between glulam and LVL is the thickness of the lamellae, the possible difference in fiber orientation and that while glulam is created for beams and columns etc. LVL can be used for both beams and to create panel boards for floors, walls etc. Since the LVL is created by slim sheets, the imperfections in timber can be reduced more efficiently than in glulam.

Formulas for timber

To be able to predict the failure modes and design specimens for the glued-in plates connection, hand calculations are performed. The capacities of interest for timber are tension in the cross section and shear along the plate.

The geometry used in the following calculation is defined according to Figure 2.3.

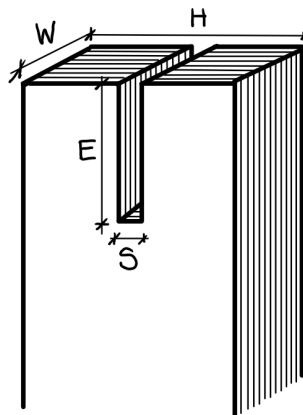


Figure 2.3: Schematic drawing of the timber specimen. W is the width of the specimen, H is the height, E is the embedment length of the plate and S is the width of the slot

Formula used for shear force in timber:

$$V_{timber} = f_{v.timber} \cdot A_{v.timber} \quad (2.1)$$

where V_{timber} [N] is the shear force in timber $f_{v.timber}$ [MPa] is the shear capacity in LVL and $A_{v.timber}$ [mm²] is $E \cdot W$ shown in Figure 2.3, which is the area subjected to shear.

Formula used for tension in timber:

$$N_{t.timber} = f_{t.timber} \cdot A_{t.timber} \quad (2.2)$$

where $N_{t.timber}$ [N] is the tension force in timber, $f_{t.timber}$ [MPa] is the tension capacity in timber and $A_{t.timber}$ [mm²] is $W \cdot (H - S)$, which is the area subjected to tension in accordance with Figure 2.3.

2.1.2 Steel

Steel is a alloy between iron and carbon, containing up to 2% of carbon by weight for structural appliances (Åstedt, 2009). Some of the most prominent features of steel, is that it is a strong and ductile material. Steel is a material that is both homogeneous and isotropic, which means it has the same properties in all directions (Al-Emrani, 2023). Steel has high capacities in all static load cases, but performs the absolute best under tensile load. It is classified depending on the yield stress, where a higher class corresponds to a higher ultimate strength.

Incorporating steel elements will also give a more predictable behaviour in connections. This is due to the possibility of ductile failure modes in steel, which is more favorable than brittle ones (Swedish Wood, 2017; Yurrita & Cabrero, 2021; Zeman et al., 2024).

Formulas for steel

To be able to predict the failure modes and design specimens for the glued-in plates connection, hand calculations are performed. The capacity of interest for steel is axial tension. Furthermore, the elongation of the steel plate is checked to ensure it does not interfere with the measuring method.

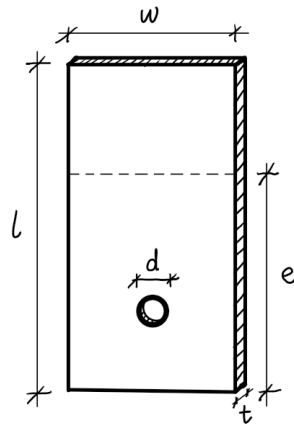


Figure 2.4: Schematic drawing of the steel plate. w is the width, l is the length and t is the thickness of the plate, d is the diameter of the hole and e is the embedment length of the plate.

Formula used for tension in steel:

$$N_{t.steel} = f_y \cdot A \quad (2.3)$$

where $N_{t.steel}$ [N] is the tension force in steel, f_y [MPa] is the yield capacity in steel and A [mm²] is $t \cdot (w - d)$, which is the area subjected to tension in Figure 2.4.

Formula used for elongation in steel:

$$\Delta L_{steel} = \frac{F \cdot l}{E \cdot A} \quad (2.4)$$

where ΔL_{steel} [mm²] is the elongation in steel F [N] is the applied force, l [mm²] is the length of the steel plate, E [MPa] is the modulus of elasticity for steel and A [mm²] is equal to $t \cdot (w - d)$ in Figure 2.4, the area of the steel plate edgewise.

2.1.3 Adhesive

There are many varying types of adhesives used in timber connections, where one of the most widely used is epoxy glue (EPX) with two components (Tlustochowicz et al., 2011). This is the type of adhesive used in this study. Tlustochowicz et al. also states that the adhesive tends to bond well with the adjacent materials, and thus making the timber the weakest part of the connection.

In many countries, the most common alternative to EPX is polyurethane (PUR) based adhesives (Tlustochowicz et al., 2011). The biggest difference between the adhesives is the ductility, as the epoxy products are often very stiff and brittle while PUR adhesives are generally flexible (Science Direct, n.d.-a, n.d.-b). This

can however vary significantly with different products, additions and ratios. Both products present good adhesion to a range of materials.

Glued joints have many benefits, especially for materials with brittle, fibrous and anisotropic materials, such as timber (Tannert et al., 2010). Firstly, it has a good weight to strength ratio. Secondly, adhesive does not necessitate any interruption of fibers and allows for a higher load-bearing capacity in comparison to mechanical anchoring methods. Furthermore, the glue does not need to be protected from environmental loads such as moisture, compared to steel connections.

The stress distribution in the bondline was first described by Volkersen's Theory in 1938 (Dillard, 2002; Science Direct, n.d.-d). The bondline is defined as where the adhesive meets the another material. Volkersen's model for stress distribution states that there are stress peaks at the end of the joint which will lead to a lower strength capacity at this point.

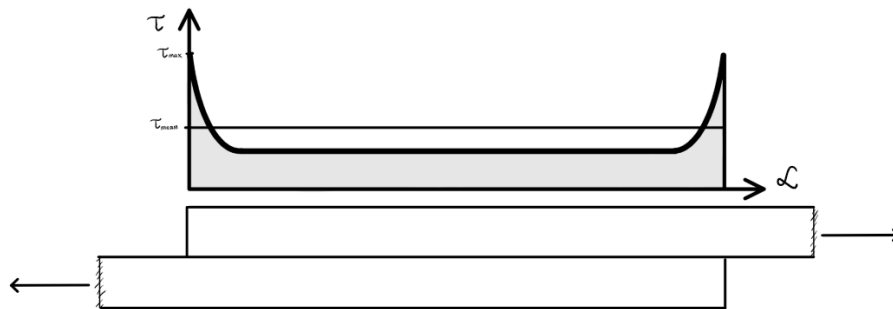


Figure 2.5: Stress distribution in bondline for a single lap joint, according to Volkersen's Model.

Multiple research projects have aimed to further develop Volkersen's theory. Ebnesajjad and Landrock (2015) describes that Volkersen's model is applicable to stiff adhesives and that the overlap length of the joint is nearly independent of the shear stress distribution in the ends. Meanwhile, the width of the joint have a proportional effect on the strength of the connection. The maximum stress in the adhesive can be lowered by increasing the thickness of the bondline, due to the shear stresses being more uniformly spread in the adhesive.

Formulas for adhesive

To be able to predict the failure modes and design specimens for the glued-in plates connection, hand calculations are performed. The capacities of interest for the testing that are going to be conducted in this project are shear in adhesives well as the adhesion to the steel.

Formula used for shear in glue dowel:

$$V_{dowel} = f_{v.a} \cdot A_{dowel} \quad (2.5)$$

where V_{dowel} [N] is the shear force in the glue dowel, $f_{v.a}$ [MPa] is the shear capacity in the adhesive and A_{dowel} [mm²] is the area of the dowel.

Formula used for adhesion between steel and adhesive:

$$V_a = f_a \cdot A_{plate} \quad (2.6)$$

where $V_{Adhesion}$ [N] is the adhesive shear force, f_a is the adhesion capacity of the adhesive, and A_{plate} is the area of the plate subtracted with the area of the perforation.

2.2 Previous testing on glued-in plates

There are certain benefits found from the limited research on glued-in plates. The connection has been proven to have a high load carrying capacity compared to a dowel connection (Vallée et al., 2011). It also acts as shear reinforcement at the end of beams, which is the place of critical shear in simply supported beams. Furthermore, they are likely more fire resistant as all steel components are embedded in timber and adhesive compared to traditional connections. Lastly, there is an aesthetical aspect of invisible connections. This section presents what tests that have previously been done on glued-in plates, as well as other similar bonded connections.

In 2011, Vallée et al. presented an article where different embedment lengths of smooth (non-perforated) glued-in plates in structural timber were tested. Embedment lengths varied from 40 mm to 160 mm with increments of 40 mm. The study shows that increased embedment length of the plate increased the capacity, from 40 mm up to 120 mm. After this, there was not an increase seen on the capacity, see Figure 2.6. This aligns with the previously mentioned Volkersen theory, where increased embedment length will only increase capacity up to the point where the stress peaks are governing. The authors compared the connection to a similar sized doweled connection, the results can be found in Figure 2.6.

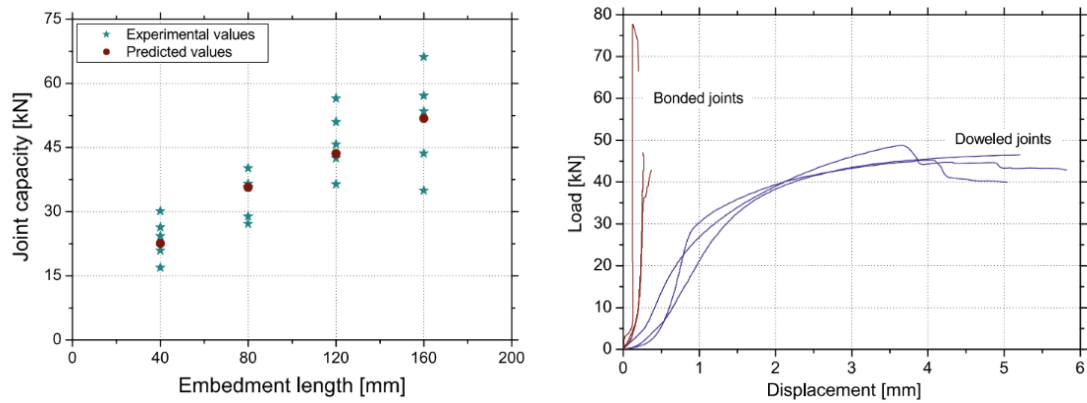


Figure 2.6: Results from Vallée et al. (2011). To the left: Relation between capacity and embedment length in glued-in plates. To the right: Load-displacement curves for bonded joints in red and doweled joints in blue.

They also performed a full scale testing on bonded and doweled trusses. The results from this test showed that the bonded truss had a perfectly linear load-displacement curve up until failure and three times the stiffness of the doweled truss, the results are displayed in Figure 2.7. With this increased stiffness, the displacement of the bonded truss was lower, as well as a 40% increase in strength capacity. The most common failure mode for the glued-in plates was local shear failure close to the bondline in the timber.

The authors note that doweled joints have large deformations compared to GIP as the initial slip is needed for the dowels to achieve full contact and to start carrying load. This is not relevant for the glued plate connection. This behaviour is one of the reasons for the lower stiffness seen for the dowel connection in Figure 2.7. The significantly lower stiffness in combination with displacement controlled loading is not to be confused with ductility. In a load controlled application as in reality, the dowels would have a brittle failure.

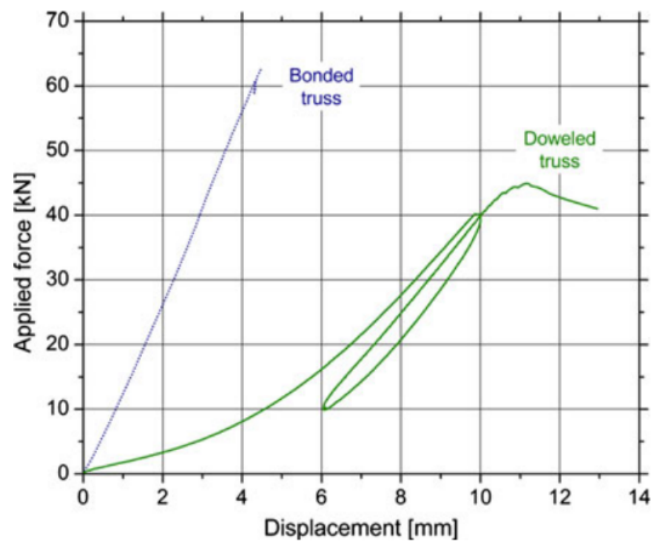


Figure 2.7: Results from Vallée et al., 2011, where the load-displacements curve for bonded and doweled trusses are shown.

Jockwer et al. (2023) tested glued-in plates with perforated steel plates. When gluing a plate with perforation, the glue will seep through the holes and connect the steel plate and adhesive further. The authors refer to these as glue dowels, as they act in a similar manner to a steel dowel in a doweled connection. Results from that study show that the dowels contribute significantly to the strength and stiffness of the connection. The testing was done on LVL specimens, with the plate glued edgewise to be able to utilize the higher shear capacity (See Figure 2.8).



Figure 2.8: Drawing of the specimens tested in Jockwer et al., 2023.

From the pictures published in the thesis (Figure 2.9), the assumption is made that the original plate is designed with 6 holes, this is however not confirmed. Three different types of plates were tested: without perforation, the original with 6 holes and double perforation, meaning 12 holes. The tests were designed so that the steel plate capacity would not be the governing factor of the connection. The test specimens were tested on a static load of 50 kN.

Two different manufacturing methods of the perforation were tested, laser cut and drilled holes, with the same amount of perforation. The results from this shows that

2. Previous research on bonded connections

there is little difference, 100% of mean max load for the laser cut compared to 101% of mean max load for the drilled holes.

The authors present the results as percentage of mean maximum load relative to the original plate. The tests done on double perforation have a higher capacity, 193% of mean max load, while tests done with plates without perforations have a significantly lower capacity, 87% of mean max load. These results concludes that the glue dowels have a significant impact on the capacity of the connection. This proves that the glue dowel provide a better shear capacity per area unit than the adhesion between glue and steel. For perforated plates, the failure occurred 100% in the glue dowel, with some partial failures in the bonded interface to steel or LVL. Some examples of failures can be observed in Figure 2.9, along with the test setup.

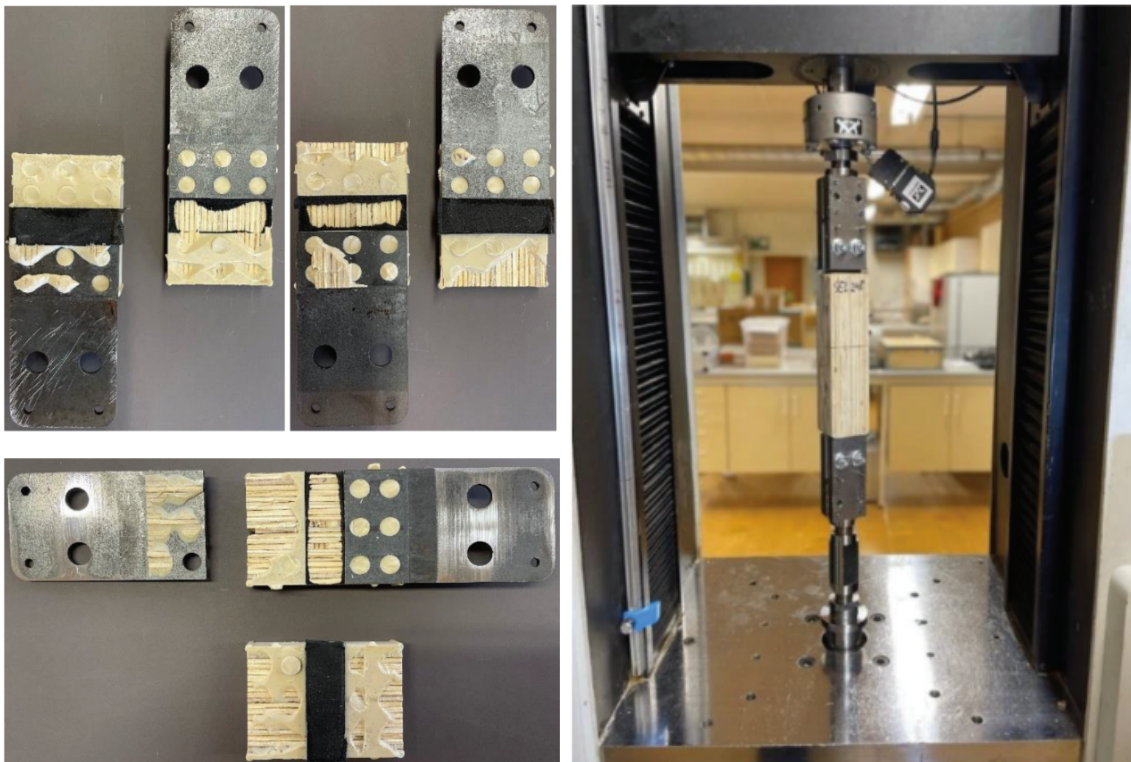


Figure 2.9: Images from Jockwer et al., 2023. To the left: The test specimen after failure, showing the present failure modes. To the right: The test rig used for static tensile testing at RISE in Borås, Sweden. Observe that the test specimen in the picture is from another test series and not of the correct geometry.

Norbäck et al. (2023) performed a study on the effect of moisture and curing time on glued-in perforated steel plates. The tests were performed on specimen cured in temperatures between 9.1-27°C and relative humidity of 25-95%. Majority of the specimens had reached full strength after one day of curing, except for specimen cured in temperatures under 12°C. It is also stated that humid conditions up to 95% RH did not affect the strength development of the joint but that it affected the final strength. The results can be seen in Figure 2.10

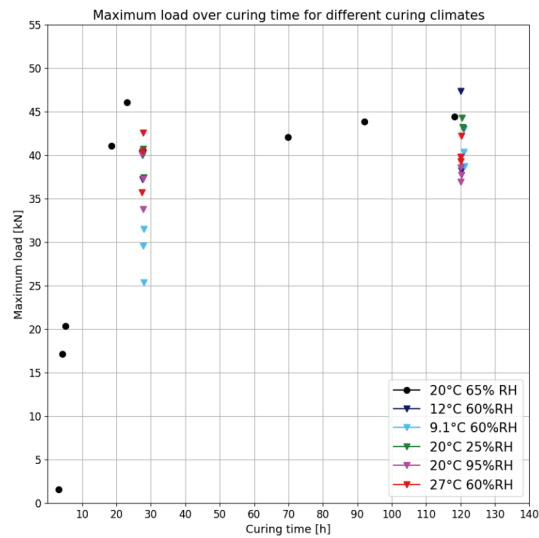


Figure 2.10: Results from temperature and moisture tests on GIP from Norbäck et al., 2023.

Norbäck et al., 2023 (2023) provides significant information regarding the method of assembly and gluing. The method consists of 3D-printed holders with guides for the steel plate, see Figure 2.11.

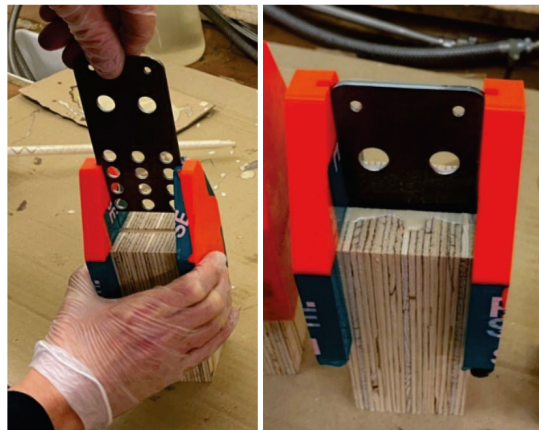


Figure 2.11: Gluing method used in Norbäck et al., 2023.

2.3 Glued-in rods and possible take aways

Tlustochowicz et al. made a state-of-the-art review in 2011 about the glued-in rods connection. An example of the connection and its main components/materials can be seen in Figure 2.12. It was stated that the geometry of the components in the connection made an impact on the capacity. Adhesive thickness is mainly influencing

the shear stress distribution, where a thicker layer can increase the distribution of stresses and lower the maximum peak shear stresses.

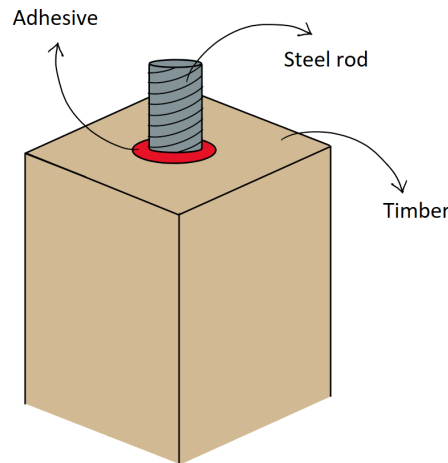


Figure 2.12: The components of a GIR connection.

An increased embedment length resulted in increased ultimate capacity for the connection, but decreased shear capacity. This can be described by Volkersen's model about shear stress distribution in the bondline, see Figure 2.5. Tlustochowicz et al. describes that the diameter of the rod can have an impact on the capacity, although a relationship has not been found. Edge distance of the glued-in rods connection should not be lower than 2.5 times the diameter of the rod, in order to not have timber splitting. For connections with multiple GIRs, group effects and shear block failures must be considered by using minimum distances between rods, as uneven stress distribution or interference between rods might lead to premature failure (Swedish Standards Institute, 2021; Tlustochowicz et al., 2011).

GIR are excellent for increasing the capacity in tension and shear for timber structures (Steiger et al., 2015). The glued-in rod acts similarly to the reinforcement bars in concrete, and prevents early cracking and crack propagation in timber. The increased capacities in shear from the GIR, will also lead to the structure having larger capacities in bending. Steiger et al. states that one of the main advantages of the connection, is how the load transfers into the center of the timber element. Traditional connections rely on shear transfer on the surface of the timber, which limits the area of effective timber and introduces moment from the distance between force and the neutral plane.

The study also by Steiger et al. (2015) includes methods of manufacturing the connection. One method is to first place the rod and then insert the adhesive. The adhesive can either be filled from the same hole the rod is inserted into or from another drilled hole at the bottom of the embedment length. By inserting glue at a drilled hole at bottom the embedment length, the risk of getting air bubbles decreases as the glue pushes out this during filling. With inserting into the same hole

as the rod, the risk is to introduce pockets of air that get trapped underneath the adhesive if the filling is not done correctly.

Another simple method is to begin filling the cavity and then push the rod into place (Steiger et al., 2015). Issues with this method are that the presence of air gaps, uneven filling or that the rod is centered in the glue are all difficult to assess. If the adhesive instead is filled from a second hole near the bottom, air gaps and even filling is assured. However, during this procedure the rod has to be fixed into place with a secondary setup in order to be centered during curing.

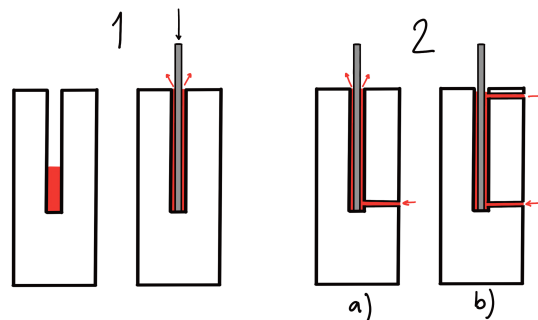


Figure 2.13: The two different adhesive insertion methods for GIR, as presented in Steiger et al., 2015.

Another study of rod embedment length between 60 - 180 mm was conducted by Otero Chans et al. in 2013, where they compared specimens in spruce and eucalyptus. The timber specimens had a size of 160 x 160 mm and the threaded steel rod a diameter of 12 mm. The sizing of the timber is larger than necessary in order to not have timber splitting as the failure mode. Instead both species failed in shear in the tests, see Figure 2.14.

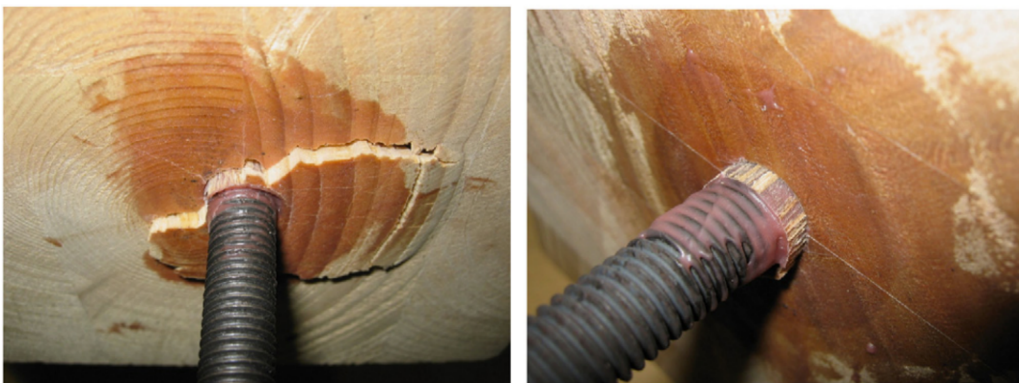


Figure 2.14: Pictures from Otero Chans et al., 2013, showing different timber failure modes. To the left: Block failure in spruce glulam specimen. To the right: Shear failure along the rod/Timber-adhesive interface failure in eucalyptus glulam.

In spruce, they recorded a shear block failure, where as in the eucalyptus there was a shear failure in the fibers immediate to the bondline. They note that eucalyptus have a higher density than spruce, and that they saw a pattern of less failure in timber for high density species and vice versa. Further testing from Otero Chans et al. concluded that there is no linear relationship between the embedment length and capacity of the connection which aligns with previously mentioned sources. If the slenderness value of the connection is increased, the capacity can even decrease with a larger embedment length. This falls in line with the requirement of minimum edge distances according to Tlustochowicz et al. (2011). Otero Chans et al. also notes that finite element analysis showed that a higher modulus of elasticity in timber results in higher stress peaks in the interface between the adhesive and timber.

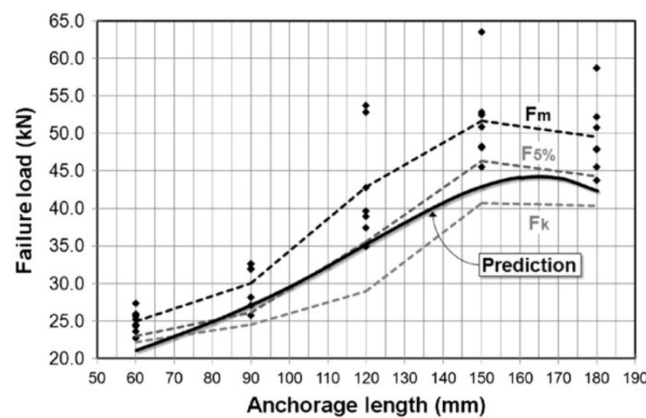


Figure 2.15: Results from Otero Chans et al., 2013, showing the failure load for spruce as a function of anchorage length.

The glue line thickness has an influence on the pull-out strength of the GIR connection, which is also depending on the diameter of the rod and which type of adhesive is used (Xu et al., 2020). It is stated that with an increased glue line thickness for brittle epoxy, the pull-out strength increases up to a limit, and then decreases for a thickness of 5 mm for rods of 10 and 12 mm. Although, for a rod with 14 mm the pull-out strength was highest for 5 mm. This suggest that there is a proportionality factor between the glue line thickness and the diameter of the rod. A too thick glue line could lead to creep, as well as most adhesives perform better with a thinner glue line (Steiger et al., 2015; Tlustochowicz et al., 2011).

Xu et al. conducted experimental testing to further investigate the manufacturing defects on GIR. Three different rod placements were investigated: centric placement, eccentric placement and with inclination (see Figure 2.16). The influence of these defects were also for three different glue line thicknesses. The testing was done on 450 mm long timber specimens and threaded rods with 10 mm diameter, with single sided pull-out testing with a rate of 2 mm/min. The most common failure mode was substrate (timber) failure for all glue line thicknesses and rod placements. Xu

et al. concludes from the testing that increasing the glue line thickness for centric and eccentric placed rods increases the the capacity, but not for an inclined rod.

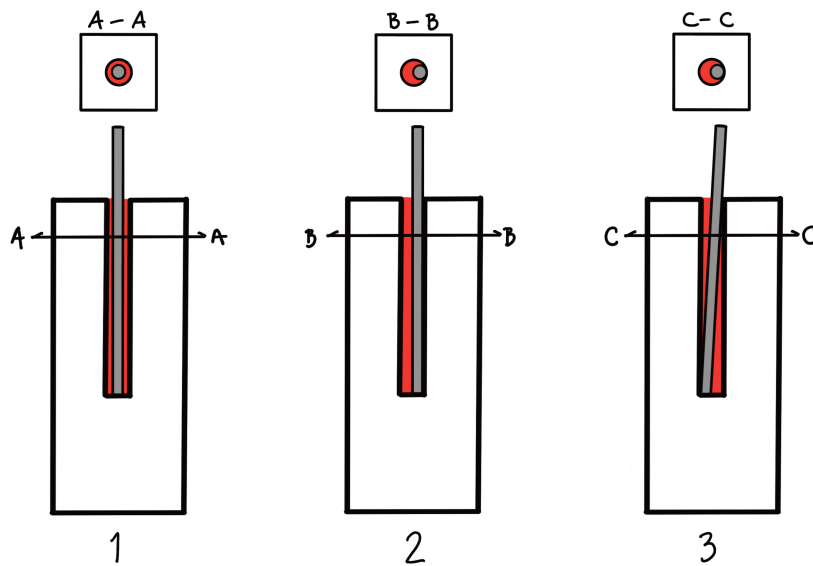


Figure 2.16: Rod placements in testing made by Xu et al., 2020. Image 1 is a centrically placed rod, image 2 corresponds to eccentrically placed rod and image 3 is inclined rod.

2.4 Other bonded connections and possible take aways

A study on bonded double lap joints (example in Figure 2.17) indicates that the thickness of the adhesive does not influence the capacity of the joint, in the studied range of 0.5 - 1.5 mm (Tannert et al., 2010).

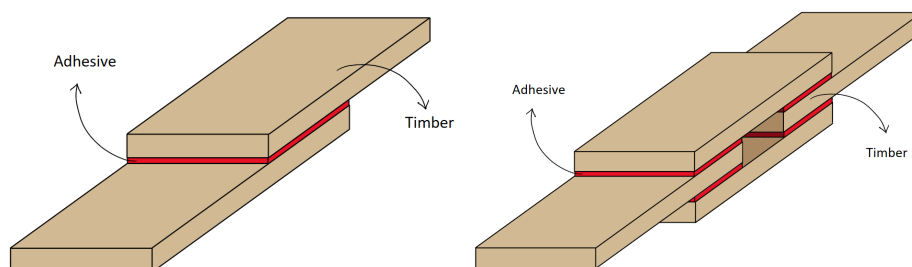


Figure 2.17: The components and layout of a lap joint. To the left, a single lap joint is displayed. To the right, a double lap joint like the specimen used in Tannert et al. (2010).

2. Previous research on bonded connections

Tests on influence of the overlap length on capacity show that there is an upper limit for when increased overlap give increased capacity (Tannert et al., 2010). Their tests ranged between 40-280 mm overlap, where after 160 mm overlap the increase in capacity was negligible. Failure mode for all specimen were brittle timber failure in the inner lamella, independent of the adhesive and adhesive thickness.

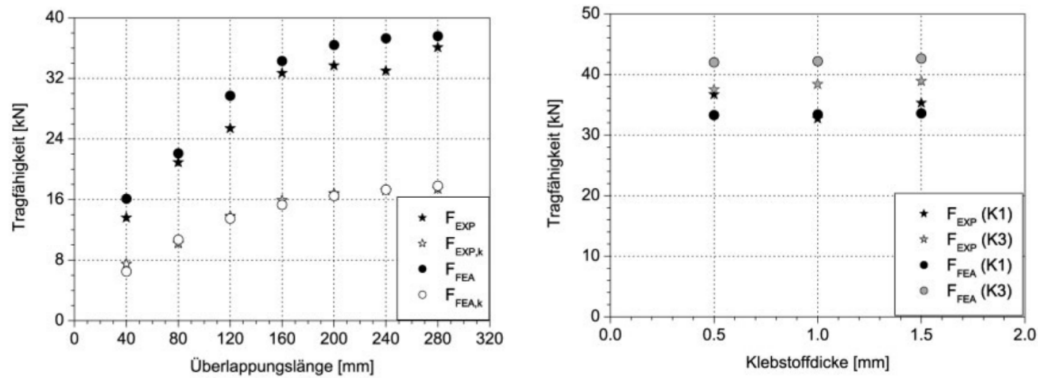


Figure 2.18: Graphs from Tannert et al. (2010). To the left: Plot of failure load as a function of anchorage length, comparing experimental and finite element results. To the right: Plot of failure load as a function of glue line thickness, comparing experimental and finite element results.

Zeman et al. (2024) compared glued steel plates to inclined screws as shear connectors in a Timber Concrete Composite (TCC) floor solution. The tests was conducted with four point bending and push-out tests. Results for the push-out tests shows that the glued-in steel plate connection had a higher load bearing capacity while the screwed connection showed a higher stiffness and ductility which can be observed in Figure 2.20.

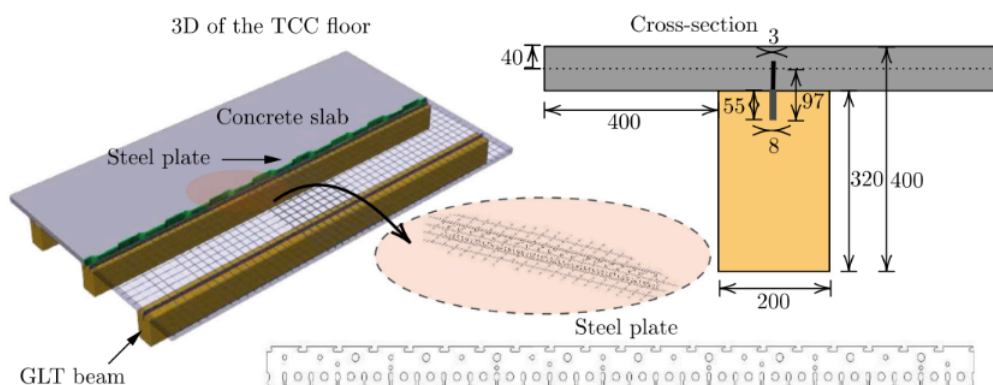


Figure 2.19: The design of the TCC floor by Zeman et al. (2024), showing the glued-in and cast-in steel plate.

Bending tests showed that the weak point in the TCC was not the connection but rather the timber beam, which shows a brittle failure with origins in areas of high

shear and moment. The authors explain that the connection display overstrength compared to the bending capacity of the cross-laminated timber (CLT) beam. When observing the different connection types, it is evident in the bending tests that the screwed connection is very brittle, despite the results of the push-out tests. In the system, the plate connection shows a somewhat brittle behaviour but acts with more ductility than screws. This is attributed to the lower stiffness which distributes the forces between slab and beam in a more efficient way. In summary, the plate connection is less stiff and ductile but contributes to a more ductile response on a system level than inclined screws.

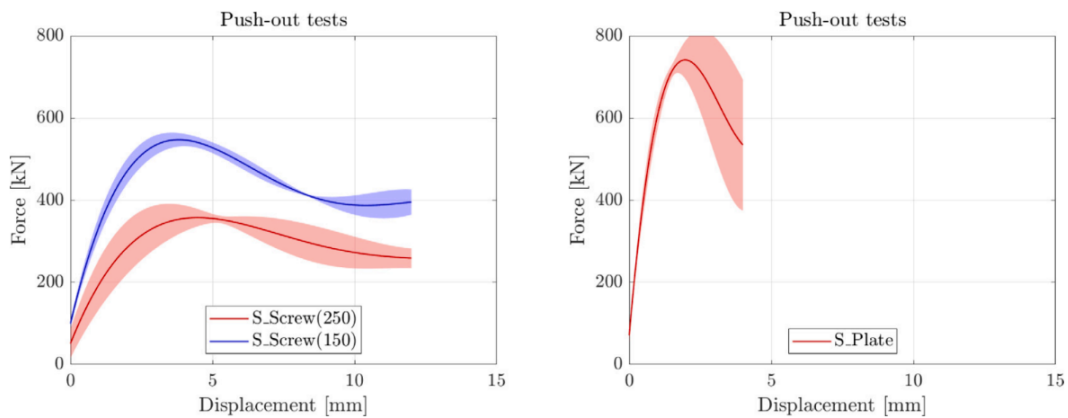


Figure 2.20: Results from pushout tests (Zeman et al., 2024). To the left: Load-displacement graph for TCC floor connected by inclined screws, distanced 150 mm in blue and 250 mm in red. To the right: Load-displacement graph for TCC floor connected with steel plate.

2.5 Method of literature review

The literature study had the main aim to review the current state of the art and present knowledge gaps.

The outcome of the literary analysis were the base for the two other phases. Previous knowledge and knowledge gaps were guiding in which types of testing will be performed. Since the connection is relatively unstudied, this part of the analysis established what parts already had been studied and what knowledge can be extrapolated from studies of similar connections. Furthermore, it has to form a direction of how the test set-up should be designed.

Searching for literature was mainly done online using databases like ScienceDirect, Scopus, Research Gate etc. to find relevant articles on the subject. As this is a rather new subject, the applicable sources were newly published. For basic knowledge such as material behaviour and manufacturing processes, course literature from

relevant courses was used together with sources from industry. Keywords for searching literature include: glued-in plates; glued-in rods; adhesive; bonded connections; etc.

The organization Swedish Wood are representatives of the Swedish sawmill industry and is a part of the Swedish Forest Industries Federation. The latter includes manufacturers of construction material, paper, pulp, bio energy etc. (Swedish Wood, n.d.-b). Furthermore, they represent Swedish glulam, CLT and packaging industries. Their goal is to spread knowledge about timber and how to use it in construction in order to promote sustainability. They aim to increase the value of the market for Swedish timber products and do so by continually educating and researching.

Publications from Swedish Wood include Design of timber structures (Volumes 1-3) from 2022, that are used repeatedly in this study, as well as as many more. They also have a large database of articles surrounding timber construction in both small and large scale, from which there is several citations. The publications are used both in education at advanced levels in Swedish universities and by industry.

2.6 Summary

Glued-in plates are a novel type of connection but from initial research it has been known that it provides high strength and stiffness compared to other similar sized connections. Glue dowels contribute significantly to increasing GIP capacity compared to flat plates. The tension capacity of GIP with non-perforated plates is proportional to the embedment length up to a certain length beyond which further embedment becomes negligible.

Glued-in rods connections share many similarities with glued-in plates, which means some design requirements and failure modes can likely be applied to GIP. For example, edge distance from GIR might be relevant to prevent splitting failure modes in GIP. Similar to what is proven for GIP, embedment length only matter up to a limited length in GIR due to stress peaks in adhesive. Thicker adhesive layers distribute these stresses more evenly.

The behaviour of steel is well studied and the goal is to make the GIP connection fail in a ductile way using the properties of steel. The behaviour of timber and adhesive are both more brittle in their respective failures than steel. These types of failures needs to be avoided in a structural connection, which can be done if the parameters affecting the components' strength are known.

3

Experimental Testing

The testing was performed in collaboration with Hilti, at the in-house test laboratory in their headquarters in Schaan, Liechtenstein. The testing consisted of static pullout tests, with load, displacement and failure mode recorded for all specimen.

3.1 Description of test series

The tests have been designed in order to evaluate the impact of geometry on the strength and stiffness of a connection with a single glued-in plate. Focus has been put on investigating the properties of the glue dowel further, as well as investigate other geometrical aspects that are proved to affect similar connections. Testing will be conducted on a greased plate in some test series to be able to investigate the capacity of only the glue dowel and not the adhesion to the steel plate.

The test series are a direct product of the literature review, where areas of interest, knowledge gaps and inconclusive results have been boiled down to geometry. Eight questions based of geometrical parameters that is believed to affect the glued-in plates connection are stated below.

1. Does hole manufacturing method have an influence on the capacity of the glue dowel?
2. How does the steel to hole area ratio affect shear capacity in the connection?
3. How is the dowel capacity influenced by the shear area and dowel length?
4. Does a thicker adhesive layer contribute to a larger distribution of stresses to the timber?
5. How will the thickness of the glue line influence the deformation behaviour of the connection?
6. How does the spacing of the perforation affect the strength of the connection?

7. How does timber size impact the failure mode, strength and stiffness of the connection?
8. Is the shear capacity of a flat plate directly proportional to its embedment length?

Each parameter stated was translated into a series of test, where one factor was varied and the others kept constant to be able to determine the influence of that singular factor. Moisture content of the timber specimens and adhesive curing time was aimed to be constant. The values were recorded, but the influence is not evaluated. Each type of test variant were tested on three instances to ensure a more rigid result.

3.1.1 Test series 1

This test series aims to answer the first question - does hole manufacturing method have an influence on the capacity of the glue dowel? It was tested on three different hole manufacturing techniques: drilling, punching and laser cut on four different plate thicknesses. The hypothesis is that the imperfections or lack thereof created while manufacturing the perforation will influence the capacity of the glue dowels which will affect the capacity of the joint.

The manufacturing methods result in different surface and edge textures. Laser cutting is very precise and creates very homogeneous surface with minimal flaws. Punching the holes will bend the edges and create more pointed edges, as they are created from high pressure. Drilling may create chips along the edges or sink edges depending on the drill used.

By also greasing the plate, the glue dowel is solely responsible for the connecting the timber and steel. Four different plate thicknesses were tested. Punching of the plate is only possible up to 4 mm, therefore testing on 6 mm is only conducted with laser cut and drilled holes. A summary of the test series is presented in Table 3.1.

Table 3.1: The different test variations for test series 1.

Variation no. [-]	Plate Thickness [mm]	Hole manufacturing [-]
1-1D	1	Drilled
1-1P	1	Punched
1-1L	1	Laser cut
1-2D	2	Drilled
1-2P	2	Punched
1-2L	2	Laser cut
1-4D	4	Drilled
1-4P	4	Punched
1-4L	4	Laser cut
1-6D	6	Drilled
1-6L	6	Laser cut

3.1.2 Test series 2

This test series aims to answer the second question - How does the steel to hole area ratio affect shear capacity in the connection? This test series investigated the contribution to the shear capacity from the adhesion of glue to the steel plate and from the shear capacity of the glue dowels. In the paper from Jockwer et al., 2023, it is stated that the glue dowels increase the strength of the connection, but it did not clearly specify the contribution from these dowels. This will be investigated by measuring the load capacity of the connection, while changing the hole diameter. Understanding this ratio aids in properly calculating the shear capacity of the glued-in plate connection. See Table 3.2 for hole diameters tested.

Table 3.2: The different test variations for test series 2.

Variation no. [-]	Hole diameter [mm]
2-6d	6
2-10d	10
2-12d	12

3.1.3 Test series 3

This test series aims to answer the third question - how is the dowel capacity influenced by the shear area and dowel length? The shear capacity in the adhesive is believed to benefit significantly from glue dowels (Jockwer et al., 2023), and understanding the ratio between shear capacity in the dowel and the adhesion to steel plate is important for the further development of the glued-in plates connection. This test series investigates two parameters independent of each other: glue dowel diameter and plate thickness. These factors will each impact the dowel size and volume, the first in thickness and the second one in length. This is helpful to understand how the geometries of the glue dowel effect the connection capacity. Increasing the glue diameter will investigate if the shear capacity of the glue dowel is proportional to the area of the glue dowel, and if there is an upper limit. Increasing the plate thickness will investigate if a longer dowel will affect the capacity, as per in GIR connections (Tlustochowicz et al., 2011). This test series was done with a greased plate to be able to only assess the influence of hole diameter and plate thickness on the glue dowel capacity. See Table 3.3 for a summary of hole diameters and plate thicknesses tested.

Table 3.3: The different test variations for test series 3.

Variation no. [-]	Plate Thickness t [mm]	Hole diameter d [mm]
3-10d	6	10
3-12d	6	12
3-16d	6	16
3-20d	6	20
3-08t	8	10
3-10t	10	10
3-12t	12	10

3.1.4 Test series 4

This test series aims to answer the fourth question - does a thicker adhesive layer contribute to a larger distribution of stresses to the timber? In literature, it is stated that shear stresses in lap joints distribute more evenly in a thicker glue line (Ebnesajjad & Landrock, 2015). This test series aims to investigate this further and see if there is a upper limit. Due to the thin glue line thicknesses, digital image correlation is not suitable and the conclusion will only be based on the strength capacity of the connection. This test series will be done on perforated plates, with the same perforation on all glue line thicknesses. The greasing of the plate leads to

the shear stresses only coming from the glue dowels. In Table 3.4 the different total glue line thicknesses are specified.

Table 3.4: The different test variations for test series 4.

Variation no.	Total glue thickness
[-]	[mm]
4-4A	4
4-6A	6
4-8A	8

3.1.5 Test series 5

This test series aims to answer the fifth question - how will the thickness of the glue line influence the deformation behaviour of the connection? In this test series, the stiffness of the connection on a plate without perforation depending on the glue line thickness is investigated. There is previously no study conducted on how the stiffness of the glued-in plates connection with perforation is influenced by the glue line thickness. Understanding how it works on plates without perforation, will help further develop the connection and implementation in industry. The total glue line thicknesses can be seen in Table 3.5

Table 3.5: The different test variations for test series 5.

Variation no.	Total glue thickness
[-]	[mm]
5-4A	4
5-6A	6
5-8A	8

3.1.6 Test series 6

This test series aims to answer the sixth question - how does the spacing of the perforation affect the strength of the connection? This testing was conducted on four different plate geometries, where the spacing of the perforation was changed but the total area of the glue dowels were kept the same. In screws and other metal fasteners as well as GIR, there are grouping effects that needs to be taken into consideration when doing capacity analysis for connections, as explained in the literature study. This test series was done to further understand the grouping effect

of the glue dowels, and how the shear capacity can be increased. See Table 3.6 for area of holes and the spacing for the different tests.

Table 3.6: The different test variations for test series 6.

Variation no.	Hole diameter	Spacing	No. holes
[-]	[mm]	[mm]	
6-1S	36	-	1
6-2S	12	20	9
6-3S	12	30	9
6-4S	12	40	9

3.1.7 Test series 7

This test series aims to answer the seventh question - how does timber size impact the failure mode, strength and stiffness of the connection? For GIR, there are design criteria on the minimum edge distance from the connection to avoid timber splitting as a failure mode (European Organisation for Technical Assessment [EOTA], 2019). This test series investigate if the same applies to the GIP connection. Three different timber sizes were tested where both the height and width was changed, see Table 3.7.

Table 3.7: The different test variations for test series 7.

Variation no.	Timber size
[-]	[mm]
7-60H	60
7-80H	80
7-100H	100

3.1.8 Test series 8

This test series aims to answer the eighth question - is the shear capacity of a flat plate directly proportional to its embedment length? In literature and studies regarding glued-in rods, there are different understandings on if the embedment length increase the capacity of the connection (Otero Chans et al., 2013; Tlustochowicz et al., 2011). Testing this on glued-in plates would help to further understand how the connection should be designed to get the desired shear capacity and to minimize material usage. During testing, four different embedment lengths were tested as per Table 3.8

Table 3.8: The different test variations for test series 8.

Variation no.	Embedment length
[-]	[mm]
8-50E	50
8-100E	100
8-150E	150
8-200E	200

3.2 Specimen geometry

Disclaimer: The LVL in test series 1-5 was designed to make use of the higher shear capacity in the edgewise direction with the slots for the steel plates perpendicular to the lamellas. However, due to a manufacturing error, this was not the case. With the limited time frame of this project, the tests were performed on these incorrect specimen. This resulted in unwanted timber shear failure in some tests.

Three different geometries were used during the experimental testing, which is shown in Figure 3.1. For all the following test series, the specific geometry can be found in Appendix A.

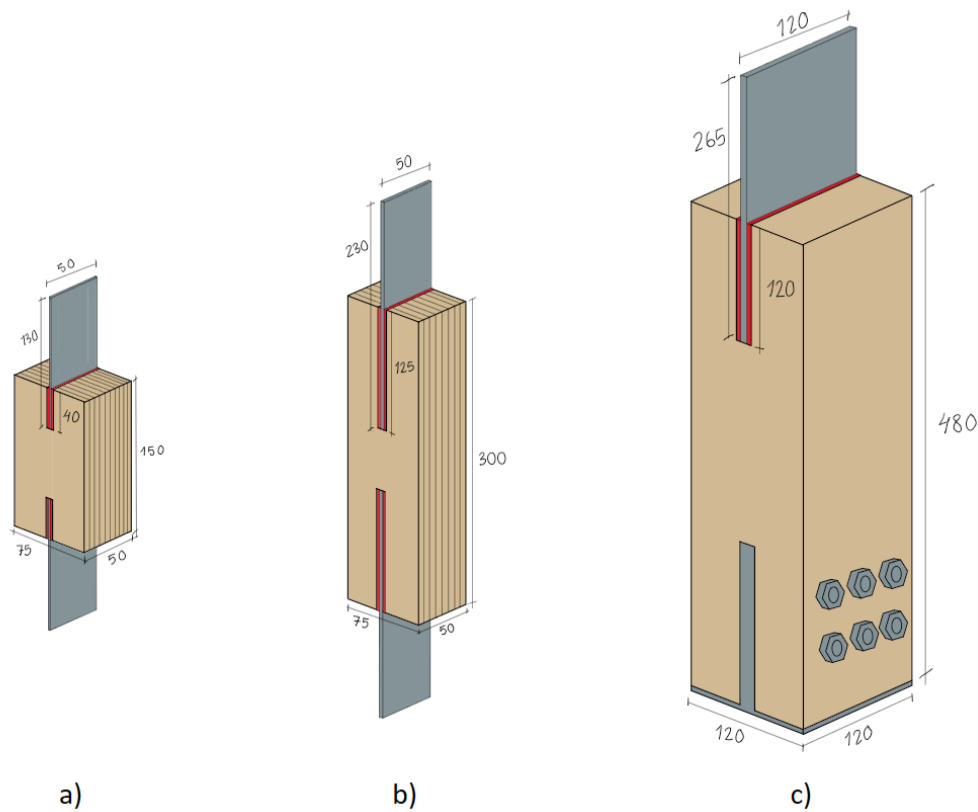


Figure 3.1: The three types of specimen in relative scale. The smallest version (to the left) is used to test hypothesis 1. The middle version (center) is used in test series 2-5. The largest version (to the right) are used in tests 6-8. Note that these measurements does not apply exactly to all test series. These are merely examples of test specimen. The largest specimen has a sufficiently strong dowel connection at one end, it does not necessarily look like the one in the drawing.

The design of the test specimen was an iterative process of hand calculations in order to achieve the desired capacities and failure modes for each test series. All test series are designed to not fail in the steel plate. Since steel is a very well researched material with predictable behaviour, it is not in the scope of this study to investigate the influence of the steel. For all specimen, S355 grade steel plates manufactured with laser cutting if else is not specified. The adhesive used is the two component epoxy HIT-RE 500 V4. The timber is specified depending on test geometry.

The first geometry, Figure 3.1 a), was used for test series 1 and was tested with double sided pulling. The specimen consisted of LVL Kerto Q with dimensions of 150 x 75 x 50 mm, with slots on each side where steel plates were slotted and glued with a bondline thickness of 2 mm. The steel plates had a length of 130 mm, where 40 mm where embedded in the timber and varying sizes of the perforation and thickness of the plate - see test series 1 for further specification.

The second geometry, Figure 3.1 b), was used for test series 2-5 and was also tested with double sided pulling. The specimen consisted of a timber specimen in LVL Kerto Q with the dimensions 300 x 75 x 50 mm. The steel plate was 230 mm long, where 125 mm was embedded in the timber, with varying plate thickness, slot width and size of perforation depending on test series (see test series 2-5 above). The slots for the steel plates were intended to be cut edgewise of the timber to be able to utilize the higher shear capacity in this direction. But due to a manufacturing error this was not the case for the delivered specimens.

The double sided testing was utilized to have a simple and effective method of assembling the test. However, this method meant more preparation of the specimens in form of more gluing.

The third geometry, Figure 3.1 c), was used for test series 6-8 and was tested with single sided pulling. The timber specimens were manufactured in GL28h. The bottom was fastened with a bolted connection to a steel plate attached to the rig. The timber length varied between the different test series, but with a constant distance between the test rig and the tested plate. The single sided testing was performed in a different hydraulic rig to enable higher loads.

3.3 Preparing of specimens

The timber specimen and steel plates were completely finalized in factory. After arrival at test facility, they were stored indoors at room climate to avoid rust and moisture.

How to inject the adhesive to ensure even filling, minimal air bubbles and a centered plate within the slot was discovered through iterations of trials. First, 3D-printed clamps similar to the ones used in Norbäck et al. (2023, see Figure 2.11) was used, see Figure 3.2. Adhesive was filled with the timber specimen standing up from two holes in the plexiglass on the sides. This method had a long assembly time and resulted in uneven filling.



Figure 3.2: Picture showing the first iteration of centering and spacing for the steel plate. Two pieces of 3D-printed plastic clamps with plexiglass slotted were screwed together. The lower clamp and the plexiglass had holes for filling the adhesive.

The second iteration was inspired by GIR methods explained by Steiger et al. (2015). Two different versions were tested, one with a hole drilled on each side of the timber to the bottom of the embedment length, perpendicular to the flatwise timber surface. The other trial had one hole drilled at a 45° angle toward the bottom of the embedment length, drilled from the edgewise surface. The adhesive was filled with the specimen lying down in an attempt at gluing both sides simultaneously. In order to see how even the adhesive had filled, the specimens were cut open after curing. The filling of adhesive was relatively even for both versions with the exception of large air pockets which can be seen in Figure 3.3.

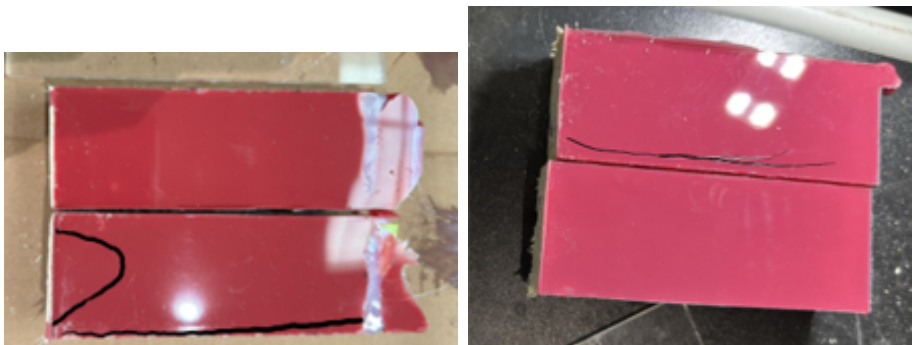


Figure 3.3: Left: Picture taken of the filling of adhesive, done with one hole drilled at 45° angle. Right: Picture taken of the filling of the adhesive, done with two holes on each side of embedment length. Both were glued laying horizontal on a flat surface. Black lines are drawn in to show the unevenness.

A simpler idea for centering the plates in the slot was to use 3D printed spacers to place onto the plates, see Figure 3.4. These were designed to be small to minimize lost glue area while also being able to glue specimen in bulk. EPX adhesive does not adhere to plexiglass, so that was utilized between each specimen to separate. The specimen were clamped together to contain the adhesive. An example of this can be seen in Figure 3.4.

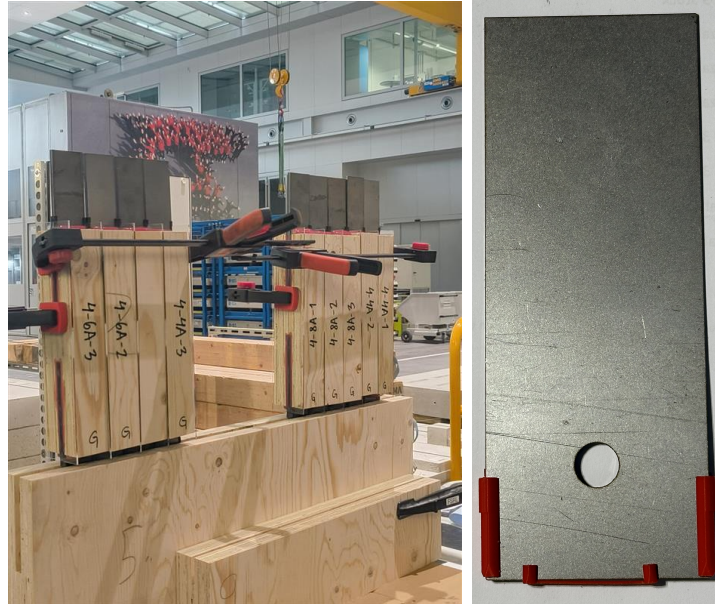


Figure 3.4: To the left: Picture showing the gluing process of multiple specimens at once. Clamps were used to keep the specimens together as well as keeping the plexiglass in place. To the right: Picture showing the spacers used to center the steel plates.

The spacers were used in the third iteration, which was also inspired by GIR gluing (Steiger et al., 2015). The method was created for filling large batches using plexiglass as separators. The idea was to pre-fill each slot with a calculated volume of adhesive and then push each plates in with spacers attached. The trial showed even filling without any voids and the method was used for test series 4. When splitting these specimens after testing, air bubbles in the glue dowel was found on 3 out of 9 specimens. It was then decided that the method should be updated even further.

The final iteration kept the spacers from the previous method but added back the filling holes. The holes was drilled at both sides of bottom of the embedment length and the plate mounted with spacers. The adhesive was filled through the hole from one side until glue overflowed on top. Filling was done from both sides for the unperforated plates. This method was used for the remaining test series, and showed fewer air bubbles in the dowels than previously. However, this method seemed to create more air bubbles along the flat of the plate than previous method. This was thought might be an effect of filling velocity as fast filling is guessed to contribute

3. Experimental Testing

to turbulence that trapped air within the glue. However, this is a mere theory and was not studied further. Regardless, this was the method that was used for the remainder of the specimen.

The adhesive was left to harden for 24 hours for all test specimens. For the double sided test specimen, one side was glued-in first and left to harden for an hour before the second plate was glued. The different sides were marked. Sizes and moisture content of the specimens were measured and recorded before gluing. For test series where a greased plate was investigated, only one side was greased to simplify the testing procedure in order to know which side would fail first.



Figure 3.5: Grease test to make sure the glue didnt adhere to the steel plate. The tested types were, from left to right: WD-40, Hilti CMA3KA grease, SKF Bearing grease, Hilti Spray lubricant, Hilti Special lubricant. The flipped pieces of glue were loose.

A grease test was also conducted on different types of greases. A picture of the test can be seen in Figure 3.5. A total of five greases were tested, in both a thick and a thin layer to see if the HIT-RE500 V4 would stick to the metal plate. Adhesive was left to harden for 48 hours before removing it from the plate. Hilti CMA3KA and Hilti Special was the only two lubricants that performed well regardless of grease quantity. After this result, it was decided that CMA3KA was the grease that would be applied during the testing, due to that there already was a big stock of this particular grease in the lab. For greased tests, the grease was applied to only one side of the timber specimens which ensured to be sure of which side would fail first.

3.4 Testing method

One simple way to test the capacity of a connection is using pullout testing (Science Direct, n.d.-c). Pullout tests can be done either single sided with another high capacity connection holding the other end, or double sided using a symmetric setup. Using double sided pullout test, also called pull-pull tests, is more like the realistic loading cases in practice. However, the double tests means that the test stops whenever the first side fails. This means that there will be an overrepresentation of weaker tests recorded than reality. From a redundancy and robustness point of

view, this is better, but it might lead to overdimensioning and wasting material if introduced in design standard.

The testing included heavy machinery such as hydraulic test rigs, using health and environmentally harmful chemicals and working in a dangerous environment with cranes, forklifts and other potential sources of harm. Before attending the test area, proper safety training is attended with educated staff. While in the test area, proper safety equipment must be used, i.e. safety goggles, gloves, safety shoes, long sleeved shirts and long pants, hair tied up, etc. During all testing there are authorized staff present, monitoring the testing to ensure it is performed in a safe and professional manner.

For testing timber connections, standard climate applies, which means testing and storing leading up to testing should be performed in $20 \pm 2^\circ\text{C}$ and $65 \pm 5\%$ RH (International organization for standardization, 1983; Swedish Standards Institute, 2021, 2023). Realistically, this was not achieved in this study. The test field had an average of $25 \pm 1^\circ\text{C}$ and $33 \pm 3\%$ RH, which means slightly warmer and much drier than code.

For brittle failures there are certain benefits using displacement-controlled loading. The GIP is stiff (Vallée et al., 2011), which means it will fail already under small displacements, but handle large loads. When testing timber joints for strength, stiffness and deformation, the ISO standard 6891 has rules of loading (International organization for standardization, 1983). Note that test series 4 does not use this loading standard, instead only had a preload added up to 0.5 kN followed by displacement controlled loading until failure. This was corrected for all remaining tests.

The method in ISO 6891/EN 26891 is based around a calculated or experienced expected load (International organization for standardization, 1983). First, the load is applied with load control up to 40% of expected max load and maintains this load for 30 seconds. From 10% of max load, up to 40% is the section for which the stiffness of the connection is evaluated. Following the 30 seconds, the load is decreased to 10% of expected max load and again maintained for 30 seconds. After this the load is applied as displacement controlled up until failure. The load curve is presented in Figure 3.6.

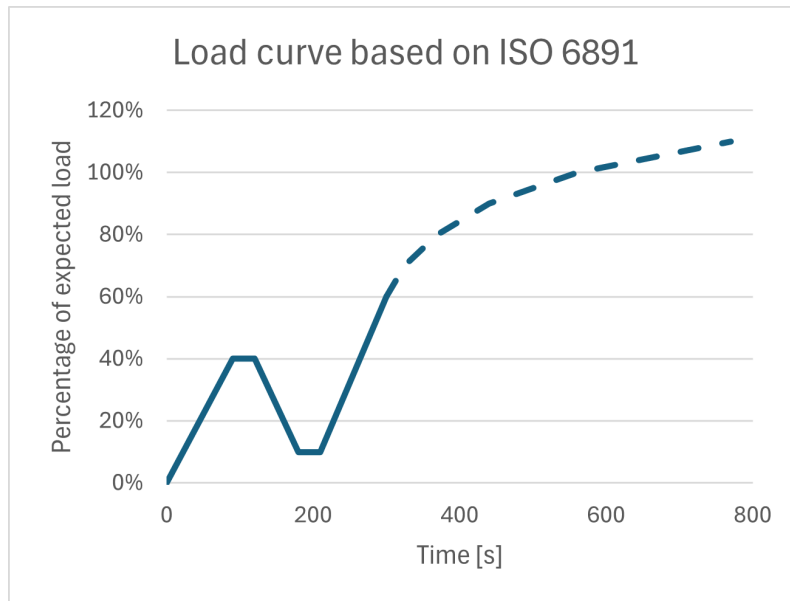


Figure 3.6: The load curve according to ISO 6891/EN 26891 (International organization for standardization, 1983).

The slope of the curve between 10% and 40% of the expected load capacity is used to calculate the stiffness of the specimen. When applicable, a trendline was created in Microsoft Excel and the R^2 , which is a coefficient of determination for variation in the dataset, had to be 0.99 or more, indicating a good match between trendline and data. For the ungreased plate, this method was not applicable due to the very stiff behaviour in combination with a too low resolution on the measuring equipment. For these tests, a linear interpolation between the start and end values was used.

Testing was done on a 70 kN hydraulic test rig for the two smaller geometries, and a 600 kN hydraulic test rig for the large geometry/single sided pull test. The double sided specimen were clamped on both sides to the machine, see Figure 3.7. To ensure that the specimen was mounted straight, a line laser was used. The single sided specimens were clamped to the hydraulic on the top and bolted to the test rig on the bottom. Lasers were used to measure the displacement during the testing. These were mounted on the timber using clamps, placed so they aligned with the steel plate. Reference points for the lasers were mounted onto the steel plate. Hence, the setup measured the relative displacement between timber and steel plate. The lasers work in a span of 10-20 mm with a resolution of 0.02 mm.

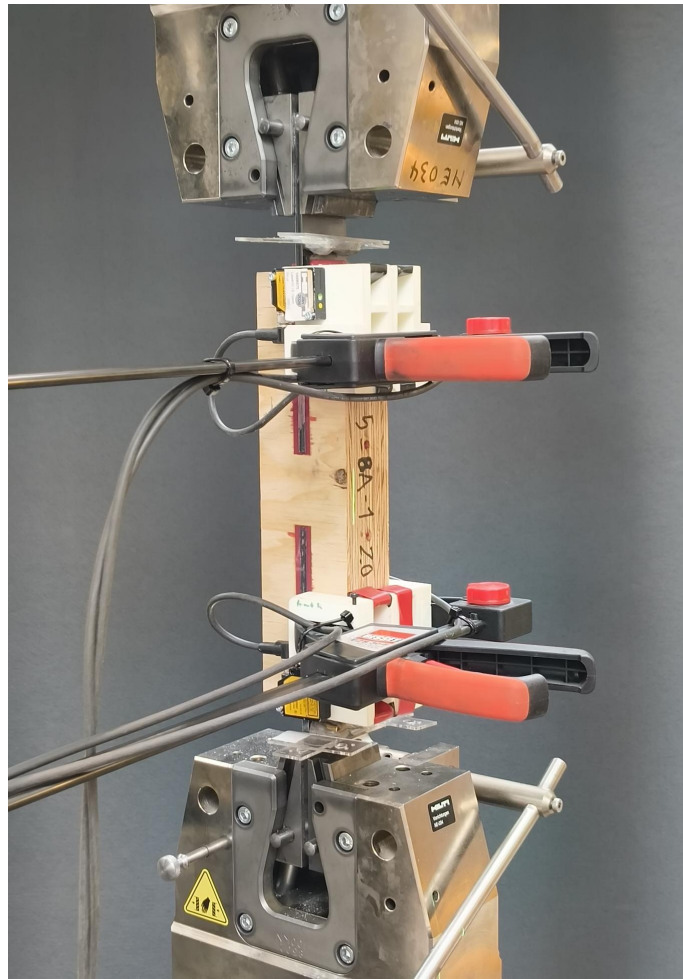


Figure 3.7: Picture showing the test rig used for double sided specimen.


4

Results



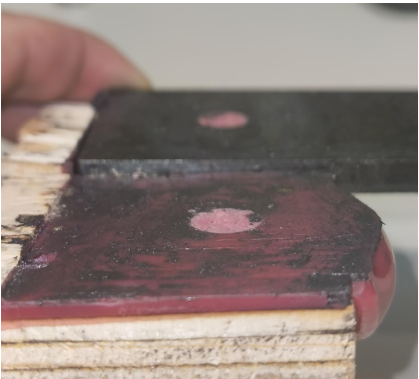
This chapter contains the results from each test series, see Appendix B for expected capacities and failure modes for all test series. The test peak load and slip modulus (where relevant) can be seen in Appendix C. In Appendix D, the load-displacement curves are shown for each test series.


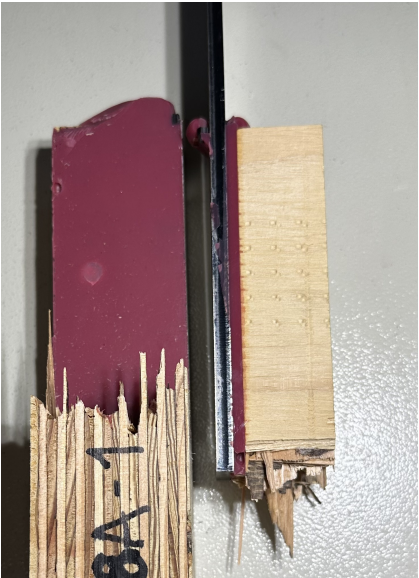
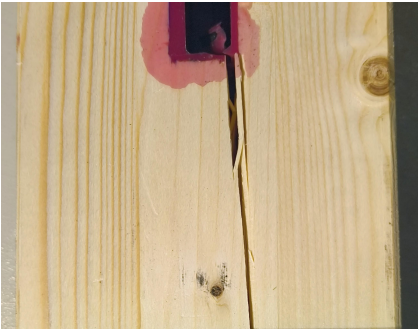
During the testing seven different failure modes were recorded; timber-glue interface, steel-glue interface, shear failure in timber, shear failure in the glue dowel, tension failure in the dowel, net section tension failure in timber, timber splitting as well as different combinations of these.

Table 4.1: Classification of failure modes.

Failure mode	Definition	Picture
Timber-glue interface	The adhesion between timber and glue is too weak, resulting in either a clean peel or a very thin layer of fibres peeling at failure	

4. Results

<p>Steel-glass interface</p>	<p>Loss of adhesion between glue and steel plate</p>	
<p>Shear failure in timber</p>	<p>The timber specimen peeling between fibers due to shear stresses</p>	
<p>Shear failure in the glue dowel</p>	<p>The glue dowel breaking of due to shear stresses, characterized by a parallel surface to the steel plate</p>	

<p>Tensile failure in the glue dowel</p>	<p>The glue dowel breaking due to tensile stresses, characterized by being cut off in an angle to the steel plate</p>	
<p>Net section tension failure in timber</p>	<p>The timber fails in pure tension due to a too small net section area. The fibers snaps in brittle failure</p>	
<p>Timber splitting</p>	<p>Tension loading creates a perpendicular outward tension effect that splits the timber along the fibers</p>	

4. Results

Combined failure	Any of the previously mentioned modes combines in more ambiguous failures. Many are also failing as a result of another failure. One very common example of this is the tension failure in dowels caused by timber splitting	-
------------------	--	---

The tension failure in the dowel, is believed to occur because the design of the specimen was too small. The tensile load causes the timber to open up, creating tensile forces perpendicular to the loading direction, which directly affects the glue dowel. For the greased plates, this is possibly more enhanced by the absence of adhesion between plate and glue. The dowel will contribute to a stress concentration which can create some bending in the timber.

In multiple of the test specimens, air bubbles were found in the dowel, see Figure 4.1. The bubbles are one form of imperfection that significantly affects the strength and stiffness of the dowel and hence lowers the capacity of the connection. These bubbles were frequent in this test campaign, and could not be erased despite many trials of gluing.



Figure 4.1: An example of an air bubble in a glue dowel.

4.1 Test series 1

This test series investigated different manufacturing types for the perforation on different plate thicknesses. Test results are presented in Table 4.2 and see Figure 4.2 for a diagram of the mean load capacity per plate thickness.

For plate thickness 1 mm and 2 mm, all specimens failed in shear in the glue dowel. For the test specimens with a plate thickness of 4 mm and 6 mm, one of the most common failure modes was shear failure in timber.

Table 4.2: The average maximum load for test series 1. Results with large CoV show air bubble in the dowel for at least one specimen.

Variation no.	Average peak load	CoV
[-]	[kN]	[-]
1-1D	2.94	8.16
1-1P	3.26	1.88
1-1L	4.23	15.09
1-2D	4.44	15.09
1-2P	4.77	5.98
1-2L	4.74	7.85
1-4D	6.31	11.36
1-4P	5.88	9.92
1-4L	5.48	5.73
1-6D	6.83	4.10
1-6L	6.25	6.16

When increasing the plate thickness, the load capacity increased. For plate thickness 1 and 2 mm, the load capacity was the highest for the laser cut plates, but this trend is not consistent. Instead the drilled holes shows the highest load capacities for plate thickness 4 and 6 mm.

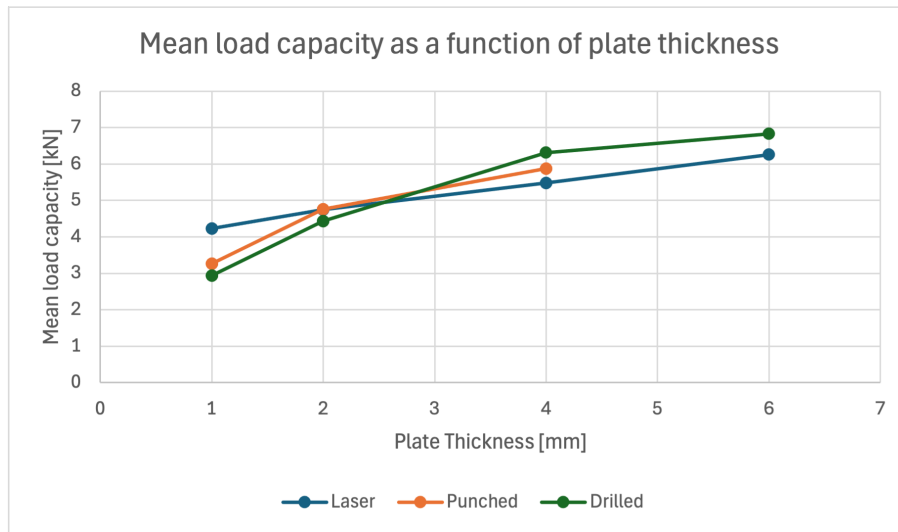


Figure 4.2: Mean load capacity as a function of plate thickness in test series 1.

For plates of 1 and 2 mm, the thin plate cut through the bottom of the dowels in the manner presented in Figure 4.3. The force transfers over a very small area, causing the adhesive to fail under the compression. This is not a pure shear failure as the whole shear area is not moving, the unloaded part of the dowel is still intact.



Figure 4.3: Partial failure in glue dowel for a 1 mm thick plate. The thin plate cuts through the dowel, actual shear failure has not occurred.

Different failure modes result in different behaviour after failure. This can be seen within this test series, in Figure 4.4, where dowel and timber failure in shear is compared. Timber shear failure result in a much more immediate drop in load-bearing capacity while dowel shear failure allows the for load increase close to peak load after a significant drop. The timber failure has a more consistent behaviour after failing while the dowel failure contribute to what is more consistent with the load-displacement curve of ductile failure. Observe however that the load-carrying capacity cease almost completely already after 2 mm of displacement and the behaviour is not actually ductile.

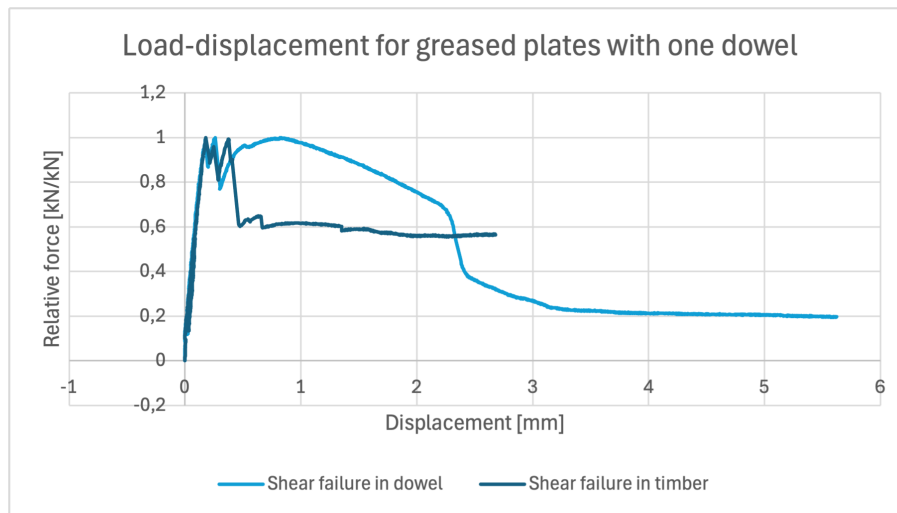


Figure 4.4: Load-displacement for two different failure modes for the same plate thickness. This shows how the failure affects the post-failure behavior.

If test data for plate thickness 8-12 mm from test series 3 were to be extrapolated for this series as well, the result would be as seen in Figure 4.5. Both test series only have one dowel with the same diameter and greased plates, meaning that the results should be applicable. Note that mean values for 8 and 10 mm plates have disregarded one measuring point each due to bubbles in glue dowels, for the purpose of showing the trend. The pattern suggests that for laser cut plates, the effect of plate thickness is only relevant for plates thinner than 6 mm.

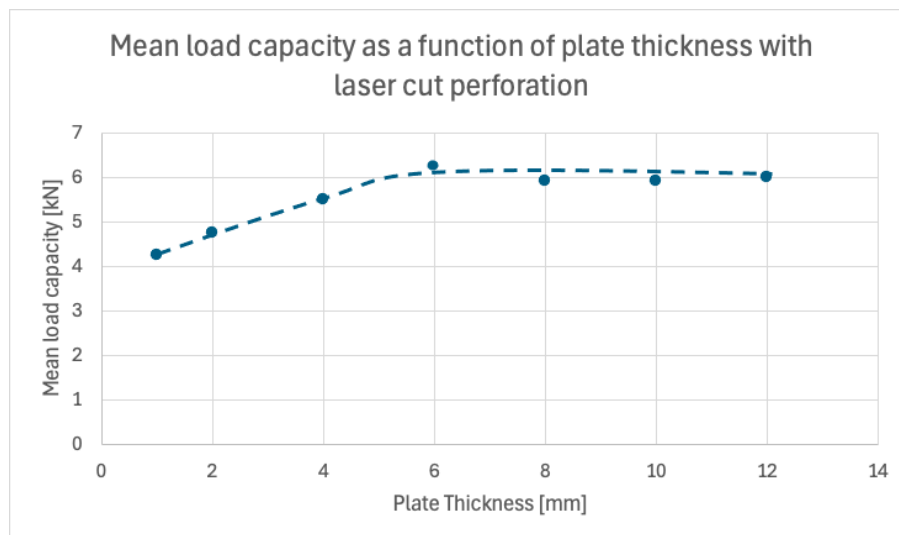


Figure 4.5: The dashed line is showing the perceived trend for laser cut plates with increasing thickness.

4.2 Test series 2

Due to the timber arriving with the wrong material strengths in the wrong direction, this test series would not work as intended. This conclusion is drawn after recalculating the capacity in combination with seeing the results from test series 1, where the timber failed unwantedly for many of the specimen. This in combination with the pressed time schedule are cause for striking this test series.

4.3 Test series 3

In test series 3, two different parameters of the glue dowel was investigated independently, the area of the glue dowel by changing hole diameter and the length of the glue dowel by increasing plate thickness. The test results are shown in Table 4.3. In the table, the specimens 3-10d and 3-06t is based on the same test specimen, but named according to the checked parameter.

Table 4.3: The average peak load and slip modulus for test series 3. Results with large CoV show air bubble in the dowel for at least one specimen.

Variation no.	Average peak load	CoV	Average slip modulus	CoV
[-]	[kN]	[%]	[kN/mm]	[%]
3-10d	7.14	0.22	39.17	13.67
3-12d	8.08	7.37	51.38	4.97
3-16d	9.33	10.61	51.09	9.96
3-20d	12.17	19.81	67.37	13.23
3-06t	7.14	0.22	39.17	13.67
3-08t	5.37	17.47	27.30	23.69
3-10t	5.20	20.96	37.46	30.47
3-12t	5.99	10.76	37.70	0.60

Despite failure in the interface between timber and glue for the 20 mm diameter, the trend for increased shear area for the glue dowels show increased load capacity. The failure for the 20 mm perforation is also an effect of the splitting due to insufficient timber strength, but also indicates that the bonding between timber and glue would could improve capacity. This could possibly be done with improving the friction on the timber surface. Regardless, as the failing component is the timber and not the dowel, the dowel can endure higher loads than the resulting maximal load for 20 mm dowels. The load-bearing capacity improves due to increased tension area

in each dowel in this case. To really evaluate the capacity of the dowels, the shear failure would also need to be evaluated.

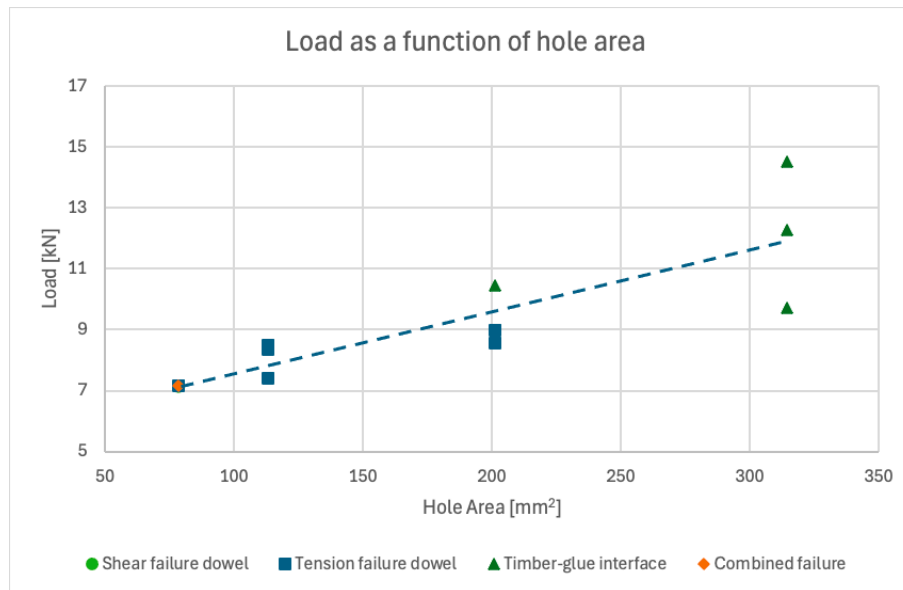


Figure 4.6: The load capacity per specimen as a function of the hole area. The dashed line is showing the perceived trend. The largest dowel size fails in timber-glue interface instead of a dowel failure. This is due to the dowel strength is increasing at a higher rate with a larger diameter than the adhesion to the timber for the increased area.

The stiffness of the connection also increases with the diameter of the glue dowel, as can be seen in Figure 4.7. The stiffness does not increase linearly between the different samples and with no clear indication as to why. However, the real trend can not be discerned from these results alone.

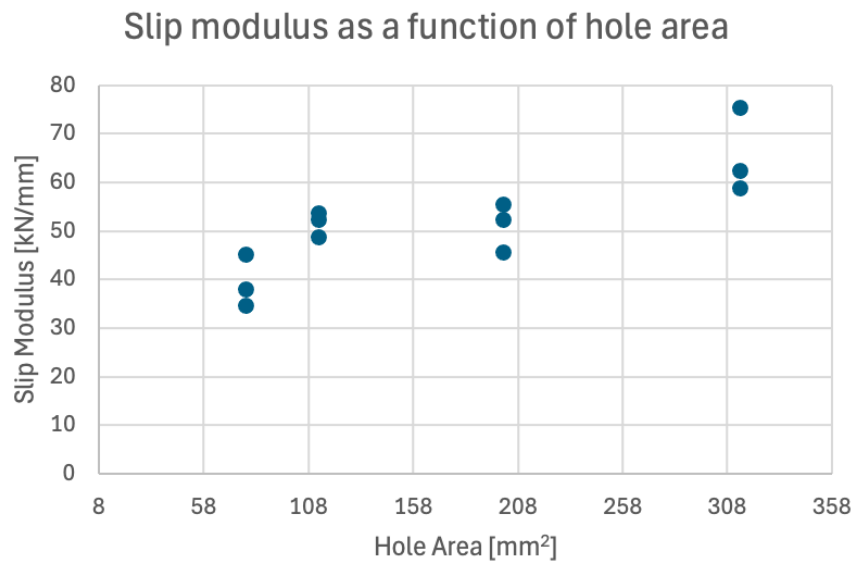


Figure 4.7: The slip modulus per specimen as a function of the hole area.

With a increased plate thickness and a greased plate, the capacity and stiffness of the connection decreases, as shown in Figure 4.9 and Figure 4.10. After testing specimen, 3-08t-1 and 3-10t-1 was cut open and investigated due to the low capacity, which showed that some grease were present in the dowel, as well as air bubbles.

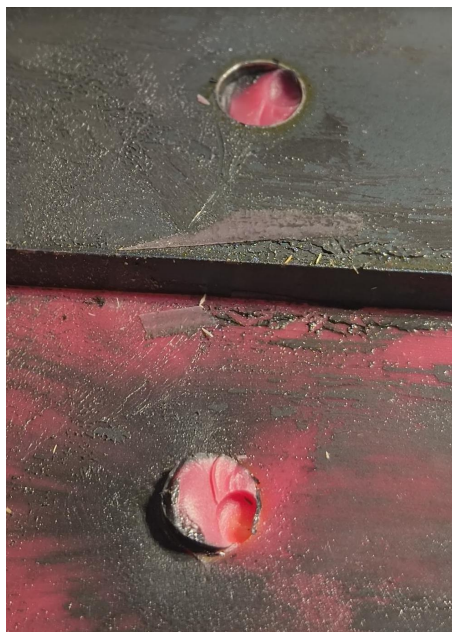


Figure 4.8: Grease has seeped into the dowel and decreased the load carrying area of the dowel (left side of the picture), combined with a big air bubble (right side).

This would explain the lower capacity of this specimen. The tensile capacity of the

dowels are lower than the shear capacity, which aligns well with the results when comparing the two failure modes present in the results.

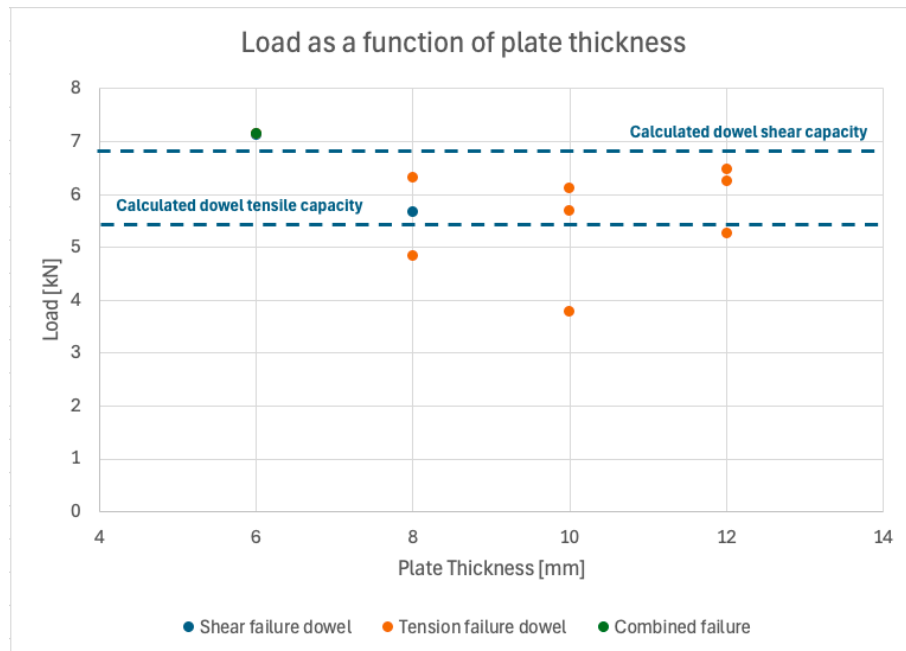


Figure 4.9: The load capacity per specimen as a function of the plate thickness. The two values under 5 kN are both specimen with air bubbles/grease in the glue dowel. Marked with dashed line is the calculated capacities for shear and tensile capacity respectively.

The load-displacement curve for the outlier in the 10 mm plate set also shows that there were large (in relation) plastic deformations before the 40% of expected load capacity, see specimen 3-10t-1 in Figure D.14, which can be found in Appendix D.

The stiffness of the dowel does not have a clear correlation with changing plate thickness as displayed in Figure 4.10.



Figure 4.10: The slip modulus per specimen as a function of the plate thickness. The two values under 20 kN/mm are both specimen with air bubbles in the glue dowel.

4.4 Test series 4

Test series 4 investigated how the capacity of the dowel and load transfer from timber to dowel were affected by the glue line thickness. The obtained test data can be seen in Table 4.4.

Table 4.4: The average peak load for test series 4.

Variation no. [-]	Average peak load [kN]	CoV [%]
4-4A	6.38	2.04
4-6A	6.03	7.87
4-8A	5.08	17.51

In Figure 4.11, the load capacity of the specimens is put into relation of the total glue thickness. It can be seen that the strength of the connection is unaffected by the change in glue thickness. This is true when excluding the outlier in the 8 mm set, that was caused by air bubble in the dowel.

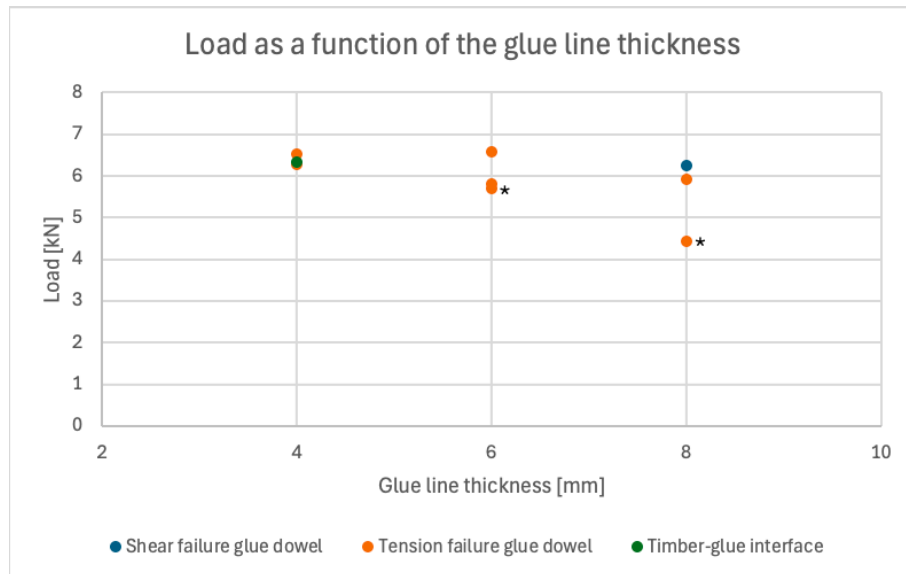


Figure 4.11: The load capacity per specimen as a function of the glue line thickness, grouped by failure mode. The data points marked have air bubbles present in the dowel, as discussed below.

The stiffness of the specimens can be seen in Figure 4.12. Here there is a slightly decreasing trend with an increased glue thickness. This suggests that a thinner glue line is preferable, as it provides the same strength but increased stiffness. All specimens were cut open after the testing to visually inspect the failure mode. In test specimen 4-6A-2 and 4-8A-2, an air bubble were found in the glue dowel. These voids also explain the lower stiffness of the test specimens.

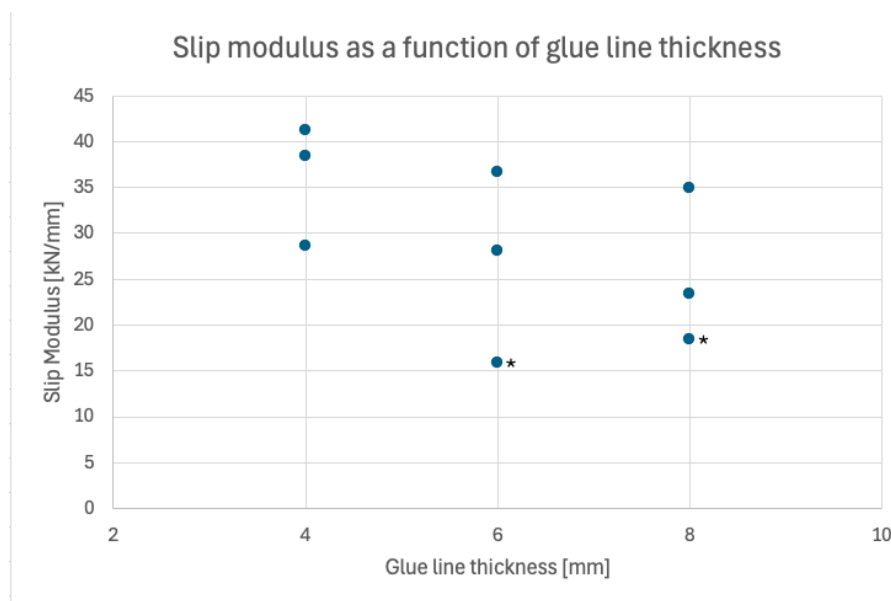


Figure 4.12: The slip modulus per specimen as a function of the glue line thickness. The data points marked have air bubbles present in the dowel, as discussed below.

4.5 Test series 5

Test series 5 was tested with ungreased and non-perforated plates to research further the influence of adhesive thickness and adhesion to steel on the behaviour of the connection. Compared to test series 4, these tests had no glue dowels that would contribute to any strength.

The test was redone due to the plates having residual grease from manufacturing that prevented proper adhesion. The following results are based on the redone test, with the correct, degreased plates. The resulting loads and stiffness can be seen in Table 4.5.

Table 4.5: The average peak load and slip modulus for test series 5.

Variation no. [-]	Average peak load [kN]	CoV [%]	Average slip modulus [kN/mm]	CoV [%]
5-4A	33.93	12.75	649.94	38.18
5-6A	30.04	26.99	622.66	4.00
5-8A	44.08	17.87	756.95	10.77

The connection is very stiff with a extremely brittle failure, most specimen had a load curve that aborted in the moment of failure due to displacement exceeding 10 mm. An example of a load-displacement curve can be seen in Figure 4.13, which is representative of the typical failure and behaviour of the flat plate.

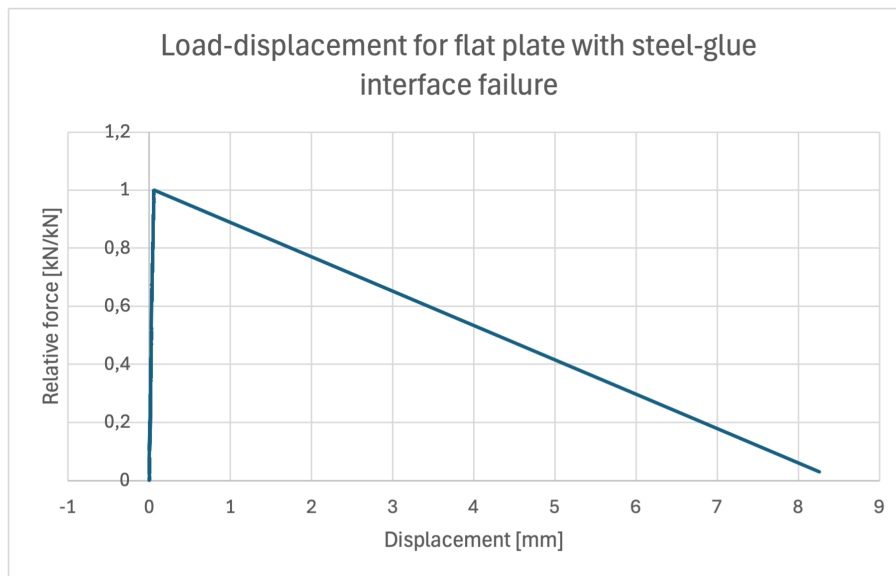


Figure 4.13: Load-displacement curve for typical specimen in test series 5. It has a very sudden failure in the interface between adhesive and steel, due to loss of adhesion.

A thicker adhesive layer seem to contribute to a larger load-bearing capacity for non-perforated plates, as shown in Figure 4.14. However, the scatter in all variations makes this hard to interpret and not a completely reliable conclusion.

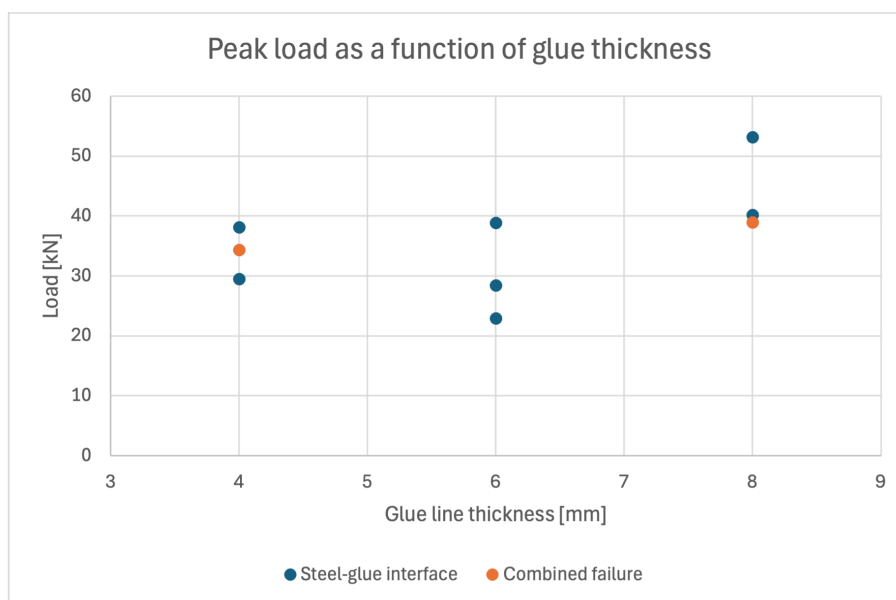


Figure 4.14: The load capacity per specimen as a function of the glue line thickness. The different failure modes are illustrated by different colours.

The results for slip influence by changing glue line thickness are inconclusive, see

Figure 4.15. No true pattern can be discerned. The scatter seen for the thinnest glue line further complicates understanding a possible trend.

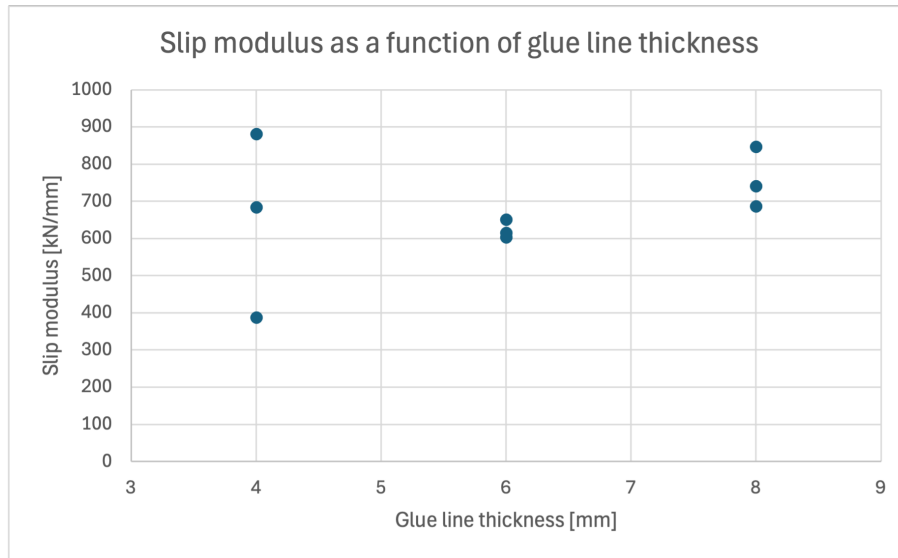


Figure 4.15: The slip modulus per specimen as a function of the glue line thickness.

4.6 Test series 6

The spacing between the perforation in the plate was varied in this test series. All plates had the same area of dowels, but spread out in one large dowel or nine smaller dowels with 20, 30 and 40 mm of centrum distance. In Table 4.6, the average values for peak load and slip modulus are presented.

Table 4.6: The average peak load and slip modulus for test series 6.

Variation no.	Average peak load [kN]	CoV [%]	Average slip modulus [kN/mm]	CoV [%]
6-1S	43.18	9.93	2332.40	47.01
6-2S	58.59	43.70	2335.41	47.21
6-3S	69.80	22.98	1867.74	11.85
6-4S	53.16	7.47	1924.10	42.02

All the specimens in 6-1S, which had one large hole with diameter of 36 mm, failed in the timber-glue interface around the glue dowel. For many of the test specimens, the timber split below the slot for the plate.

Timber glue interface was the most common failure model for the 6-2S specimens, while the 6-3S variation showed tension failure in dowels. The highest average peak load was recorded for the 6-3S's, see Figure 4.16. In the 6-4S specimens, timber shear failure was observed for the dowels close to loaded end, and timber-glue interface failure for remaining dowels. The timber fails for edge distances somewhere under 2.5 times the diameter of the dowel. The lowest capacities were displayed in the single dowel (6-1S) as well as the 6-4S.

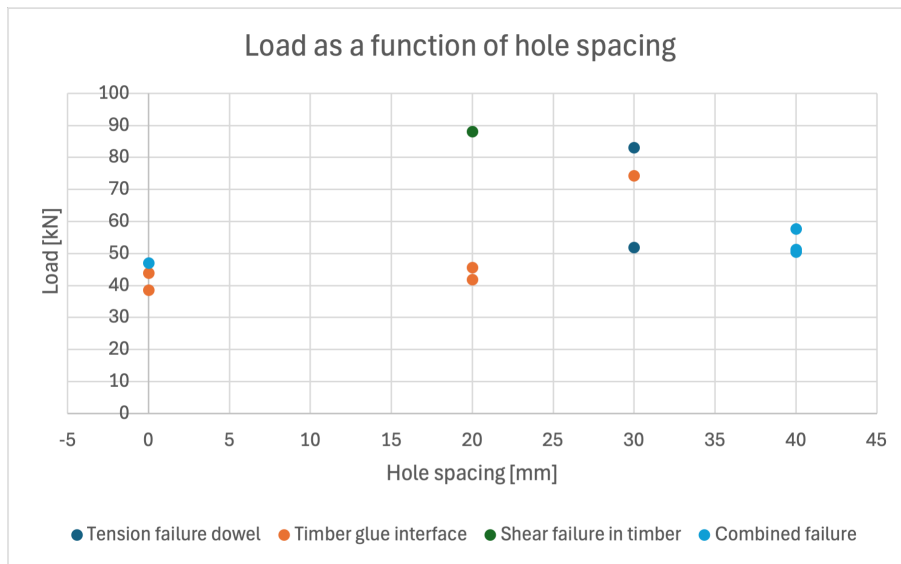


Figure 4.16: The peak load per specimen as a function of hole spacing.

The stiffness for the low distribution of perforation was higher than for the two more distributed alternatives. The values are plotted in Figure 4.17.

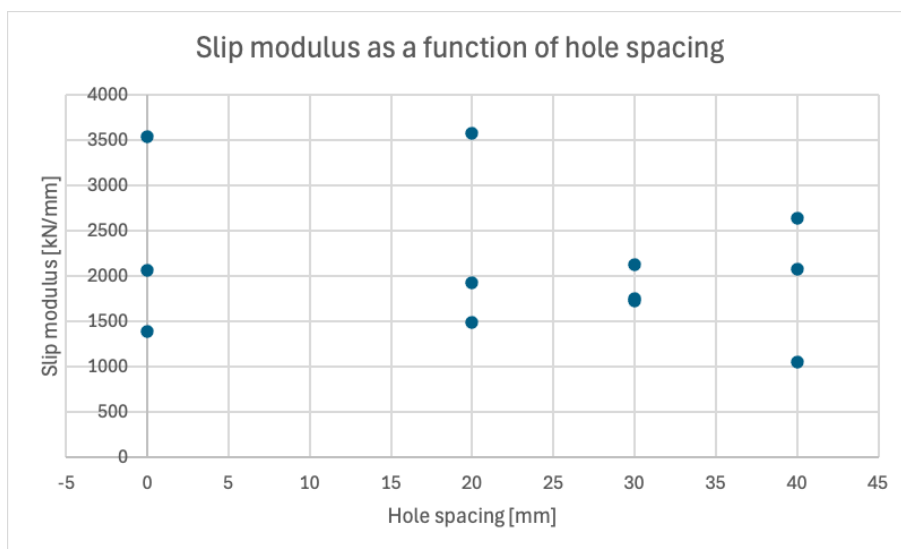


Figure 4.17: The slip modulus per specimen as a function of hole spacing.

4.7 Test series 7

The available net section of timber was decreased in this series, to see if this influenced the failure mode. This was mainly done to assess if the risk for timber tensile failure or timber splitting was increased with less timber. Both the width and height of the timber was decreased for each variation. The results are displayed in Table 4.7.

Table 4.7: The average load capacity and slip modulus for test series 7.

Variation no.	Average peak load	CoV	Average slip modulus	CoV
[-]	[kN]	[%]	[kN/mm]	[%]
7-60H	45.69	15.41	1088.15	28.33
7-80H	45.24	3.99	1912.70	24.75
7-100H	44.48	16.57	1385.53	17.30

The degreasing of the plates used in this test series was not sufficiently good, and residue was visible on the adhesive after the tests had been done, see Figure 4.18. The plates were degreased using the same method and product as for the other plates, but for these plates, it did not work. These plates must have been treated differently or be from another manufacturing batch than the other plates, and unfortunately this affects the resulting capacity.

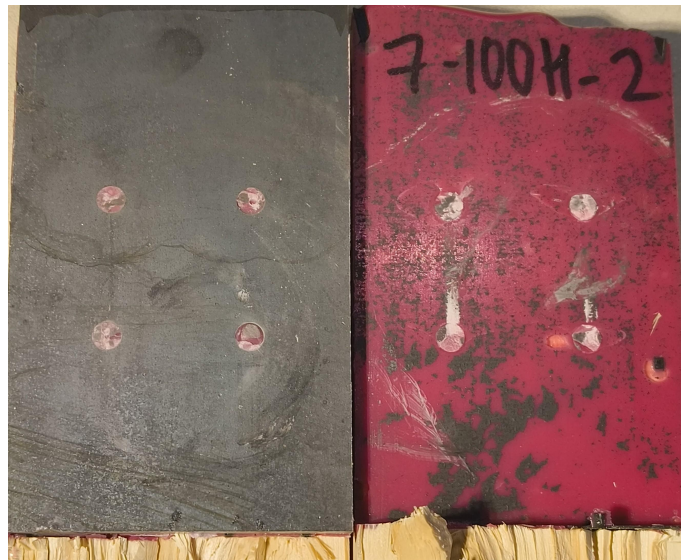


Figure 4.18: Opened specimen from series 7. Black is residue on from plates on glue, in red. As visible, a significant portion of the area has this residue.

The maximum peak load is surprisingly found for the specimen with the smallest specimen, as shown in Figure 4.19. This should not be the case as this both have a smaller expected capacity tension/splitting in timber as well as a smaller adhesion area. In some capacity, all of the specimens failed in the steel-glue interface due to the degreasing not being sufficient enough.

These results need complete retrial, which was not performed in this study due to time limitation. The load and slip of the specimens are presented below in Figure 4.19 and Figure 4.20, but do not contribute to any conclusions.

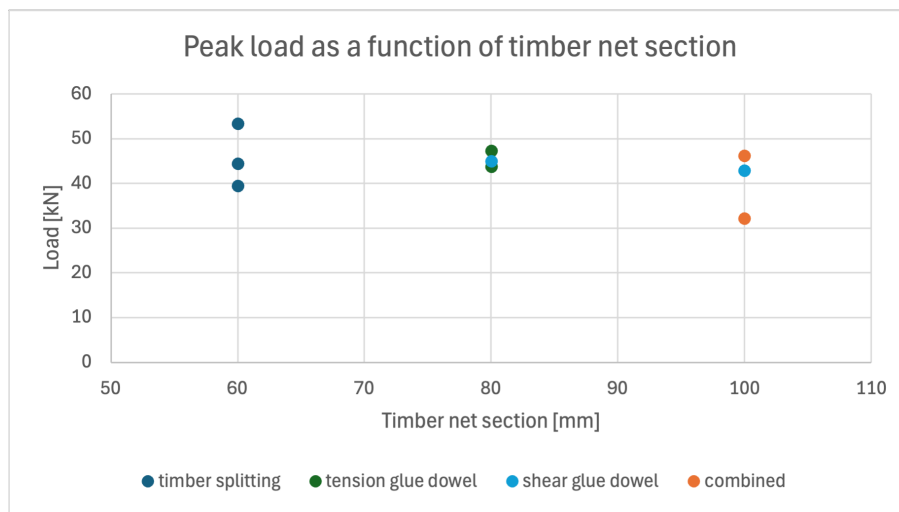


Figure 4.19: The load capacity per specimen as a function of the timber net section.

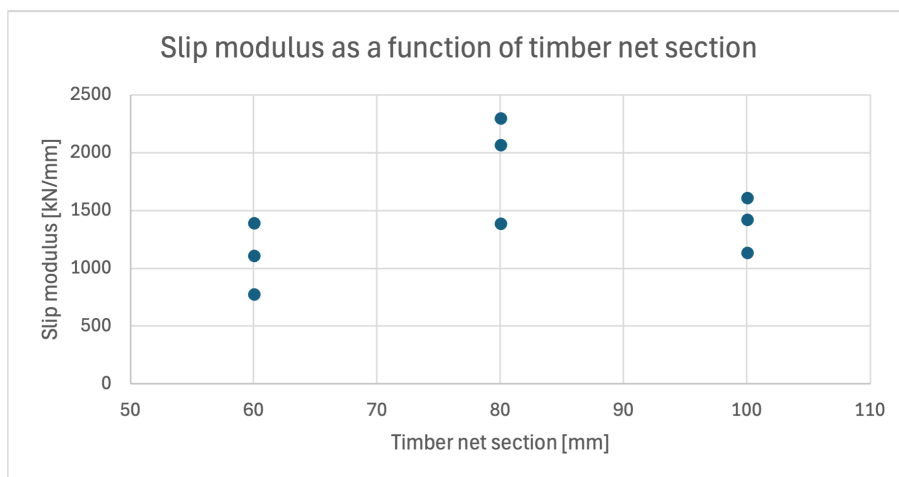


Figure 4.20: The slip modulus per specimen as a function of the timber net section.

4.8 Test series 8

Four different embedment lengths were tested, between 50 mm and 200 mm with 50 mm increments. The steel plate was unperforated in this test series. See Table 4.8 for the average peak load and slip modulus for each variation in the test series.

Table 4.8: The average peak load and slip modulus for test series 8.

Variation no. [-]	Average peak load [kN]	CoV [%]	Average slip modulus [kN/mm]	CoV [%]
8-50E	25.07	41.16	695.72	70.62
8-100E	45.37	21.38	2347.41	37.02
8-150H	63.87	36.77	2259.38	25.62
8-200H	64.94	27.35	1973.87	30.66

When looking at the increased embedment length, it can be seen that the load capacity increases up to 150 mm and then plateaus for 200 mm. All of the specimens failed in the steel-glu interface. For embedment length of 200 mm the timber split below the slot on one specimen as well. This aligns with studies on glued-in rods and lap joints (Otero Chans et al., 2013; Tannert et al., 2010).

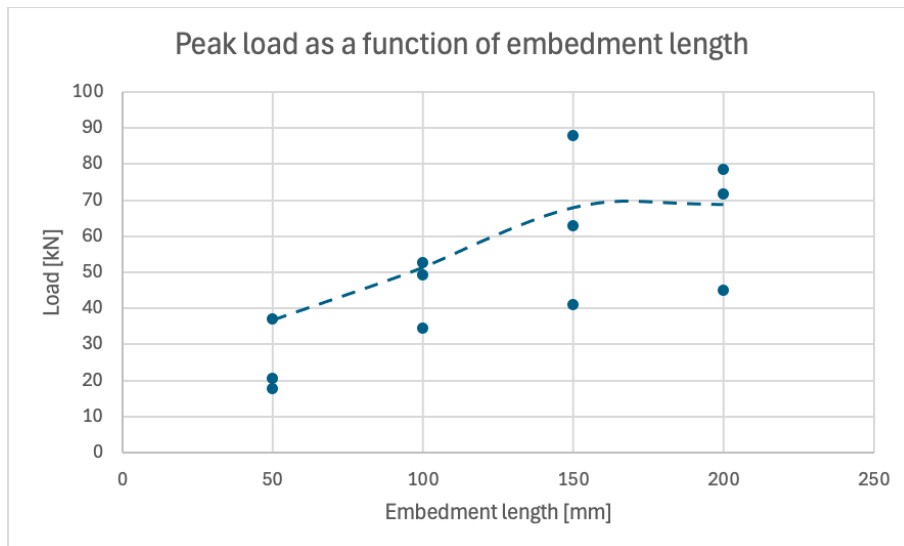


Figure 4.21: The peak load per specimen as a function of embedment length. The dashed line is showing the perceived trend.

The slip modulus peaks at 100 mm embedment length, as can be seen in Figure 4.22.

This peak occurs earlier than what can be seen for the load capacity. There is also a decrease of the slip modulus after 100 mm embedment length.

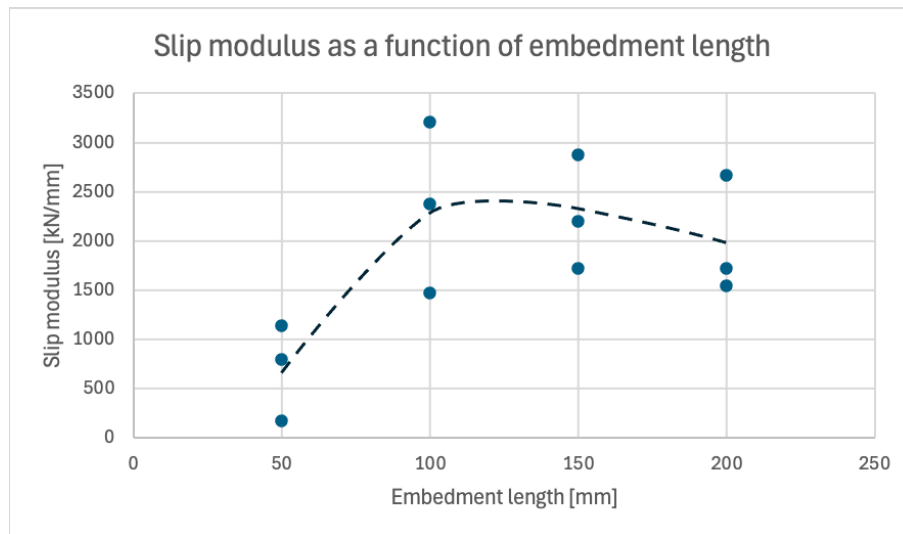


Figure 4.22: The slip modulus per specimen as a function of the embedment length. The dashed line is showing the perceived trend.

5

Discussion

The intention was to contribute with basic knowledge of the mechanics of the connection, as to build a foundation for future research. Over a hundred tests have been done during this testing campaign, where many of the results have not contributed to a conclusive answer or learning. Due to this, the takeaways from the results may rather be what to look out for in future studies.

5.1 The glue dowel and its geometry

The glue dowel is mainly affected by its diameter, according to the results from test series 3. When the hole diameter was increased, the load capacity increased linearly with the increased area, which aligns with the calculations. The capacity of the glue dowel exceeds the capacity of timber-adhesive bonding and needs to be further tested for diameters larger than 20 mm and for different adhesive/timber combinations. A large scatter in the capacities can be seen for the 20 mm diameter glue dowel. These three specimens failed in the timber-glue interface, and due to the properties in timber, a large scatter is not unconventional. The stiffness increased with an increased hole diameter, which aligns with theory. A larger diameter increases the inertia of the dowel, which allows for a larger stiffness.

In test series 6, three specimens with one large hole of diameter 36 mm was tested which failed in the timber-glue interface. As stated earlier, if the diameter is increased, the capacity of the glue dowel is therefore also increased. However, the capacity of the bond line timber-adhesive does not increase to the same extent and becomes the governing failure. This has only been tested on a glue line thickness of 2 mm. It is stated in literature that a thicker glue line can distribute the stresses more (Ebnesajjad & Landrock, 2015; Tlustochowicz et al., 2011). If the area for stress distribution is increased, it will lead to a lower stress concentration at the bond line. Hence, it is possible that this failure mode can be reduced with a thicker bond line.

When comparing the load-displacement curves from the test where the plates were perforated or unperforated, Figure 4.4 and Figure 4.13, it can be seen that there is some post failure capacity with a glue dowel. The failure with smooth plates, is

very brittle. The failure with glue dowels present in the connection, the failure is less brittle. However, this does not mean that it is a ductile failure.

The length of the dowel or thickness of plate does however not impact the strength or stiffness of the connection in any discernible way for plates thicker than 6 mm. See Figure 4.9 and Figure 4.10. This will be further discussed below.

5.2 The influence of plate thickness on connection behaviour

The results from test series 1 shows that increasing the plate thickness from 1 mm to 6 mm increases the capacity. More specifically, for plates 4 and 6 mm thick, specimens failed in the timber and not in the adhesive. This does mean that the glue dowel is stronger than the maximum load capacity in the timber for the specimens with 4 and 6 mm thick plates. To be able to draw conclusions regarding this, more test data would be needed.

For the thinnest plate of 1 mm, the plate cut into the dowel, like shown in Figure 4.3. For the 2 mm plates, the effect was still present, specifically for the drilled and punched plates, but the effect decreased compared to previously mentioned plates. For very thin plates, the area of stress distribution will be very small and the pressure of the plate onto the dowel very large, which aligns well with the results. The combination of visual inspection of the plates as well as these results leads to the conclusion that for thin plates, punching and drilling lead to sharper edges of the hole. This will in turn lower the capacity of the dowel.

Regarding the manufacturing methods, it was difficult to assess this influence due to the failure being in the timber rather than in the adhesive for the plates with thickness 4 and 6 mm. This can not be assessed from the collected data and needs to be further investigated in the future.

For plates with thickness 1 mm, there was a difference between the manufacturing methods. The laser cut holes showed a larger capacity compared to the drilled and punched holes. This is due to the laser cut holes having a cleaner cut with less sharp edges, which does not cut into the dowel in the same capacity as the other two. The edges of the drilled and punched holes had larger inconsistencies. In 2 mm plates, the difference between the load capacity for the different manufacturing methods was negligible. The uneven edges can here then be of advantage, since there is more surface area for the adhesive to adhere to. Epoxy glue does also adhere better to uneven surfaces.

The lower capacity in laser cut plates compared to drilled and punched, can be an effect of lower mechanical interlocking due to smoother edges. This also leads to shear failure in the glue dowel being the dominating failure mode for the specimens with plates that were laser cut. The opposite can be said for drilled and punched

for the thicker plates, where higher load capacity can be due to the unevenness seen in the hole, increasing the mechanical interlocking.

The drilled holes have a decrease in stiffness at 6 mm plates. This is believed to be because the edges of the hole become more prominent with a thicker plate. The laser cut plates have cleaner edges that it not affected by the plate thickness. Furthermore, the laser cut plates have a very linear trend compared to the other plates. That is likely due to them being very uniform and lacking imperfections. This contributes to a more predictable behaviour.

When comparing all of the tests done with different plate thicknesses, it can be seen (in Figure 4.5) that the capacity increases and then plateaus after 6 mm. Different embedment length and adhesive area was used for test series 1 and 3 where this was tested, but due to the plates being greased the capacity of the dowel should be the same. For plate thickness 4 and 6 mm from test series 1, multiple tests failed in the timber. Therefore the capacities of the glue dowel is larger than the presented test data.

A suggestion is to investigate this further and suggest a reduction factor for very thin plates. As a side note, these are minimally small plates that carry barely any load in a structural context. For the application, the plates will most probably be of larger scale and thicknesses sub 6 mm will most likely be unnecessary.

Plate thicknesses above 6 mm does not seem to have a clear influence on the load capacity. There is also a larger scatter for the specimens with 8 and 10 mm thick plates that influence the results. All the specimens in test series 3 failed in the glue dowel, but with different failure modes. Specimens that failed in tension in the glue dowel, showed a lower load capacity than expected shear failure in the glue dowel. The shear failure was calculated with two shear planes, and gave therefore a larger capacity than the tensile capacity. The tension failures are a direct consequence of the incorrect timber specimen, as the tension creates a splitting effect and the specimen split much easier with the lamella directioned in the same way as the plate. The assumption was that the capacity would increase with a increased plate thickness. This was based on the fact that with a thicker plate, there would be a larger compressive area of the glue dowel. With the data collected, this can not be stated.

5.3 Geometry of the adhesive and the effect on connection stiffness

In test series 4 the adhesive thickness was increased and tested on a greased perforated plates. The results shows that the load capacity of the glue dowel is unaffected by the thickness of the surrounding adhesive layer. It was not possible to use digital image correlation to measure the stresses, since the glue line thicknesses tested were too slim to be able to get a reliable result from this. Due to this, it was not

possible to measure the stress distribution in the glue line, and instead only load and displacement was measured. A lower load capacity on the thicker bond lines, could be explained by eccentricity is easier induced. None of the test specimens for test series 4, failed in shear of the glue dowel but rather in tension.

Test series 4 was also not tested with the loading curve according to standard for timber fasteners. The loading curve used for these tests was a preload up to 0.5 kN, and then displacement controlled loading of 0.03 mm/s until failure. The loading method was corrected for the remaining tests to the loading curve (see Figure 3.6) that is proposed in the standard ISO 6891/EN 26891 for timber fasteners (International organization for standardization, 1983) as mentioned in Chapter 3. Even if the loading curve is not according to standards, the results should still answer the hypothesis in question. The loading up to 40% of expected capacity is used to measure the stiffness of the connection, and this was not part of this test series. The stiffness of the connection is still possible to be calculated with the provided test graphs, where the slope of the curve between 10% and 40% of expected load was taken.

When looking at the load-displacement curves for the test series 4, it can be seen that there is more inconsistencies in the graphs compared to the other test series. This could be due to the loading and unloading phase used in other test series removes some internal stresses, which then removes some of the noise in the graphs. During the testing cracking could be heard from the test specimens, which is believed to be force redistribution in the glue. Specifically this was seen in the specimens in 4-4A, which were very unclear and irregular, having no internal pattern or likeness. Fortunately, we had some overlaps in the testing for this specific test, where 3-10d was identical to 4-4A, which could then be included to clarify and improve the results.

Test series 5 was done in two sets of specimens. This was due to the plates used for the first test set was not degreased before assembly. It was clear when testing that the specimen did not reach their ultimate load when comparing to hand calculations. This is due to the film of grease that prevented total adhesion. For the second set of test specimens, a different kind of LVL was used and the manufacturing of the specimens was in the first intended way of the design and a larger shear capacity could be utilized. However, since the timber was not the failing component, this should not impact the validity or comparability of the results.

5.4 Geometry of the timber section

The degreasing on the plates for test series 7 was not successful, and the results for this test series is therefore not reliable or conclusive. The load capacity was even for all three variations of the timber net section, but was all well below the expected capacity for the timber. This is because the adhesion between the steel and the adhesive not being fully developed due to residual grease being present. There are

no conclusive results on this, and needs the testing needs to be conducted again in the future.

5.5 The influence of plate design

The distribution of the perforation influence the capacity of the connection. Having the glue dowels close together leads to stress concentration and therefore failure in the timber-glue interface. However, placing the glue dowels to close to the edge leads to lower capacities as well. In these test results, a edge distance below 2.5x dowel diameter leads to failure on the timber side.

When looking at the embedment length of the connection, it is seen that increasing up to 150 mm increases the capacity and then plateaus for 200 mm. This aligns with the literature, where it is stated that increasing the embedment length above a certain limit does not decrease the stress peaks in the adhesive (Otero Chans et al., 2013; Tlustochowicz et al., 2011).

Seeing as timber splitting is such a vital aspect of the design of the GIP, along with the fact that the specimens in this study with the longest embedment length failed by splitting. This indicates, that there should be a minimum design requirement for timber size in correlation to the embedment length. To be able to determine ratios between this, further testing is needed.

5.6 Gluing method and air bubbles

One of the sources of error in this study is that it is difficult to visually assess during the gluing process that the adhesive was evenly filled, especially in the perforation of the plate. Voids in the adhesive are difficult to avoid. Epoxy has a exothermic reaction during the hardening and the gases released during the hardening will therefore create small air bubbles. However, these bubbles are not the problem and does not cause significant decrease in load-bearing capacity. The larger voids are created by air being trapped in the adhesive during the injection. Multiple different gluing methods were investigated during this testing campaign, where both ease of installation and quality of the filling was assessed.

It was found that filling adhesive from holes at the bottom of embedment length after that the plate had been centered, gave the more reliable results compared to when filling adhesive first and then mounting the plate. Filling the adhesive in batches with plexiglass in between was found to be a functioning method, that did not influence the results of the gluing.

In some of the test series conducted, there was larger air bubbles recorded that could affect the load carrying capacity. There could be many influencing factors, where one could be that the grease on the plate is affecting how the glue moves in the slot. This however is more of a possible testing error rather than a fault with the GIP

as this is not a method that would be used in real world application. This is rather only used in this study to gather information of the glue dowel. Another possible reason could be the speed of injection of the glue. If the glue is injected with a high speed in a narrow slot, turbulence within the glue could trap air.

Air bubbles in the adhesive is difficult to avoid, and more importantly, impossible to visually inspect after filling the adhesive in GIP application. The air bubbles influence the results, especially if they are located in the glue dowel. Since it cannot be determined after installation how many air bubbles are, it could be wise to have a design criteria where the adhesive strength is reduced. To ensure no bubbles, a similar method to what is found in GIR would be an improvement. For GIR, there is a possibility to use a rubber sealing cuff that travels with the adhesive by the change of volume and that allows air to slip out and creates a type of vacuum. Another type would be to seal and use actual vacuum to remove air bubbles. These techniques are not developed for GIP and would both be very labour and time intensive.

The centering pieces used for installing the plate, was found to work very well in this study. Ease of installation, how well it centered the plate and the low material usage speaks in this methods advantage. However, it is not investigated how this method works on larger plates.

During the testing of the specimens, the curing time of the adhesive was not always identical since multiple specimens where glued at the same time. The testing of specimens was done within 3 h of 24 h curing time. According to the attached user guide for the RE500 V4 (Hilti, n.d.), the adhesive should be fully cured after 7 hours in the temperature range 20-24° C, and therefore the adhesive was fully cured.

5.7 Design of geometry and calculation method

It was decided to use LVL Kerto Q for the small tests due to a higher shear capacity perpendicular to the veneers compared to glulam. For the larger tests, glulam was used due to shorter delivery times. When the LVL arrived, the manufacturer had produced the pieces with the lamelleas parallel to the slot for the plate. This results in a significantly lower shear capacity, 1.3 MPa compared to the 4.5 MPa the tests were designed for. With a limited time frame before this mishap, there was no time to wait for new specimen, but rather to try to adapt the tests to the new circumstances. Due to this, it is difficult to properly evaluate the influence of some of the parameters since the timber failed in shear instead of the intended failure in the adhesive.

After the specimens had been tested, they were cut open to assess the failure mode. For many of the specimen, the dowel failure was not in shear as expected, but rather tension. The reason for the tension in the glue dowel is the timber bending outwards due to the applied tensile force. The reason for this, is both due to the design of the specimens being too small and that the lamellae of the specimens were manufactured in the wrong direction. It was decided during the testing phase that the specimens

should not be clamped together to increase the stability, since this could effect the friction in the connection. In the post processing of the data, it was chosen to look at the first load peak and evaluate this capacity.

The calculation method used when designing the specimens, was too simplified and did not take all of the possible factors into consideration. Timber splitting was not considered, and this was found to be a dominating failure. For future studies, the timber size and relation to timber density should be considered in calculations by calculating the tensile forces created perpendicular to loading direction but also studied to find a formula for assuring avoiding timber splitting.

5.8 Greased plates

The smaller specimen were mainly tested with greased plates. A grease test was done on steel prior to the testing, where the Hilti RE500 V4 was applied to the greased and left to harden, as shown in Figure 3.5. After the curing time, the adhesive could be removed with hand force. It was therefore decided that the greased area of the steel plate was not contributing to the load capacity with any adhesion.

There could be inconsistencies with the greasing, both with a too thin layer and a too thick layer. A too thin or uneven layer could lead to adhesion between the steel plate and the adhesive, and therefore contributing to added load capacity. A too thick layer could lead to excess grease flowing with the adhesive during filling, and therefore creating pockets that lower capacity. When comparing test data with the same size of the dowel, but with different embedment lengths, it can also be seen that the capacity of the dowel is in a similar range. Due to this, it can be said that the greasing of the plate is sufficiently good for the testing.

5.9 Testing method

The loading program was designed according to ISO 6891/EN 26891 and can be seen in Figure 3.6. The curve is based upon the estimated/calculated capacity of the connection. The estimated maximum capacity calculated in a simplified way, since there is no standard for the load capacity for glued in plates should be calculated. Therefore, there are cases where the calculated max capacity is higher than the actual capacity of the specimen. This could be seen in the load-displacement curves, where there are cases where plastic deformation can be seen before the 40% mark. In some of the test series where this could be seen, the expected load was decreased in the loading protocol to be able to evaluate the stiffness of the connection.

Each test was manually ended when the load-displacement curve plateaued, hence there was no stiffness left in the specimen, or when the displacement exceeded 10 mm. Since this was manually done from visual inspection, there might be a small risk that tests have been stopped before the maximum capacity has been reached.

With double sided testing, it is only the side that fails first where the max load can be recorded and the other side it can only be stated that the capacity is higher but not by how much. The double sided testing has both advantages and disadvantages. The main two disadvantages are that there is a extra material usage as well as double the time for installation process. The main advantage of this testing, was that the test rig used for double-sided testing had an easy installation. This in both regards of the speed and being able to have the specimen straight in the test rig. However, for the specimens with greased plate, only one of the two plates were greased. This ensured failure at the greased plate and measurement only needed to be done for the failing plate.

With the single sided pull-out tests, a plate was mounted with bolts in the bottom. The plate was thinner than the slot in the timber to be able to mount it, but also lead to some eccentricity of the tensile force in the bottom specimen. It was only visibly inspected if the bottom plate was mounted in the center, and not with a line laser as the case with the double-sided testing. This leads to it not being as reliable.

When the testing campaign was investigated, many different parameters were of interest. It was decided to make a broad investigation to fill knowledge gaps and find which parameters that could have an influence on the connection. Due to time limitations, it was not possible to make multiple variations on all of the parameters. When in later stage the data from testing were analysis, it was found that it could be difficult to find trends with few variations. In future research, if it is possible, it would be valuable to have more variations per parameter to be able to define trends. Having three parameters per parameter, also means that scatter in the data have a large impact on the results.

5.10 Further research

For further research on the topic, it needs to be investigated how the application of this connection can be implemented in the practical field. The adhesive needs to be filled evenly and with consideration of air bubbles. Also how this should be assured on site and when implemented in codes and national standards should be further assessed.

This study focuses on the geometry of the connection. Other interesting parameters are different materials, most prevalently adhesives. A few studies (Vallée et al., 2011; Zeman et al., 2024) have already looked at the bonded plate connection in systems and their contribution to the global response, but this would need further investigation. Also with different load cases to this, particularly the combined action from bending in a beam.

In this testing campaign, it is not investigated how the load capacity is affected by plates that are not centered. Uneven adhesive on the sides of the plate, as well as a plate with eccentricity, leads to the load transfer not being ideal.

The adhesive used in this study, HIT-RE 500 V4, is a two component epoxy developed by Hilti. It has a service range between -40°C and $+40^{\circ}\text{C}$ (Hilti, 2024). Above $+40^{\circ}\text{C}$, the adhesive softens and loses strength. For fire safety, this is a very important topic. Other connections are expected to resistance time of 15-30 minutes (Swedish Standards Institute, 2004).

6

Conclusion

The conclusion of this thesis can be summarized in the following four main points.

The influence of glue dowels and their geometry

Glue dowels increase the load capacity of the connection, and also give the connection some post-failure capacity, which leads to a less brittle failure compared to unperforated plates. Although, this does not mean that the failure is ductile.

The area of the glue dowel has a linear increasing correlation with the load capacity. If the area of the glue dowel is increased so that the capacity of the glue dowel exceeds the capacity of the bond line, the governing failure mode will be timber-glue interface.

Increasing the glue line thickness, will increase the load capacity and the stiffness of the connection on unperforated plates. For GIP with glue dowels, the load capacity decreases with an increased glue line thickness.

The influence of plate design

Distributing the perforation of the plate, gives a higher load capacity due to a better stress distribution in the adhesive according to the test results. Although, the perforation should not be placed closer than 2.5 times the dowel diameter to the edge of the plate to ensure that there is no shear failure in the timber. Distribution will ensure that the dowels can redistribute the stresses into the timber effectively and not cause premature failure through stress concentrations.

Both plate thickness and embedment length have a certain limit to their contribution to increased load carrying capacity. After the limit, the load carrying capacity will not increase further from increasing these parameters. Increasing the plate thickness above 6 mm does not contribute to a higher load-bearing capacity if the steel is not failing. The embedment length above 150 mm only contribute to a larger material usage for a width of 120 mm. According to literature, the width/length does have an impact and should be studied for GIP specifically, as well as scale factors for GIP.

Gluing method and centering of plates

When filling epoxy glue blindly, which is the case for glued-in plates, it is difficult to assess the quality of the filling. This means there may be air bubbles present which lowers the capacity of the connection. Filling the adhesive after the plate is centered in the slot, gives a more reliable and even filling. The filling method for adhesive needs to be further investigated, and perhaps a reduction factor could be implemented into the design calculations.

The centering pieces used for testing worked well for this scale of specimens. They were material efficient, had a simple installation process, and worked well for centering the plate both at the bottom and the top. However, they would need to be tested for scaling issues and practical applications.

Specimen design and calculations

Many of the tests presented in this thesis needs to be re-run, since the results are inconclusive due to too small test specimens and/or unwanted failure mode. During the testing campaign, timber failure - both in shear and splitting - was dominating. The calculation method used, was too simplified and did not account for the needed timber net sectional area.

When analysing the data for some test series, it was difficult to find trends. More variations per parameter would be recommended for future testing to be able to see more clear trends.

Final remarks

This study has found that glued-in plate connections offer high load capacity and stiffness, that get further improved by using perforated plates that form glue dowels. The presence of air bubbles is inevitable and could significantly reduce connection performance. While some findings are inconclusive, there are also results that align with theory and previous research and findings that could be confirmed by further study.

While the findings are promising, the connection's practical application in structural design requires further research and implementation into standard. Future work should focus on refining gluing methods as well as developing calculation methods.

References

- Al-Emrani, M. (2023). *Steel Structures : Course literature - VSM 191*. Chalmers University of Technology, Department of Architecture; Civil Engineering.
- Åstedt, B. (2009, October). *Stålets egenskaper*. https://media.sbi.se/2019/11/Stalets_egenskaper.pdf
- Dillard, D. A. (2002). *Fundamentals of stress transfer in bonded systems. Adhesion Science and Engineering*, 1–44. <https://doi.org/10.1016/B978-0-444-51140-9.50028-7>
- Ebnesajjad, S., & Landrock, A. H. (2015). *Adhesives Technology Handbook* (3rd ed.). Elsevier. <https://doi.org/10.1016/C2013-0-18392-4>
- European Organisation for Technical Assessment [EOTA]. (2019, October). *Design of Glued-in Rods for Timber Connections* (tech. rep.).
- Hilti. (n.d.). *Hilti HIT-RE 500 V4 1400 Jumbo Användaranvisning* (tech. rep.). https://www.hilti.se/c/CLS_FASTENER_7135/CLS_CHEMICAL_ANCHORS_7135/r12560055
- Hilti. (2024). *HIT-RE 500 V4 INJECTION MORTAR Product Technical Datasheet* (tech. rep.).
- International organization for standardization. (1983). *Timber structures - Joints made with chemical fasteners - General principles for the determination of strength and deformation characteristics* (tech. rep.).
- Jockwer, R., Landel, P., Norbäck, V., Ziethén, R., Dölerud, E., Naveda, L. A., & Åkerström, C. J. (2023). *Fatigue resistance of adhesive bonded connections with and without internal steel plates in large timber structures. 13th World Conference on Timber Engineering, WCTE 2023, 4*, 2118–2124. <https://doi.org/10.52202/069179-0281>

- Norbäck, V., Landel, P., Dölerud, E., & Wickström, A. (2023). *On-site gluing and weather effects on tall wooden wind turbine towers. 13th World Conference on Timber Engineering, WCTE 2023, 3*, 1336–1341. <https://doi.org/10.52202/069179-0182>
- Otero Chans, D., Estévez Cimadevila, J., & Martín Gutiérrez, E. (2013). *Withdrawal strength of threaded steel rods glued with epoxy in wood. International Journal of Adhesion and Adhesives, 44*, 115–121. <https://doi.org/10.1016/j.ijadhadh.2013.02.008>
- Science Direct. (n.d.-a). *Epoxy Adhesive - an overview*. <https://www.sciencedirect.com/topics/engineering/epoxy-adhesive>
- Science Direct. (n.d.-b). *Polyurethane Adhesive - an overview*. <https://www.sciencedirect.com/topics/engineering/polyurethane-adhesive#chapters-articles>
- Science Direct. (n.d.-c). *Pullout Test - an overview*. <https://www.sciencedirect.com/topics/engineering/pullout-test#related-terms>
- Science Direct. (n.d.-d). *Volkersens Model - an overview*. <https://www.sciencedirect.com/topics/engineering/volkersens-model>
- Steiger, R., Serrano, E., Stepinac, M., Rajčić, V., O'Neill, C., McPolin, D., & Widmann, R. (2015). *Strengthening of timber structures with glued-in rods. Construction and Building Materials, 97*, 90–105. <https://doi.org/10.1016/j.conbuildmat.2015.03.097>
- Swedish Standards Institute. (2004). *Eurocode 5: Design of timber structures - Part 1-2: General - Structural fire design* (tech. rep.).
- Swedish Standards Institute. (2021). *Glued-in rods in glued structural timber products - Testing, requirements and bond shear strength classification* (tech. rep.).
- Swedish Standards Institute. (2023). *Adhesives for load-bearing timber structures* (tech. rep.).
- Swedish Wood. (n.d.-a). *Choosing glulam*. https://www.swedishwood.com/building-with-wood/about-glulam/choosing_glulam/
- Swedish Wood. (n.d.-b). *Om Svenskt Trä*. <https://www.svenskttra.se/om-oss/>
- Swedish Wood. (n.d.-c). *Trä i byggprocessen*. <https://www.svenskttra.se/bygg-med-tra/byggande/bygga-i-tra/>

- Swedish Wood. (2017, January). *Förband och anslutningsdetaljer*. <https://www.traguiden.se/konstruktion/limtrakonstruktioner/projektering-av-limtrakonstruktioner/forband-och-anslutningsdetaljer/>
- Swedish Wood. (2022). *Design of timber structures - Volume 1* (Vol. 1). www.swedishwood.com.
- Tannert, T., Hehl, S., & Vallée, T. (2010). *Probabilistische Bemessung von geklebten Anschlüssen im Holzbau*. *Bautechnik*, 87(10), 623–629. <https://doi.org/10.1002/bate.201010043>
- Tlustochowicz, G., Serrano, E., & Steiger, R. (2011). *State-of-the-art review on timber connections with glued-in steel rods*. <https://doi.org/10.1617/s11527-010-9682-9>
- Vallée, T., Tannert, T., & Hehl, S. (2011). *Experimental and numerical investigations on full-scale adhesively bonded timber trusses*. *Materials and Structures/Materiaux et Constructions*, 44(10), 1745–1758. <https://doi.org/10.1617/s11527-011-9735-8>
- Xu, B. H., Guo, J. H., & Bouchaïr, A. (2020). *Effects of glue-line thickness and manufacturing defects on the pull-out behavior of glued-in rods*. *International Journal of Adhesion and Adhesives*, 98, 102517. <https://doi.org/10.1016/J.IJADHADH.2019.102517>
- Yurrita, M., & Cabrero, J. M. (2021). *On the need of distinguishing ductile and brittle failure modes in timber connections with dowel-type fasteners*. *Engineering Structures*, 242, 112496. <https://doi.org/10.1016/J.ENGSTRUCT.2021.112496>
- Zeman, M., Sejkot, P., Mikes, K., Fragiaco, M., & Aloisio, A. (2024). *Glued-in steel plate and screwed connections in Timber–Concrete Composites systems: Mechanical performance and design implications*. *Journal of Building Engineering*, 96. <https://doi.org/10.1016/j.job.2024.110477>

A

Appendix A - Geometry of test specimen

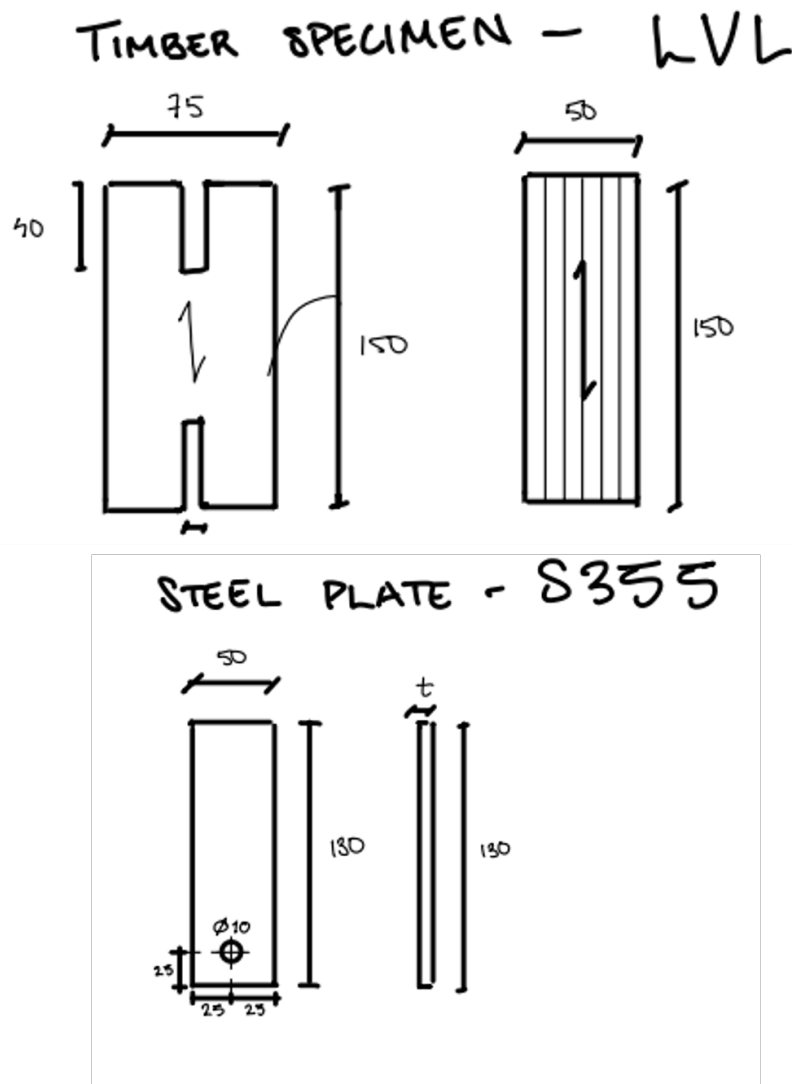


Figure A.1: The geometry of the specimen in test series 1

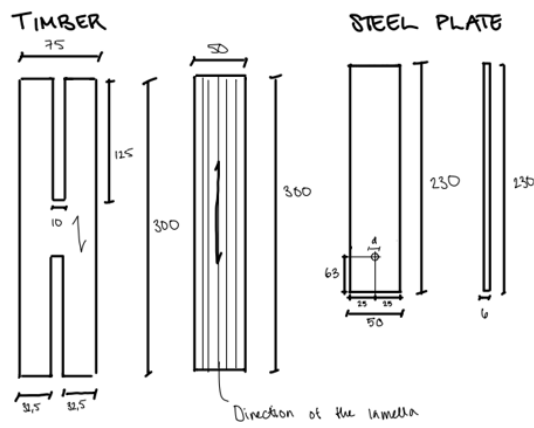


Figure A.2: The geometry of the specimen in test series 2

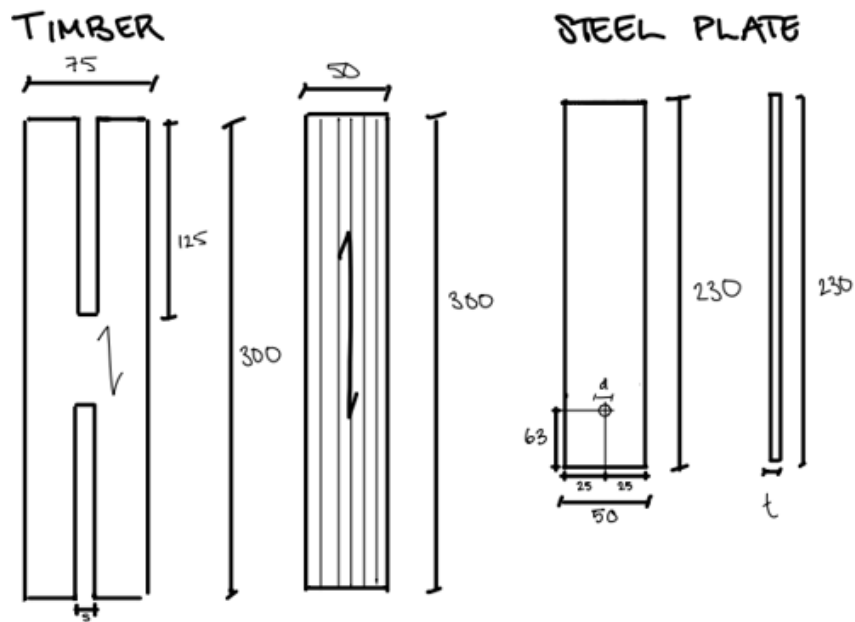


Figure A.3: The geometry of the specimen in test series 3

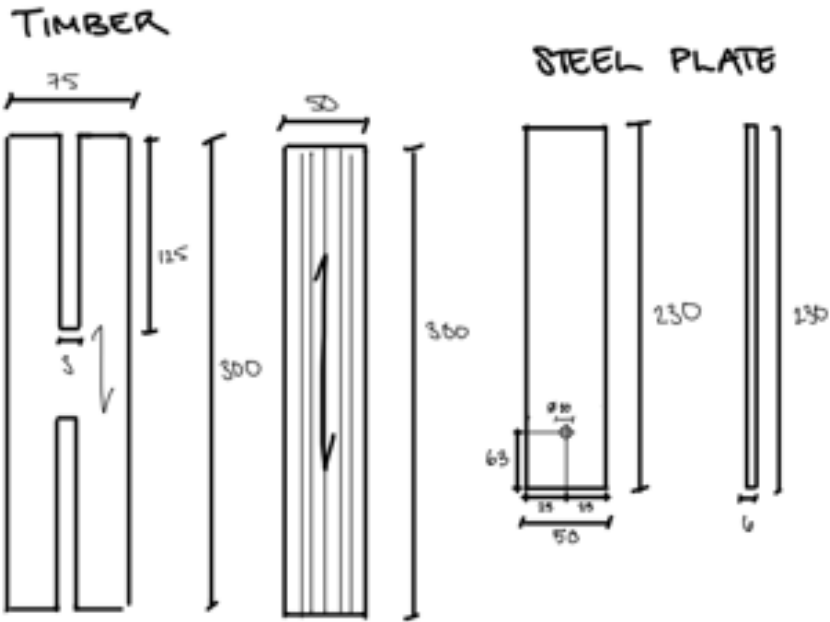


Figure A.4: The geometry of the specimen in test series 4

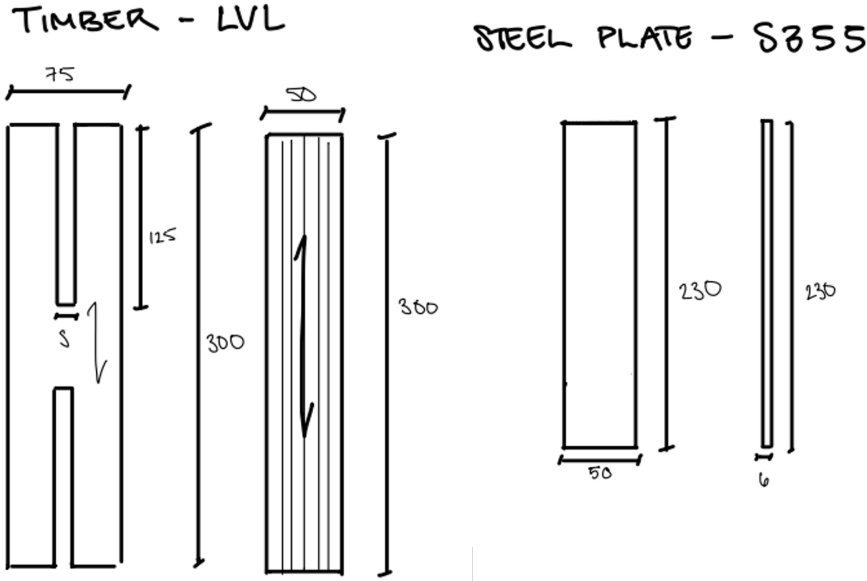


Figure A.5: The geometry of the specimen in test series 5

A. Appendix A - Geometry of test specimen

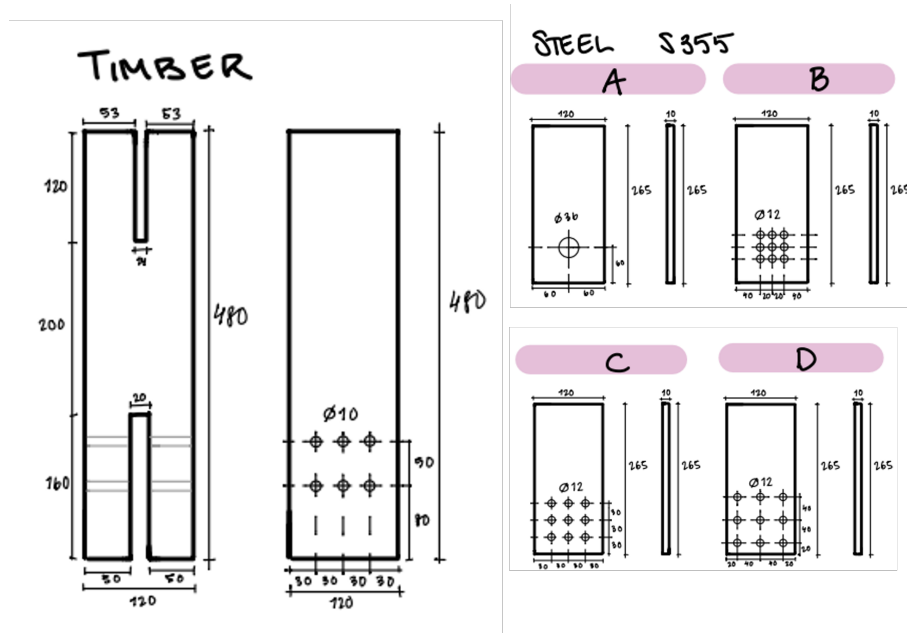


Figure A.6: The geometry of the specimen in test series 6

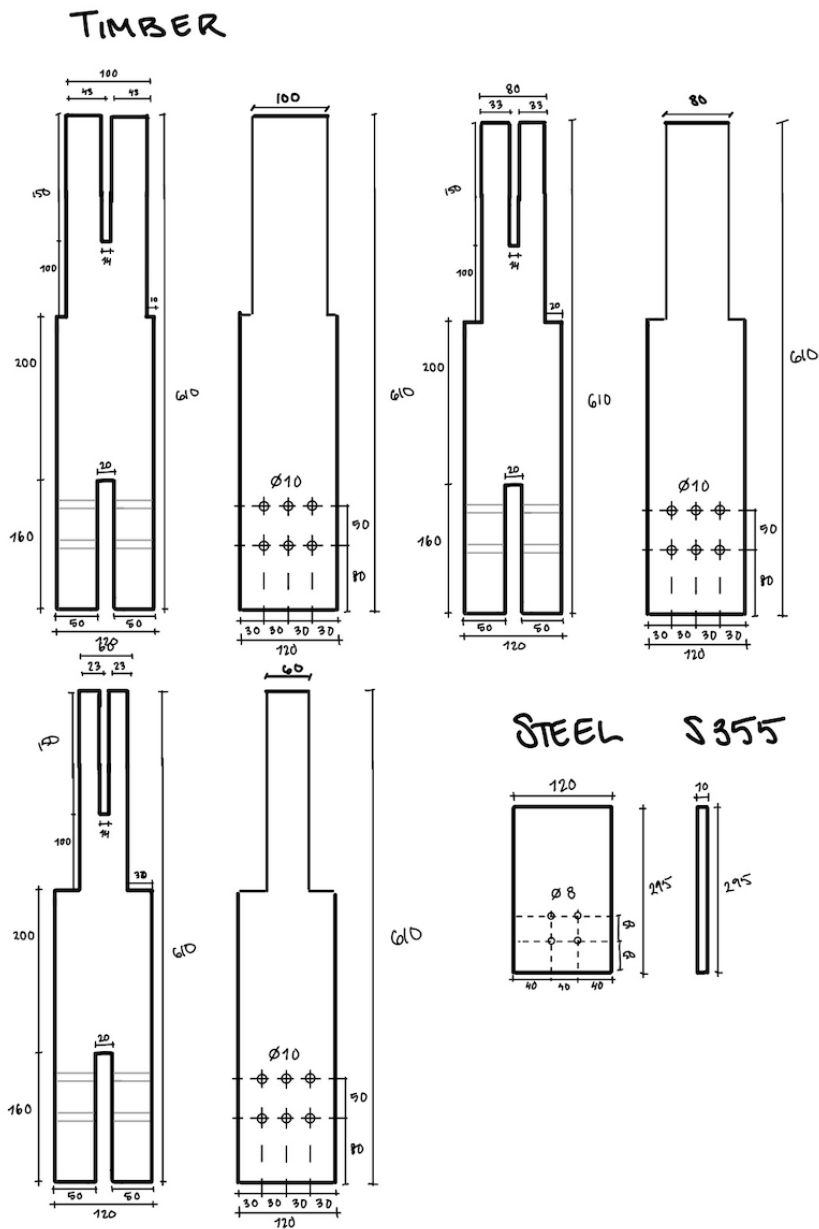


Figure A.7: The geometry of the specimen in test series 7

A. Appendix A - Geometry of test specimen

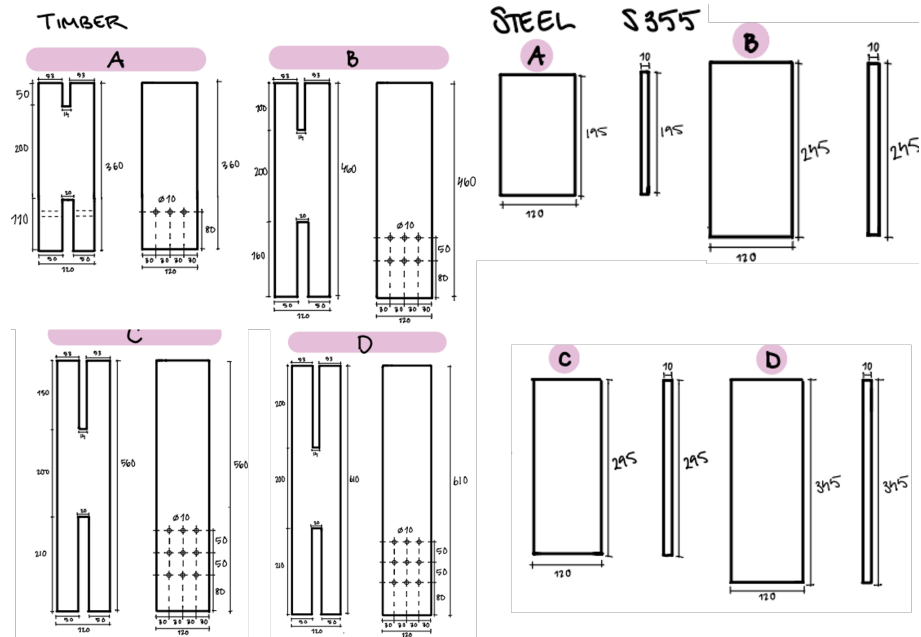


Figure A.8: The geometry of the specimen in test series 8

B

Appendix B - Tables of results from hand calculations

Table B.1: Results from test series 1

Variation no. [-]	Predicted capacity [kN]	Predicted failure [-]
1-1D	6.75	Shear failure in glue dowel
1-1P	6.75	Shear failure in glue dowel
1-1L	6.75	Shear failure in glue dowel
1-2D	6.75	Shear failure in glue dowel
1-2P	6.75	Shear failure in glue dowel
1-2L	6.75	Shear failure in glue dowel
1-4D	6.75	Shear failure in glue dowel
1-4P	6.75	Shear failure in glue dowel
1-4L	6.75	Shear failure in glue dowel
1-6D	6.75	Shear failure in glue dowel
1-6L	6.75	Shear failure in glue dowel

Table B.2: Results from test series 2

Variation no.	Predicted capacity	Predicted failure
[-]	[kN]	[-]
2-6d	42.25	Shear failure in adhesive
2-10d	46.25	Shear failure in adhesive
2-12d	49.00	Shear failure in adhesive

Table B.3: Results from test series 3

Variation no.	Predicted capacity	Predicted failure
[-]	[kN]	[-]
3-10d	6.75	Shear failure in glue dowel
3-12d	9.73	Shear failure in glue dowel
3-16d	17.29	Shear failure in glue dowel
3-20d	27.02	Shear failure in glue dowel
3-08t	6.75	Shear failure in glue dowel
3-10t	6.75	Shear failure in glue dowel
3-12t	6.75	Shear failure in glue dowel

Table B.4: Results from test series 4

Variation no.	Predicted capacity	Predicted failure
[-]	[kN]	[-]
4-4A	6.75	Shear failure in glue dowel
4-6A	6.75	Shear failure in glue dowel
4-8A	6.75	Shear failure in glue dowel

Table B.5: Results from test series 5

Variation no.	Predicted capacity	Predicted failure
[-]	[kN]	[-]
5-4A	39.50	Shear failure in adhesive
5-6A	39.50	Shear failure in adhesive
5-8A	39.50	Shear failure in adhesive

Table B.6: Results from test series 6

Variation no.	Predicted capacity	Predicted failure
[-]	[kN]	[-]
6-1S	87.54	Shear failure in glue dowel
6-2S	87.54	Shear failure in glue dowel
6-3S	87.54	Shear failure in glue dowel
6-4S	87.54	Shear failure in glue dowel

Table B.7: Results from test series 7

Variation no.	Predicted capacity	Predicted failure
[-]	[kN]	[-]
7-60H	123.65	Tension failure in timber
7-80H	126	Shear failure in timber
7-100H	126	Shear failure in timber
7-120H	126	Shear failure in timber

Table B.8: Results from test series 8

Variation no. [-]	Predicted capacity [kN]	Predicted failure [-]
8-50E	38.4	Shear failure in adhesive
8-100E	76.8	Shear failure in adhesive
8-150E	115.2	Shear failure in adhesive
8-200E	153.6	Tension fail- ure in adhe- sive

C

Appendix C - Results from experimental testing

Table C.1: The max load and failure mode for test specimens in test series 1.

Variation no. [-]	Max load [kN]	Failure mode [-]
1-1D-1	2.68	Shear failure dowel
1-1D-2	3.15	Shear failure dowel
1-1D-3	2.99	Shear failure dowel
1-1P-1	3.32	Shear failure dowel
1-1P-2	3.20	Shear failure dowel
1-1P-3	3.26	Shear failure dowel
1-1L-1	3.50	Shear failure dowel
1-1L-2	4.56	Shear failure dowel
1-1L-3	4.65	Shear failure dowel
1-2D-1	4.76	Shear failure dowel
1-2D-2	4.88	Combined shear and tension failure
1-2D-3	3.67	Shear failure dowel
1-2P-1	5.09	Shear failure dowel
1-2P-2	4.56	Shear failure dowel
1-2P-3	4.65	Shear failure dowel
1-2L-1	5.07	Shear failure dowel
1-2L-2	4.34	Shear failure dowel
1-2L-3	4.81	Shear failure dowel
1-4D-1	6.77	Timber-glue interface
1-4D-2	6.67	Shear failure dowel

C. Appendix C - Results from experimental testing

1-4D-3	5.48	Timber-glue interface
1-4P-1	6.51	Shear failure dowel
1-4P-2	5.36	Shear failure timber
1-4P-3	5.76	Shear failure dowel
1-4L-1	5.58	Shear failure timber
1-4L-2	5.13	Shear failure timber
1-4L-3	5.73	Shear failure timber
1-6D-1	6.53	Shear failure timber
1-6D-2	7.10	Shear failure timber
1-6D-3	6.85	Shear failure timber
1-6L-1	5.81	Shear failure timber
1-6L-2	6.51	Timber-glue interface
1-6L-3	6.44	Shear failure timber

Table C.2: The max load and failure mode for test specimens in test series 3.

Variation no.	Max load	Failure mode
3-10d-1	7.12	Shear failure dowel
3-10d-2	7.15	Combined shear and tension failure
3-10d-3	7.14	Tension failure dowel
3-12d-1	7.40	Tension failure dowel
3-12d-2	8.50	Tension failure dowel
3-12d-3	8.35	Tension failure dowel
3-16d-1	10.45	Timber glue interface behind the dowel
3-16d-2	8.57	Tension failure dowel
3-16d-3	9.29	Tension failure dowel
3-20d-1	12.27	Timber-glue interface
3-20d-2	9.72	Timber-glue interface
3-20d-3	14.54	Timber-glue interface
3-08t-1	4.27	Tension failure dowel
3-08t-2	5.52	Shear failure dowel
3-08t-3	6.32	Tension failure dowel
3-10t-1	3.80	Tension failure dowel
3-10t-2	5.70	Tension failure dowel

3-10t-3	6.11	Tension failure dowel
3-12t-1	6.25	Tension failure dowel
3-12t-2	6.47	Tension failure dowel
3-12t-3	5.26	Tension failure dowel

Table C.3: The max load and failure mode for test specimens in test series 4.

Variation no.	Max load	Failure mode
4-4A-1	6.35	Tension failure dowel
4-4A-2	6.53	Tension failure dowel
4-4A-3	6.99	Timber glue interface behind the dowel
4-6A-1	6.57	Tension failure dowel
4-6A-2	5.70	Tension failure dowel
4-6A-3	5.81	Tension failure dowel
4-8A-1	6.25	Shear failure dowel
4-8A-2	4.43	Tension failure dowel
4-8A-3	5.92	Tension failure dowel

Table C.4: The max load and failure mode for test specimens in test series 5.

Variation no.	Max load	Failure mode
5-4A-1	26.37	Steel glue interface
5-4A-2	21.38	Steel glue interface
5-4A-3	22.68	Steel glue interface
5-6A-1	17.34	Steel glue interface
5-6A-2	16.01	Steel glue interface
5-6A-3	22.09	Steel glue interface
5-8A-1	26.55	Steel glue interface
5-8A-2	20.31	Steel glue interface
5-8A-3	23.71	Steel glue interface

Table C.5: The max load and failure mode for test specimens in test series 6.

Variation no.	Max load	Failure mode
6-1S-1	47,03	Combined failure
6-1S-2	38,56	Timber-glue interface
6-1S-3	43,95	Timber-glue interface
6-2S-1	41,98	Timber-glue interface
6-2S-2	45,71	Timber-glue interface
6-2S-3	88,08	Shear failure timber
6-3S-1	51,99	Tension failure in glue dowel, splitting in timber
6-3S-2	83,09	Tension failure in glue dowel, splitting in timber
6-3S-3	74,34	Timber-glue interface
6-4S-1	57,73	Timber-glue interface combined with shear in timber
6-4S-2	50,51	Timber-glue interface combined with shear in timber
6-4S-3	51,25	Timber-glue interface combined with shear in timber

Table C.6: The max load and failure mode for test specimens in test series 7.

Variation no.	Max load	Failure mode
7-100H-1	32,04	Combined failure
7-100H-2	42,82	Shear failure glue dowel
7-100H-3	46,14	Combined failure
7-80H-1	43,63	Tension failure glue dowel
7-80H-2	44,90	Shear failure glue dowel
7-80H-3	47,19	Tension failure glue dowel
7-60H-1	39,40	Splitting in timber
7-60H-2	44,36	Splitting in timber
7-60H-3	53,29	Splitting in timber

Table C.7: The max load and failure mode for test specimens in test series 7.

Variation no.	Max load	Failure mode
8-50E-1	20,59	Steel glue interface
8-50E-2	17,75	Steel glue interface
8-50E-3	36,87	Steel glue interface
8-100E-1	34,35	Steel glue interface
8-100E-2	52,64	Steel glue interface
8-100E-3	49,11	Steel glue interface
8-150E-1	87,89	Steel glue interface
8-150E-2	62,76	Steel glue interface, shear in timber
8-150E-3	40,96	Steel glue interface, timber splitting
8-200E-1	71,65	Steel glue interface
8-200E-2	44,79	Steel glue interface
8-200E-3	78,36	Steel glue interface

D

Appendix D - Load-displacement curves from experimental testing

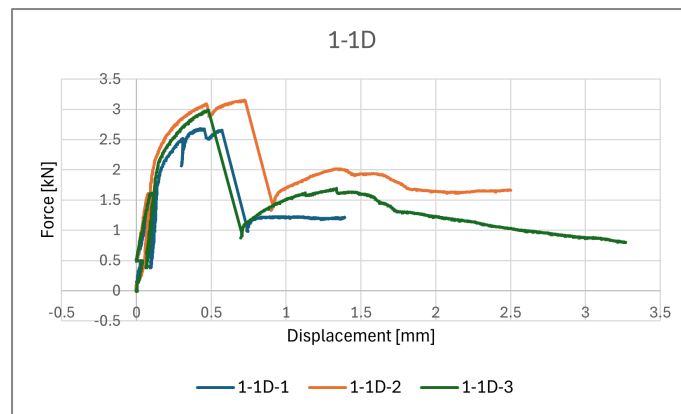


Figure D.1: Load-displacement curve for test 1-1D

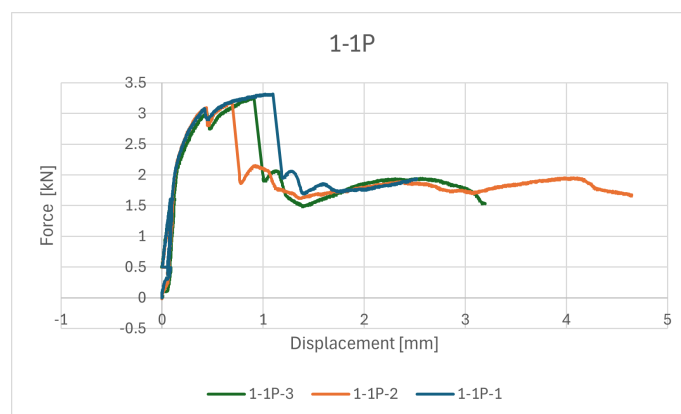


Figure D.2: Load-displacement curve for test 1-1P

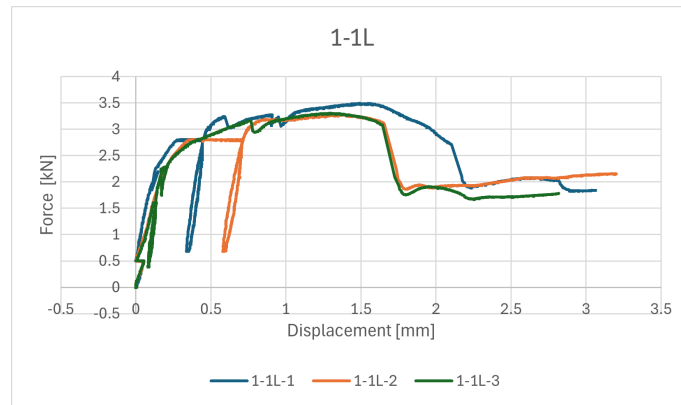


Figure D.3: Load-displacement curve for test 1-1L

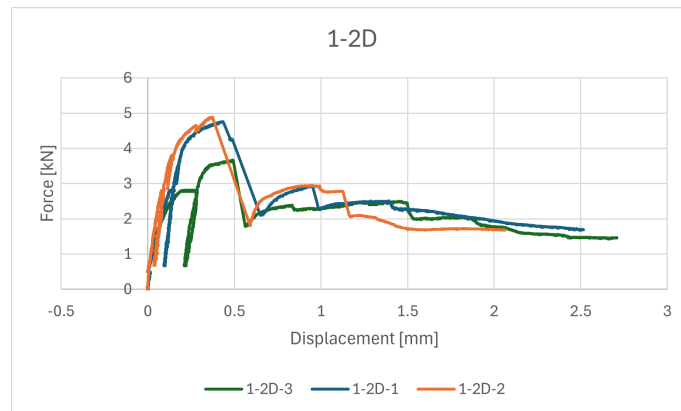


Figure D.4: Load-displacement curve for test 1-2D

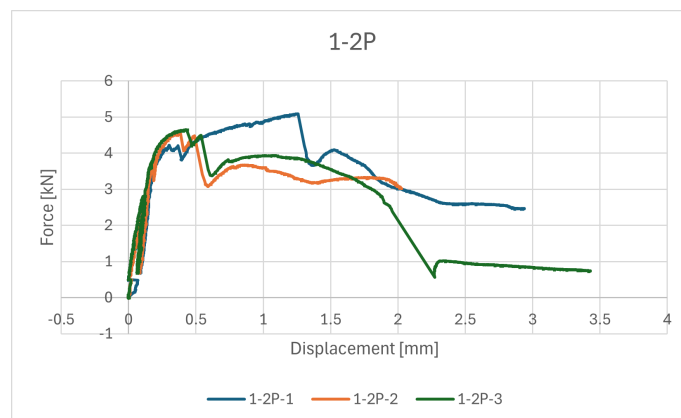


Figure D.5: Load-displacement curve for test 1-2P

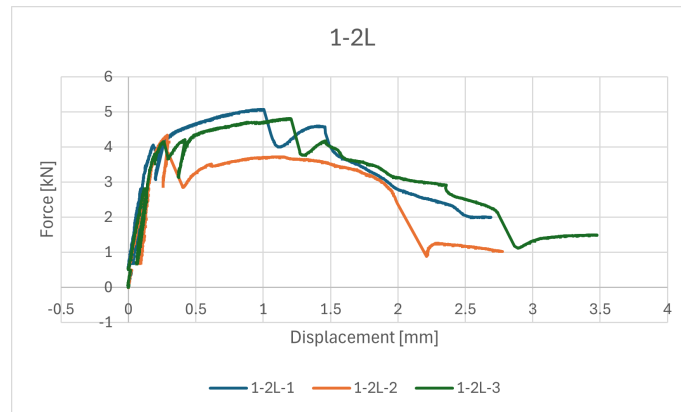


Figure D.6: Load-displacement curve for test 1-2L

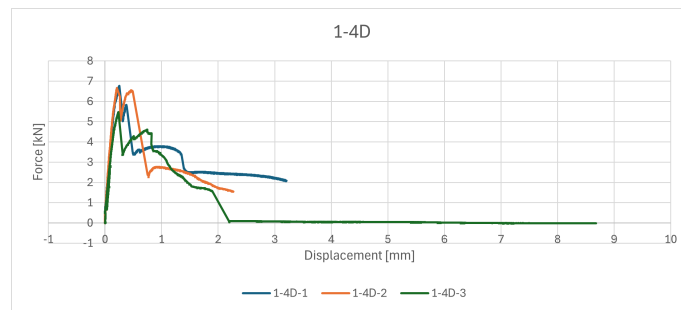


Figure D.7: Load-displacement curve for test 1-4D

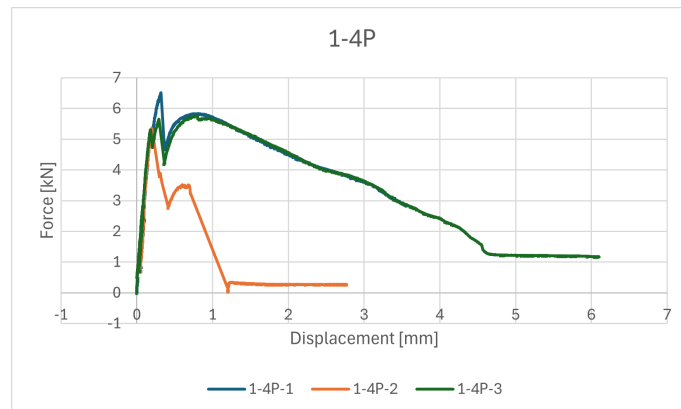


Figure D.8: Load-displacement curve for test 1-4P

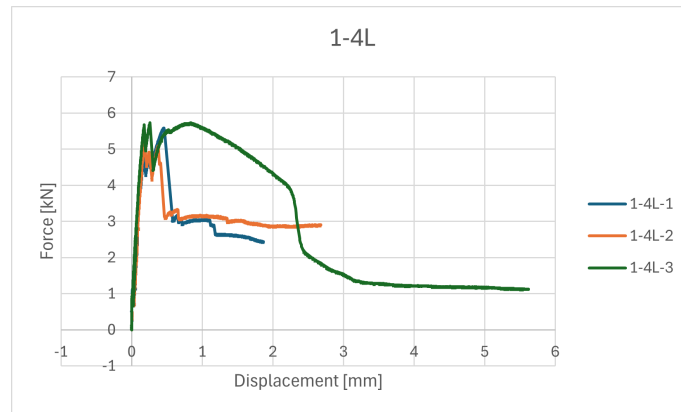


Figure D.9: Load-displacement curve for test 1-4L

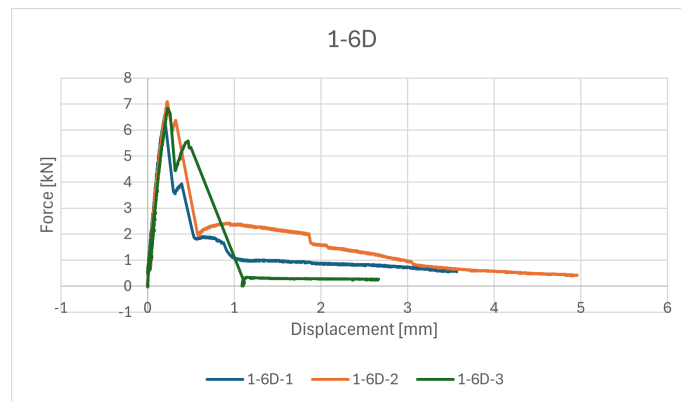


Figure D.10: Load-displacement curve for test 1-6D

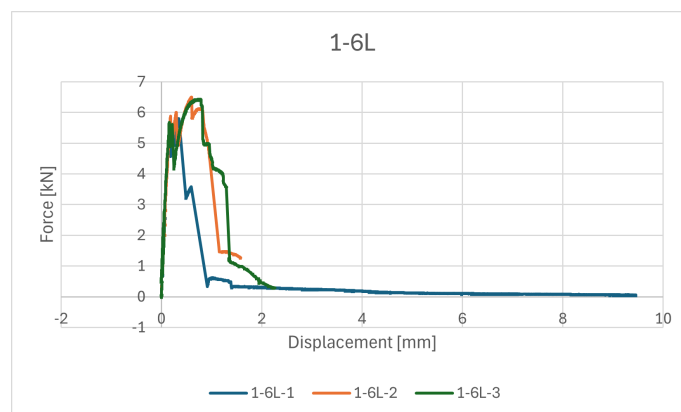


Figure D.11: Load-displacement curve for test 1-6L

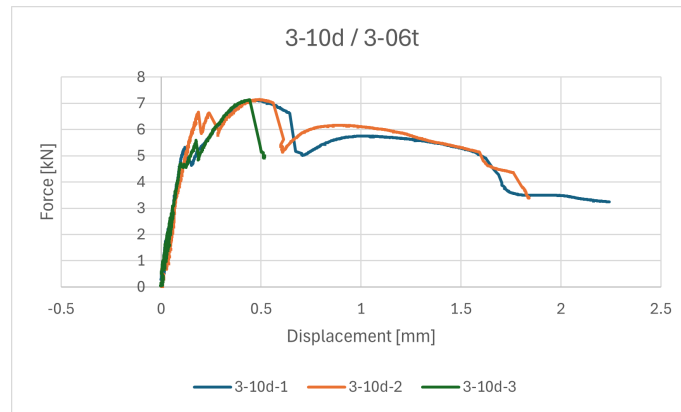


Figure D.12: Load-displacement curve for test 3-10d and 3-06t

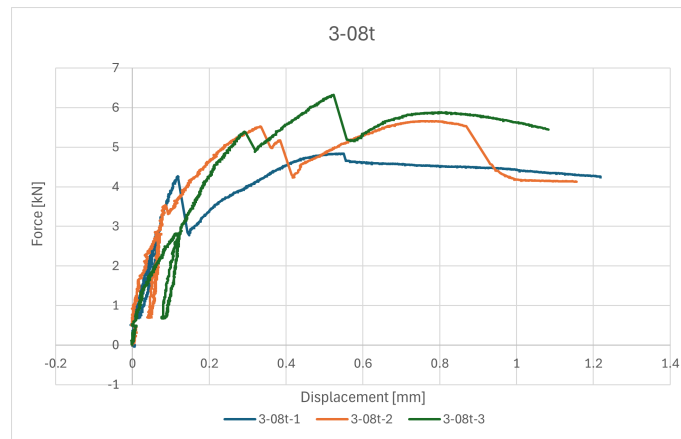


Figure D.13: Load-displacement curve for test 3-08t

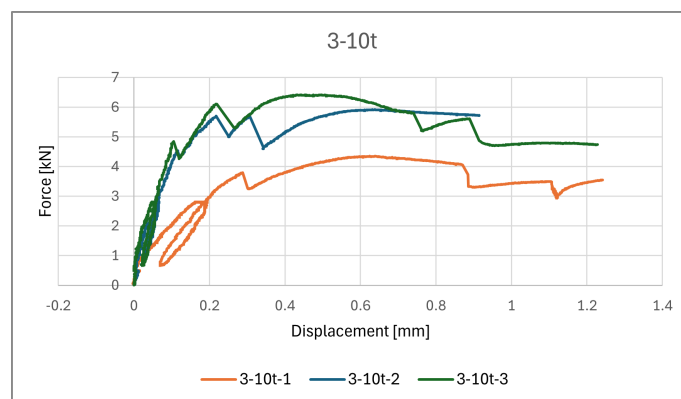


Figure D.14: Load-displacement curve for test 3-10t

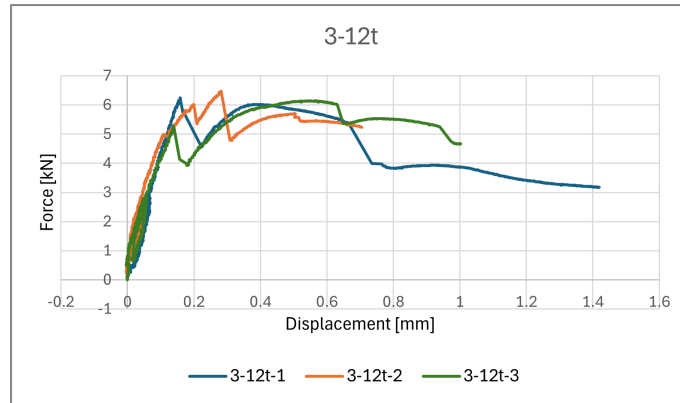


Figure D.15: Load-displacement curve for test 3-12t

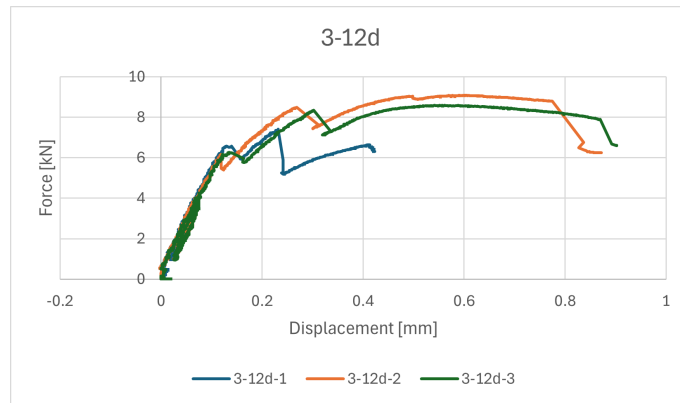


Figure D.16: Load-displacement curve for test 3-12d

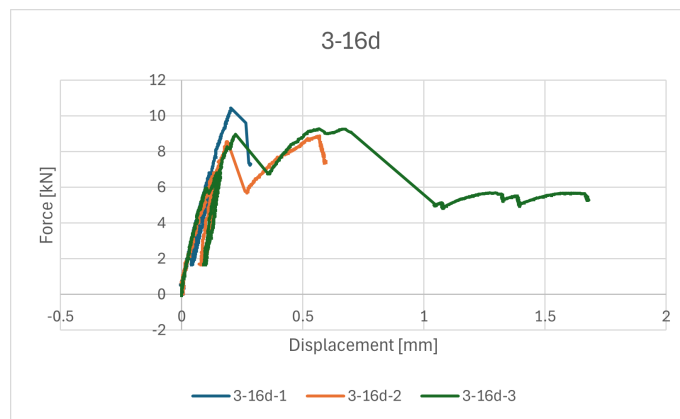


Figure D.17: Load-displacement curve for test 3-16d

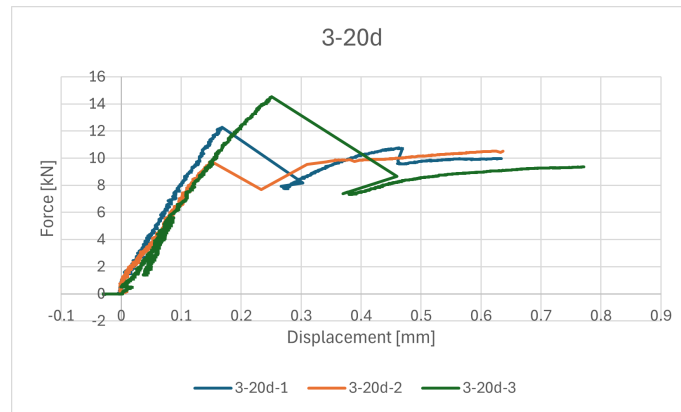


Figure D.18: Load-displacement curve for test 3-20d

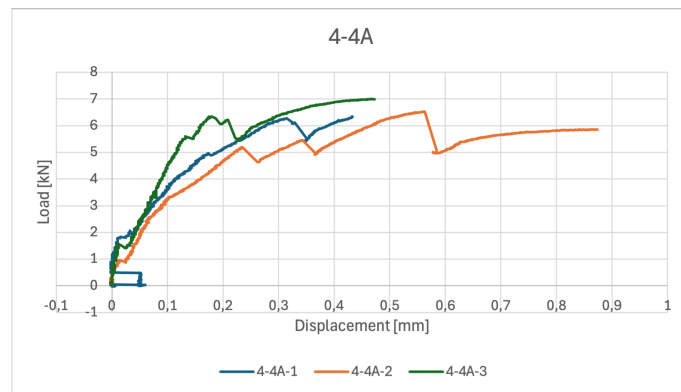


Figure D.19: Load-displacement curve for test 4-4A

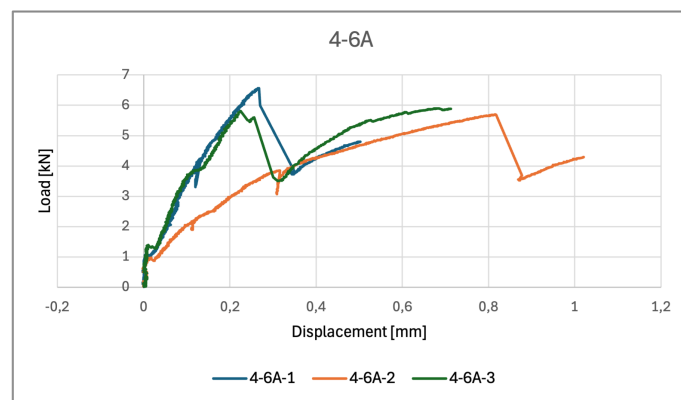


Figure D.20: Load-displacement curve for test 4-6A

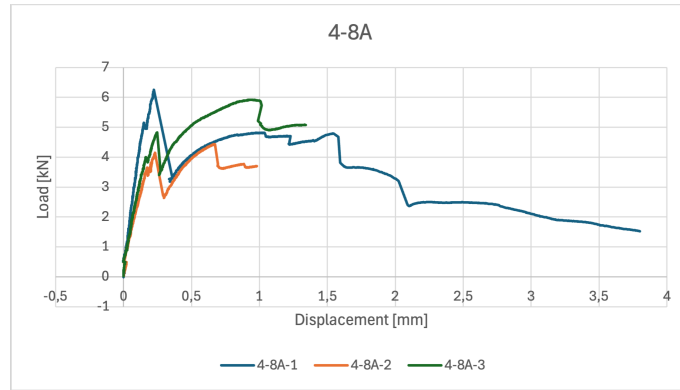


Figure D.21: Load-displacement curve for test 4-8A

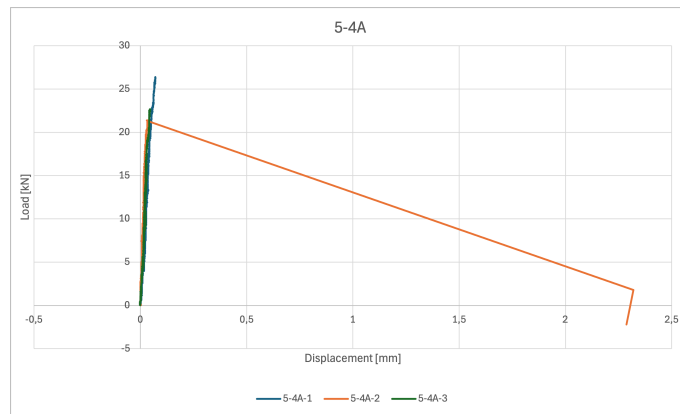


Figure D.22: Load-displacement curve for test 5-4A

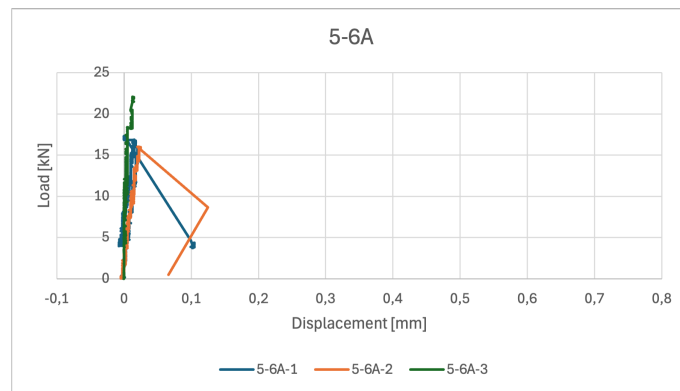


Figure D.23: Load-displacement curve for test 5-6A

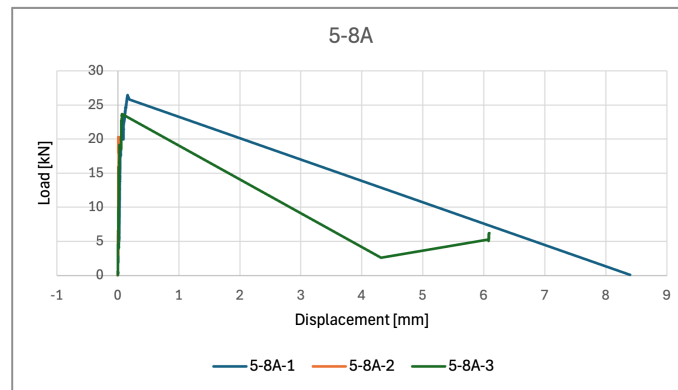


Figure D.24: Load-displacement curve for test 5-8A

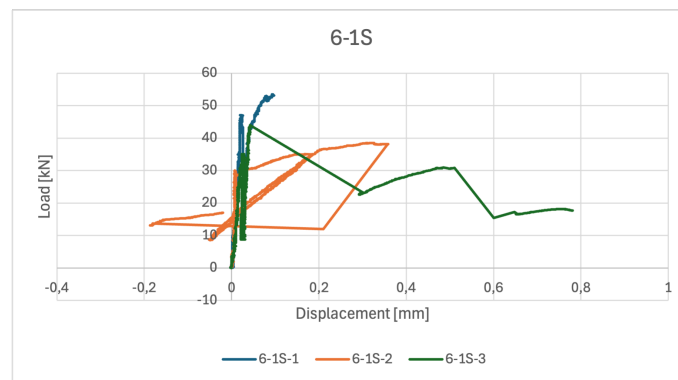


Figure D.25: Load-displacement curve for test 6-1S

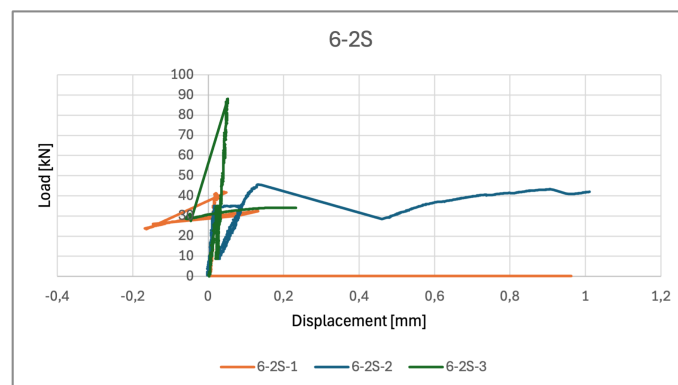


Figure D.26: Load-displacement curve for test 6-2S

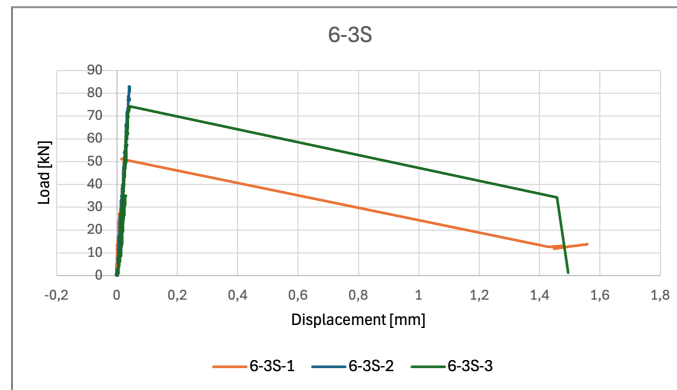


Figure D.27: Load-displacement curve for test 6-3S

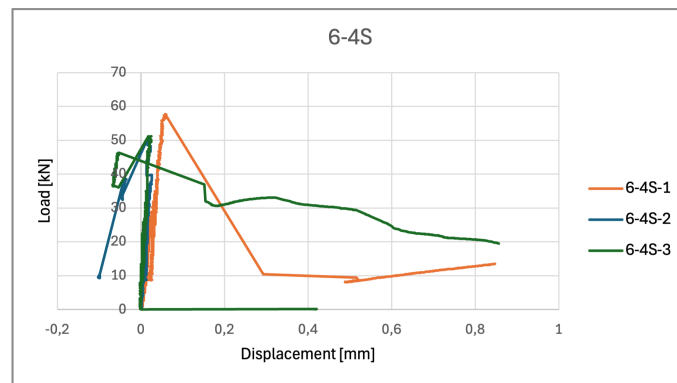


Figure D.28: Load-displacement curve for test 6-4S

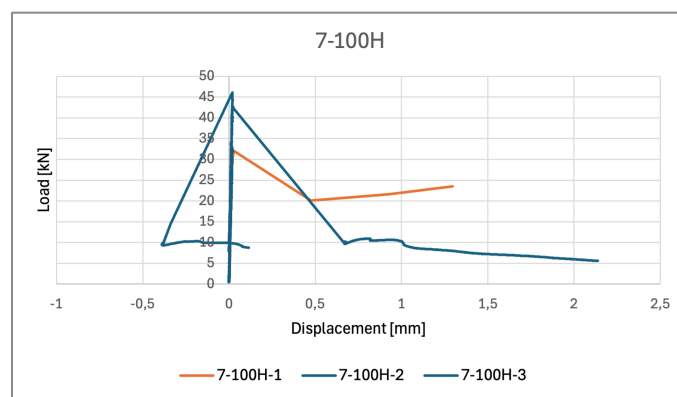


Figure D.29: Load-displacement curve for test 7-100H

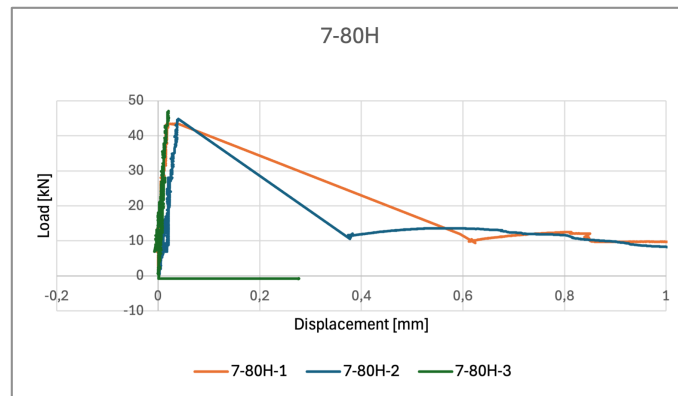


Figure D.30: Load-displacement curve for test 7-80H

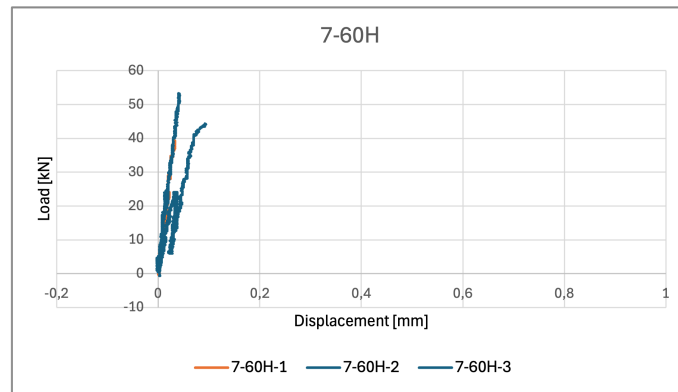


Figure D.31: Load-displacement curve for test 7-60H

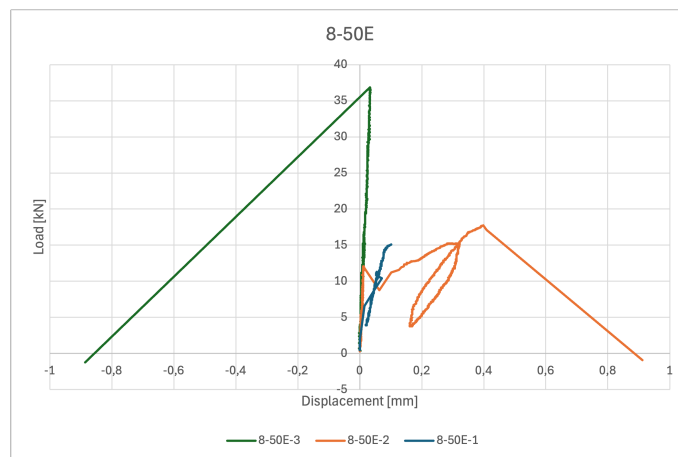


Figure D.32: Load-displacement curve for test 8-50E

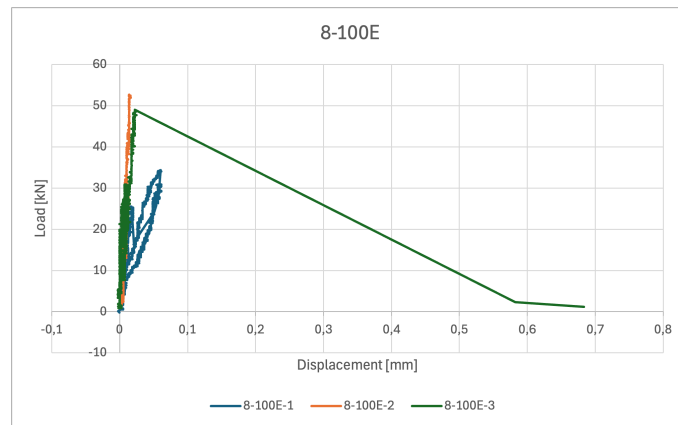


Figure D.33: Load-displacement curve for test 8-100E

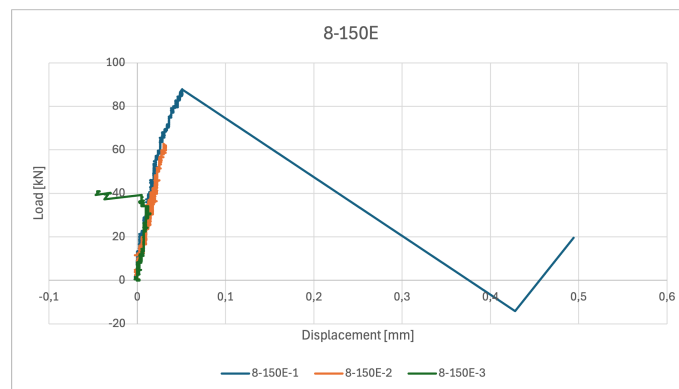


Figure D.34: Load-displacement curve for test 8-150E

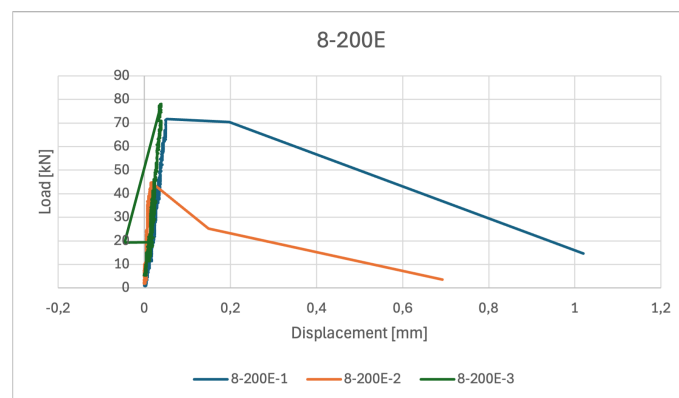


Figure D.35: Load-displacement curve for test 8-200E

DEPARTMENT OF ARCHITECTURE AND CIVIL ENGINEERING
CHALMERS UNIVERSITY OF TECHNOLOGY

Gothenburg, Sweden

www.chalmers.se



CHALMERS
UNIVERSITY OF TECHNOLOGY